PRECIPITATION ESTIMATES BY RADAR: A ZENITH POINTING RADAR PERSPECTIVE

A Thesis Submitted to

The Faculty of Graduate Studies and Research
of
McGill University
by
Frédéric Fabry

In Partial Fulfillment of the
Requirements for the Degree
of
Master of Science

Department of Meteorology
McGill University
Montréal, Quebec
Canada
H1P 1C0

July 1990

ABSTRACT

Data collected from zenith pointing radar is used to study the range dependence of some meteorological radar errors associated with different sampling methods between radar and gauges in stratiform precipitation. Errors due to the vertical variation of reflectivity such as those related with the bright band or with snow growth cause a much larger bias in radar estimates than those due to beam filling or gradients. The maximum useful range varies with the bright band height and the elevation angle program used, a CAPPI giving superior results especially for snow. The sudden changes in bright band height over short distances and the large scatter of its thickness limit the accuracy of current corrections for the vertical variation of reflectivity based on scanning radar data. The possibility of using a zenith pointing radar to obtain this correction is discussed.

RESUME

Des données provenant d'un radar à visée verticale sont utilisées pour l'étude de certaines erreurs d'estimations de précipitations stratiformes associées aux différences d'échantillonage entre radars et pluviomètres en fonction de la distance. Les erreurs dues aux variations verticales de la réflectivité comme celles causées par la bande brillante ou par la croissance de la neige sont de beaucoup plus importantes que celles reliées au faisceau rempli de façon non uniforme ou aux gradients. La portée utile du radar varie en fonction de l'altitude de la bande brillante et du programme d'élévation, un CAPPI donnant de meilleurs résultats surtout pour la neige. Les changements soudains d'altitude de la bande brillante sur de courtes distances ainsi que la grande variabilité de son épaisseur limitent la justesse des présentes corrections pour la variation verticale de la réflectivité qui sont basées sur les données d'un radar à balayage panoramique. L'utilisation possible d'un radar à visée verticale pour ce travail est discutée.

ACKNOWLEDGEMENTS

The completion of this thesis would have been significantly delayed without the help of almost all the staff of the McGill Radar Observatory. Above all thanks are due to Geoff Austin, my supervisor, for his advice and support over the course of the work on this project. I also want to thank Abnash Singh for his precious help in the mechanical assembly of the radar, Ernest Ballantyne for his help with the digitizer and the calibration of the radar, Brian Katz and Mario Ivanich for their advice on the computer interface, Aldo Bellon and Mike Duncan for stimulating discussions and their help in the proof-reading of this manuscript. The list would not be complete without Alan Seed and David Tees whose guidance at the early stage of the thesis proved to be extremely valuable.

Next, I must also thanks my parents, Nicole and Roland Fabry for their ample moral support through all the stages of the thesis preparation. This moral support included the use of a car for transportation to the McGill Radar during the collection period of weather data which often occurred when public transportation was unavailable.

TABLE OF CONTENTS

LIST OF FIGURES

LIST OF TABLES

STATEMENT OF ORIGINALITY

To the author's knowledge, high resolution zenith pointing radar data was used for the first time for the quantitative study of the degradation of the accuracy of scanning radar estimates of stratiform precipitation with range. Using this data, it was found that the bright band was the main limiting factor to the accuracy of the estimations.

The mean vertical reflectivity profile varied significantly from event to event and even within events. Hence, corrections based on a standard reflectivity profile or on climatological statistics from raingauges for example are of limited accuracy. Reflectivity gradients and beam filling problems which were formerly considered very important sources of error have in fact a limited impact on the accuracy of these estimates.

Bright band thickness was measured using rainfall data for 3 months and was found to follow a log-normal distribution. It also showed a power law dependence with rainfall.

1 INTRODUCTION

1.1 RADAR ESTIMATES OF STRATIFORM PRECIPITATION

In the past forty years, a great deal of research has been done on the use of radar for measuring precipitation. By providing instantaneous and continuous precipitation information over large areas, the radar has rivaled the dense rain gauge network as the main tool for obtaining precipitation estimates. Moreover, radar enables the generation of short term quantitative precipitation forecasts. However, there is still little concensus on the accuracy of the radar estimates because the radar does not measure rainfall directly. Radar measures the reflectivity of the hydrometeors, Z, which corresponds to the average over the illuminated volume of the sum of the sixth powers of the drop diameters per unit volume. Rainfall is proportional to the volumes of the drops (and hence to the third power of drop diameters) times the fall velocity. The latter is also a weak function of drop diameters. In addition, the reflectivity of the precipitation is measured at several kilometers above the ground and during an instant, while the quantity of interest is the accumulation over time of precipitation at the ground. In order to convert reflectivity into rainfall information, several Z-R relationships of the form $Z = aR^b$ have been proposed by assuming or measuring drop-size distributions.

To verify the accuracy of the radar, it is essential to compare its estimates with some sort of ground truth. This comparison is usually done with rain or snow gauges which are assumed to have measured the precipitation accurately at a set of points. Wilson and Brandes (1979) recognizes three types of error in radar-gauge comparisons. The first type

is the error in estimating the radar reflectivity factor. This includes errors from various sources such as calibration, attenuation, beam blockage, anomalous propagation and errors related to the fluctuating nature of the precipitation echoes and to the technique used to average pulses. For snow, missed echoes because of reflectivity below the radar threshold could be added to the list. These errors have received a lot of attention and are well documented by several papers (Wilson and Brandes list 16 references on the subject). The second type of error is related to variations of the Z-R relationships from storm to storm and within storms. In order to determine the correct Z-R relationship for a storm, dual wavelength (Ulbrich and Atlas, 1975) and dual polarization radars (Seliga and Bringi, 1976) have been proposed. Good results are obtained if the drop size distribution is a main source of the radar error (Doviak, 1983). The third type of error listed by Wilson and Brandes is caused by the differences in the gauge-radar sampling methods. Radar estimates the mean rainfall illuminated by its kilometers wide beam at a significant height above the ground and during an instant every 5 to 15 minutes. Gauges measure the accumulation of rainfall at the ground over an area of a few decimeters square. Sampling errors include those due to time sampling differences, evaporation or accretion and to non-uniform reflectivity in the beam caused by storms edges, bright band contamination and missed small scale features. These errors can be very important in the case of stratiform precipitation where there are rapid changes in the reflectivity field as a function of height particularly in snow and around the melting layer.

However, until recently, the sampling errors were generally much less discused than the other ones because they are more difficult to study. For example, the errors associated with vertical and horizontal variations of reflectivity in the radar beam as a function of range cannot be estimated unless high resolution reflectivity information is available.

This lack of a correct field has inhibited research on radar-gauge sampling problems. If any progress is to be made, one must assume that some "wrong" field is in fact "correct" enough to be a plausible "correct" field. There are a number of ways to do this. First, an hypothetical reflectivity profile can be assumed and then calculations can be made. This reflectivity field can be purely theoretical or based on measurements. Donaldson (1964) used such a technique to examine the variation of echo top measurements with range using plausible model storms. Secondly, a stochastic model can be used to generate a plausible correct field (see Chandrasekar and Bringi, 1987). Thirdly, scanning radar data at the highest resolution possible (for example at close range) can be used. This high resolution data will then be simulated to be observed by a radar at different ranges (Tees and Austin, 1989).

1.2 RADAR ACCURACY AND RANGE

Excluding attenuation and beam blockage, the decrease of the radar accuracy with range is related to the sampling differences between radar and gauges. It also varies with the type of precipitation (Figure 1.1, Wilson, 1976). There are several reasons for the degradation of radar estimates with range. First, the beam widens with range. For example, a 1 degree beam widens by 1 km every 60 km of range. At a range of 30 km, the beam would be 500 meters wide while it would be 4 km wide at 240 km. Assuming a constant bin length, the sampling volume is then 64 times larger at 240 km than at 30 km. Gradients in the reflectivity field are more likely to be present and stronger at far range in a larger volume than at close range, causing a range dependent bias. Zawadzki (1982, 1984) computed errors associated with beam smoothing in the presence of reflectivity gradients. He presented a simple example of range dependent sampling in the presence of

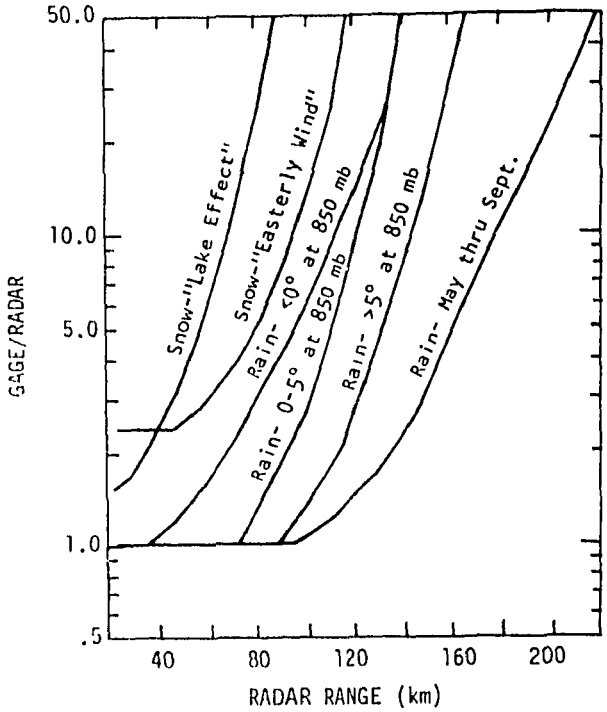

Fig. 1.1 - Graph of gauge to radar ratio as a function of range (from Wilson, 1976).

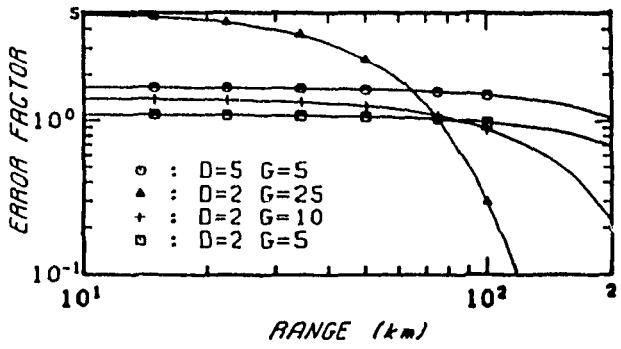

Fig. 1.2 - Curves from Zawadzki (1984) showing the error factor vs range for various combinations of gradient and measurement cell size.

gradients. Consider a Gaussian beam sampling a field with a constant reflectivity gradient G (dB/km) along one direction, the field being constant in the other two. Assuming that a single Z-R relationship governs the transformation from Z to R, he shows that when the gradient has been sampled with the beam and then averaged into a Cartesian grid of size D (in km), the ratio of the "measured" rainfall to that "actually" there at the center of the grid is:

$$F = \frac{cA}{GD}\exp\left(-\frac{(\delta G)^2}{Ac^2}\right)\sinh\left(\frac{GD}{cA}\right) \qquad where \quad c = 20\log_{10} e$$

where F is the Error Factor, δ is the distance (in km) subtended by the beam and A is the exponent in the Z-R relationship used to convert Z to rainfall. This relation helps to predict the discrepancies in radar-gauge comparisons (Figure 1.2). Furthermore, a wide beam is also more likely to include different types of hydrometeors such as snow, rain, sleet, hail or melting precipitation in unknown proportion making the precipitation estimates more difficult. Secondly, the height of the beam axis changes with range. When precipitation is estimated using a 0.5 degree PPI (Plan Position Indicator), the height of the beam axis is 600 meters at a range of 50 km but 2.6 km at 150 km and 5.9 km at 250 km. This can cause serious biases at far range since the precipitation rate or the reflectivity measured at these heights by the radar is often significantly different than that at the surface. This problem can be somewhat alleviated by using a CAPPI (Constant Altitude Plan Position Indicator) which combines data from several elevations angles in one radar map (Marshall, 1957). A good example of the problem is shown in Joss and Waldvogel (1990). They used mean vertical reflectivity fields such as those derived by Koistinen (1986) to look at the effect of range on radar derived vertical precipitation

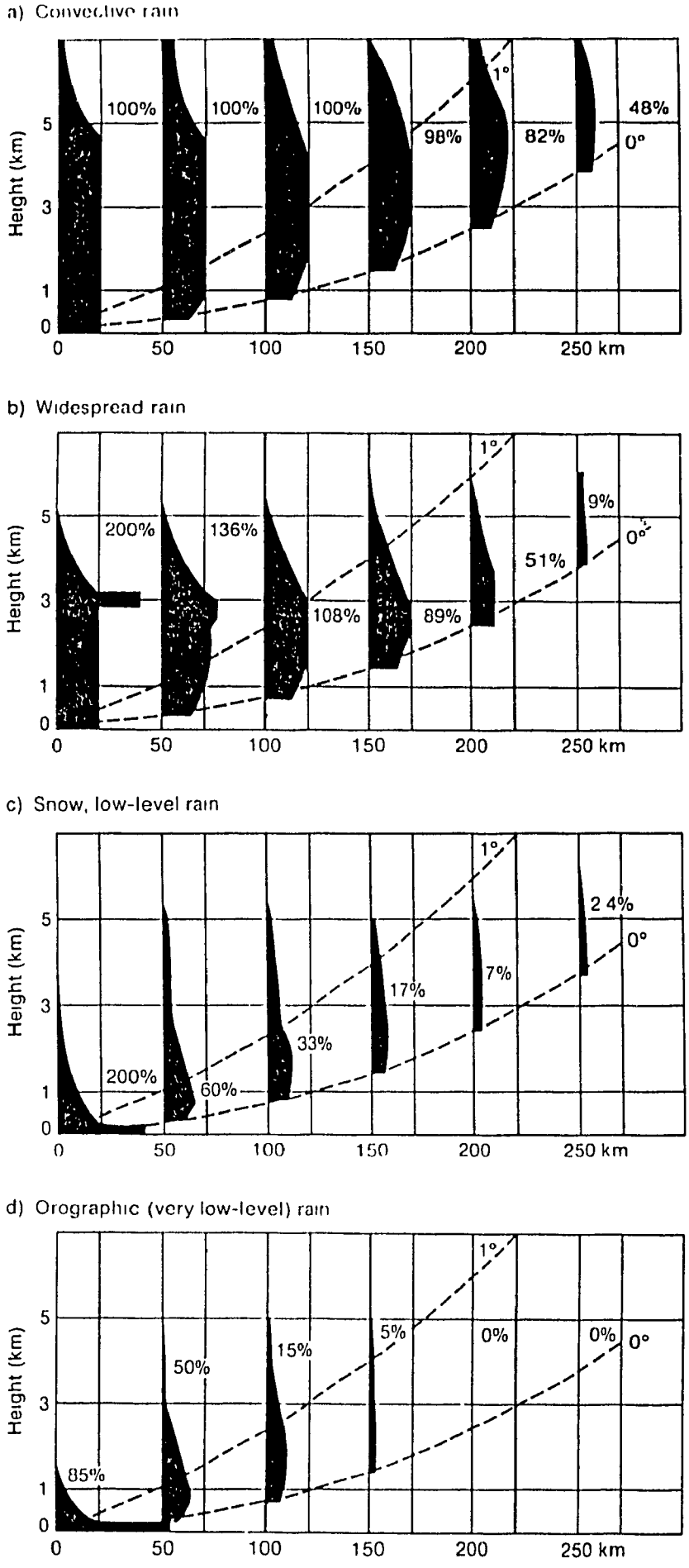

Fig. 1.3 - Vertical profiles seen by the radar at various ranges in convective and widespread rain, in low-level rain or snow, and in orographic rain. The numbers in each figure give the percentage (referred to the true melted water value which would be measured at ground level using a rain gauge) of rain rate deduced from a maximum reflectivity in the profile. A radar with a 1° beam width is assumed, in a flat country. If the radar is lower than nearby obstacles, then much less precipitation can be observed at far ranges. The top and bottom of the main part of a 1° beam elevated at 0.5° are shown as dashed lines labeled 0° and 1° (from Browning and Collier, 1989; partly after Joss and Waldvogel, 1990).

profiles for different types of precipitation (Figure 1.3). They clearly demonstrate the importance of the range dependance of precipitation measurements, especially when the precipitation is limited to low levels as in stratiform rain or snow (see also Joss and Waldvogel, 1989). Tees and Austin (1989) used high resolution radar data from summer precipitation at close range and mapped it at far range to simulate what the radar would have measured. Sub-bin gradients were assumed to be negligible. Seven storms were studied by a radar generating CAPPIs at 3 km and the "measured" accumulation as a function of range was plotted (Figure 1.4). Here again the estimation decreases considerably as a function of range.

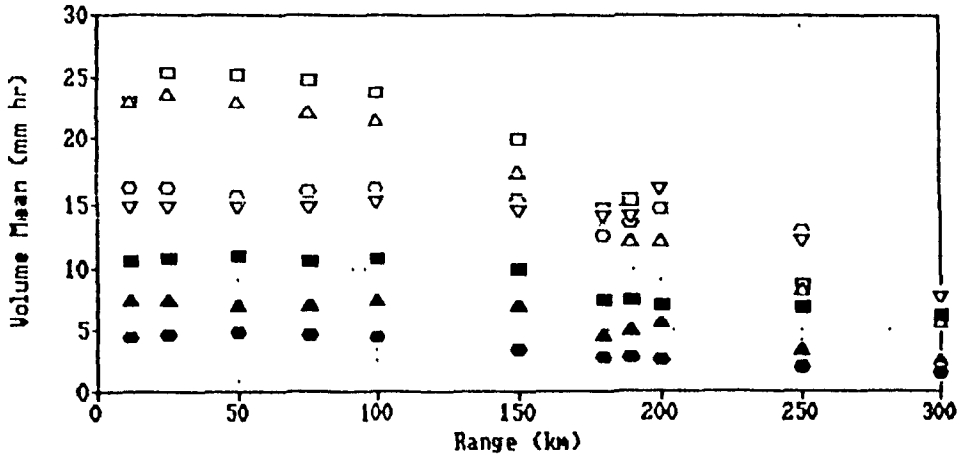

Fig. 1.4 - Volume Mean rainfall rate vs range for the curved earth simulation for seven summer storms in Montreal (from Tees and Austin, 1989).

One approach to correct for range variations of the reflectivity field, suggested by Calheiros and Zawadzki (1987), is based on mapping the cumulative probabilities of rainfall in raingauges to the cumulative probability of radar reflectivity. Since the intensity distributions change with range, this method produces range dependent Z-R relationships. This method attempts to match the radar to the climatology of the gauges. However, this method is only intended to work "on the average" since the comparison of any particular event with the climatology is doubtful. It also treats similarly convective and stratiform events which have different vertical reflectivity profiles and hence different range dependent biases.

To study stratiform precipitation where vertical reflectivity variations are strong, high resolution reflectivity field is needed. But using scanning radar data even at close range does not give the necessary vertical resolution to resolve accurately strong and narrow features like the bright band. However, actual radar data would make a more realistic input field than a mean vertical profile without gradients or a stochastic model or fractal precipitation field. The best way to obtain a high resolution field based on radar data is to combine a zenith pointing radar transmitting short pulses and a very fast digitizer. This data is ideal to study the range dependance of radar estimates and to separately evaluate the contribution from different terms. This thesis will describe how zenith pointing radar data from rainfall and snowfall events was used to investigate the range dependance of radar estimates and to what extent the different phenomena causing a non uniform reflectivity in the beam affect these estimates. As will become apparent in the following chapters, the case to case and time to time changes in the shape of the vertical profile of precipitation are important, leading to some reservations about the applicability of an average vertical profile as a real-time correction.

1.3 ATTACKING THE SAMPLING PROBLEM WITH A ZENITH POINTING RADAR

A zenith pointing radar measures the height-time variation of precipitation as it moves over it. Since this two-dimensional picture of precipitation is of little interest in an operational environment, it is mostly used for research in microphysical and dynamical studies of precipitation at relatively small scales. Radars measuring only reflectivities were first used together with vertically scanning radars to look at features like the bright band (Austin and Bémis, 1950), snow trails (Marshall, 1953), generating cells (Gunn et al., 1954; Douglas et al., 1957; Sauvageot, 1976) and echo shapes (Boucher, 1957) Doppler technology has yielded new data on particle sizes and fall speeds in bright band cases. These results were obtained either using radar alone (Lhermitte and Atlas, 1963) or by combining radar with other instruments (Waldvogel and Steiner, 1986). Increase in sensitivity and resolution together with the development of FM-CW radars (Richter, 1969) expanded research on clouds and clear air echoes (Gossard and Strauch, 1983).

The main advantage of using a zenith pointing radar to study radar-gauge sampling problems is that its sampling method more closely resembles that of a rain or snow gauge than that of a scanning radar. First, it can evaluate the precipitation very close to the ground using the first bins rather than higher up as for scanning radars. It also takes measurements continuously instead of every 5 minutes; hence accumulations can be computed in the same fashion as for gauges. Furthermore, the surface over which the precipitation is estimated is of the order of a few meter square against decimeter square for a gauge and kilometer square for a scanning radar. Therefore, the precipitation rate statistics determined from zenith pointing data would more closely approximate those by

gauge than those from a scanning radar.

By definition, the zenith pointing radar measures only the reflectivity from weather echoes moving above it. Changes in the measured quantity occur at a much slower rate than for a scanning radar whose field of view vary significantly in a tenth of a second. Thus the zenith pointing radar has more time to average the reflectivity data from several pulses in order to reduce the echo fluctuations. This gives the stable and accurate measurements necessary to make reliable simulations. In addition, the data collected can have high vertical and time resolutions. As an example, the radar used in this study allow us to get a new reflectivity measurement every 20 meters and a new series of measurements every second or two. This high resolution makes it possible to compute the effects of the bright band or the reflectivity gradients on radar precipitation estimates.

The main limitation of using zenith pointing radar measurements for simulations is that the data is only available in two dimensions. Indeed, the radar only obtains data in one spatial dimension, height, the other dimension being time. The observed time variations of the data recorded arise from a combination of the translation across the beam of spatial variations in the precipitation patterns and of the evolution of the structure in time. The physical interpretation of the measurements is therefore difficult and their use for simulations limited unless some assumptions are made about the behavior of the reflectivity data in the two other spatial dimensions. However, if the zenith pointing radar is operated in conjunction with a scanning radar, then considerable additional information is available to aid in the interpretation.

Measurements from a zenith pointing radar seem singularly appropriate to study the accuracy of precipitation estimates by scanning radar since the initial field produced using this data is closer to the real field than can be generated by most other methods, whether they are based on model rainfalls or scanning radar data.

2 EXPERIMENTAL WORK

2.1 MECHANICAL AND ELECTRONIC SET-UP

The zenith pointing radar was installed in a trailer located in the parking lot of the McGill Radar Observatory from the fall of 1989 (Fig. 2.1). The transceiver was installed on a structure inside the trailer build previously for an iceberg remote detection experiment. Above the structure, two aluminium bars were put across the trailer's sunroof opening and were used as a support for the 1.2 meter diameter vertically pointing antenna. The rest of the sunroof opening was covered with rubber to prevent the entry of precipitation into the trailer and a plastic radome was added over the dish. A schematic of the experimental arrangement is shown in Figure 2.2.

The transceiver used was obtained from an X-band Decca RM926 marine radar. The specifications for the zenith pointing radar are given in table 2.1.

Table 2.1 - Radar specifications

Wavelength	3.2 cm
Peak Transmitted Power	25 kW
Pulse Length used	0.25 μs
Pulse Repetition Frequency	1700 Hz
Receiver Transfer Function	Logarithmic
Receiver Sensitivity	-97 dBm
Antenna Size	1.2 m
Beam Width	2.3 º
Minimum Detectable Signal	7 dBZ (0.1 mm/hr) at 10 km

Fig. 2.1 - McGill zenith pointing radar on its trailer.

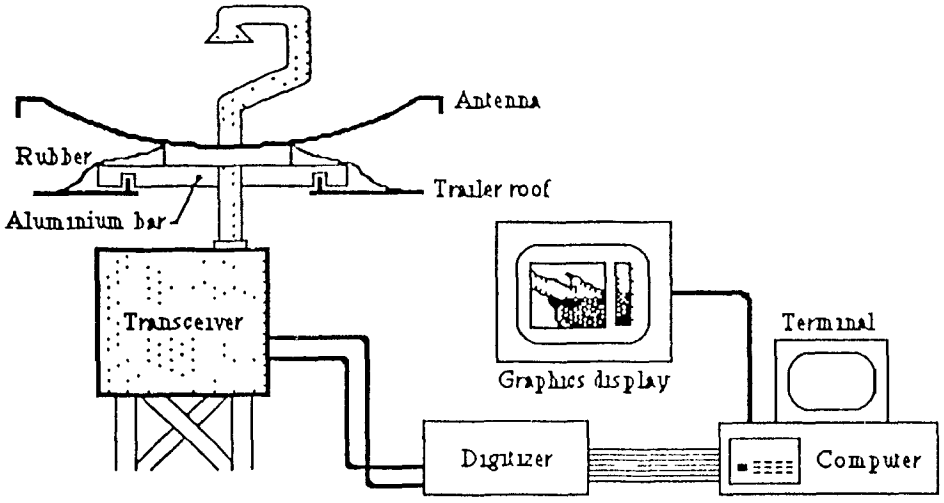

Fig. 2.2 - Sketch of the experimental set-up in the trailer.

The output of the receiver was fed to a digitizer also made previously for the iceberg experiment. It has 6 bit resolution and a sampling rate of 7 MHz which yields an excellent vertical resolution with bins every 21.4 meters. The digitizer was slightly modified and then calibrated so that its input range matched the receiver's output voltages. The returned power data was then sent to a Micro PDP-11 which processed and then archived the data for analysis. The computer also sent the data to a graphics screen which acted as a real time display.

2.2 DATA ARCHIVAL PROGRAM

The archiving program on the PDP-11 was written in assembly language in order to minimize processing time. The program starts by reading the initial parameters such as the number (k) of pulses to be averaged for each final measurement and the frequency of measurements. It then starts executing its main (infinite) loop until stopped by the operator.

The first part of the loop is devoted to the data collection. In order to attempt to reduce the fluctuations in the measurements due to the Observer's Problem (Marshall and Hitschfeld, 1953; Wallace, 1953; Smith, 1964), the program reads k independent pulses of data proportional to the logarithm of the returned power from the digitizer. For all the data sets used in this thesis, k is equal to 20. To further reduce the fluctuations, the program averages the returned power measurements linearly instead of summing their logarithms. In order to do this in real time, an averaging technique was developed and is described in more detail in Appendix A.

The stable returned power values are then converted into reflectivities. The power received (Pr) and the reflectivity (Z) are related by

$$Pr = C\frac{Z}{r^2}$$

where C is a constant which depends on radar parameters and r is the range at which the reflectivity is measured. Since the power received data fed to the computer are proportional to ln(Pr),

$$\ln(Z) = \ln(Pr) + 2\ln(r) - \ln(C)$$

We then obtain reflectivity data proportional to ln(Z), a convenient form for radar meteorology purposes.

The next step in the data processing is to correct the near range values for the attenuation made by the transmit-receive cell. The purpose of the T-R cell is to avoid the situation where the 25 kW transmitter pulse power goes directly to the receiver designed to detect powers 15 orders of magnitude weaker. When the radar is transmitting, the gas in the T-R cell is ionized and this plasma protects the receiver. When the transmission is completed, the gas deionizes but this takes some time and causes a notable attenuation for reflectivities up to about 1.2 km in range. Since after activation the ion population follows a gaussian function and since attenuation is proportional to the number of ions, then

$$Z_{real} = \frac{Z_{mes}}{1 - \exp\left(-\left(\frac{r}{r_{3dB}}\right)^2\right)}$$

where r_{3dB} is the distance corresponding to the time constant of the ion deionization. For this radar, r_{3dB} is about 750 meters. While this correction allowed us to use the data collected at much closer range, it is not perfect. The reflectivity information at a range closer than around 300 meters tended to be unreliable, although the first 150 meters were dominated by ground clutter anyway. After this correction, the data was saved on disk and displayed in real time on a graphics monitor.

2.3 DISPLAY PROGRAMS

Two small communication programs were written to transfer the data from the PDP to IBM PC compatible microcomputers. This was done because the author was more familiar with the latter family of computers and because the tools for data analysis such as language compilers and the computers themselves were more available. A display program was written and allowed any height-time window of the data set to be viewed and to be printed on a laser printer. An example of the output of this program is shown in Figures 2.3 and 2.4. Figure 2.3 shows 14 hours of precipitation associated with the passage of a cold front, giving a synoptic scale picture of the situation. Figure 2.4 on the other hand focuses on a small window in the early part of the event. We can see snow trails starting from "generating cells" and merging further down, giving some information on what is happening in the microscale.

2.4 DATA COLLECTED

The data set collected for this thesis is primarily height-time indicators (HTI) for about half the precipitation events at the radar site from mid-October 1989 until the end

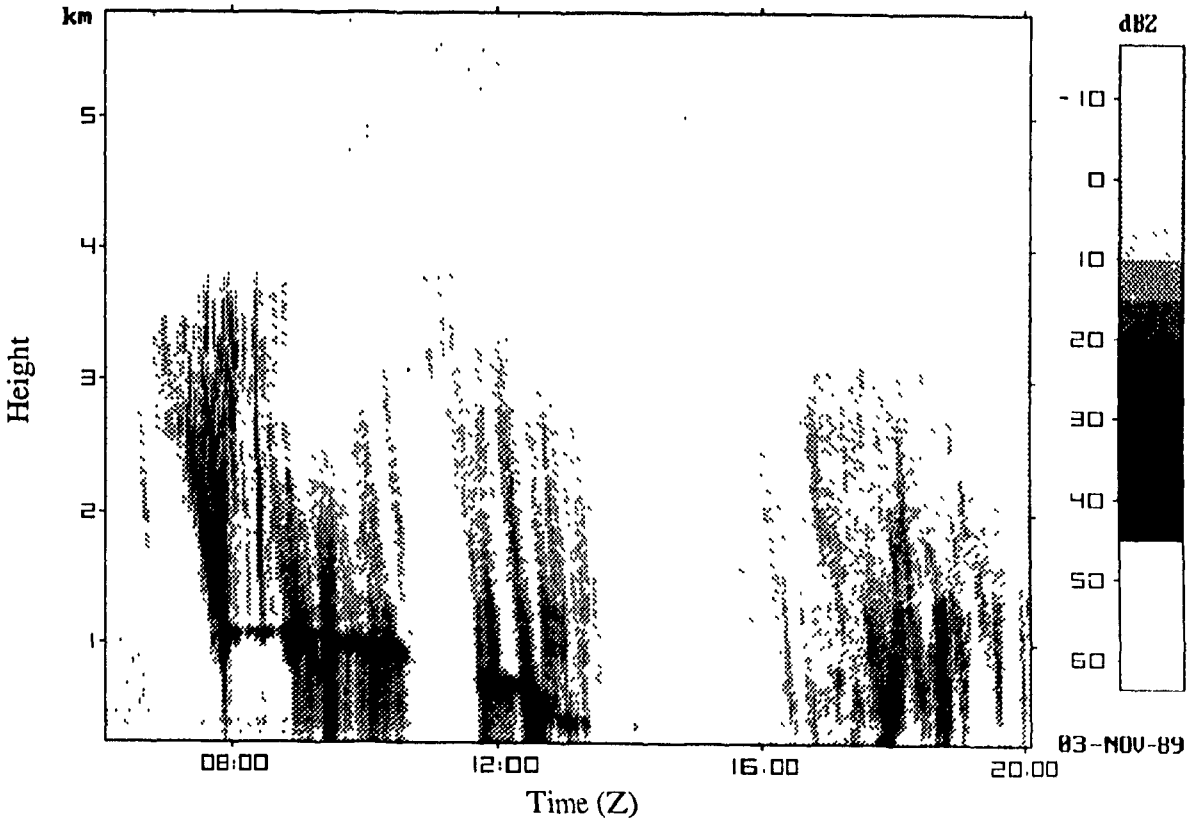

Fig. 2.3 - Height-time indicator of rain changing to snow on November 3rd 1989.

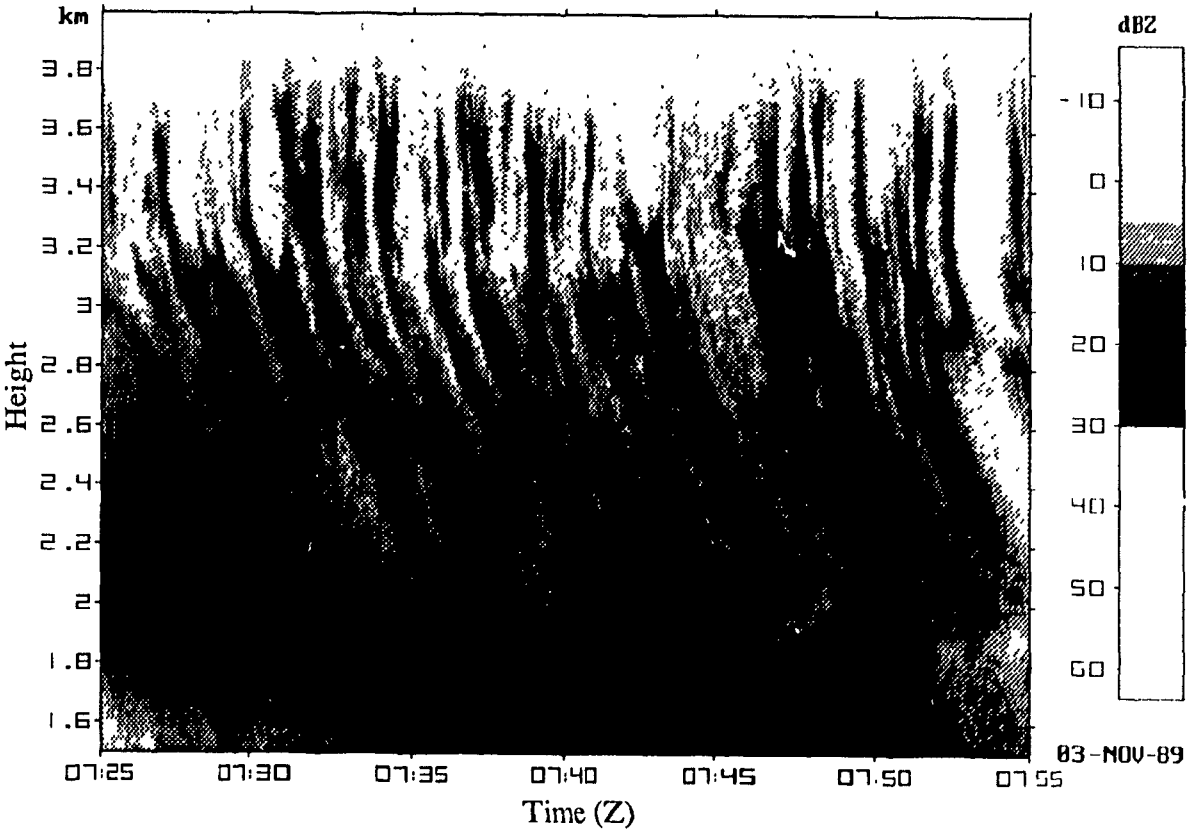

Fig. 2.4 - Close up on the snow formation in the early part of the event.

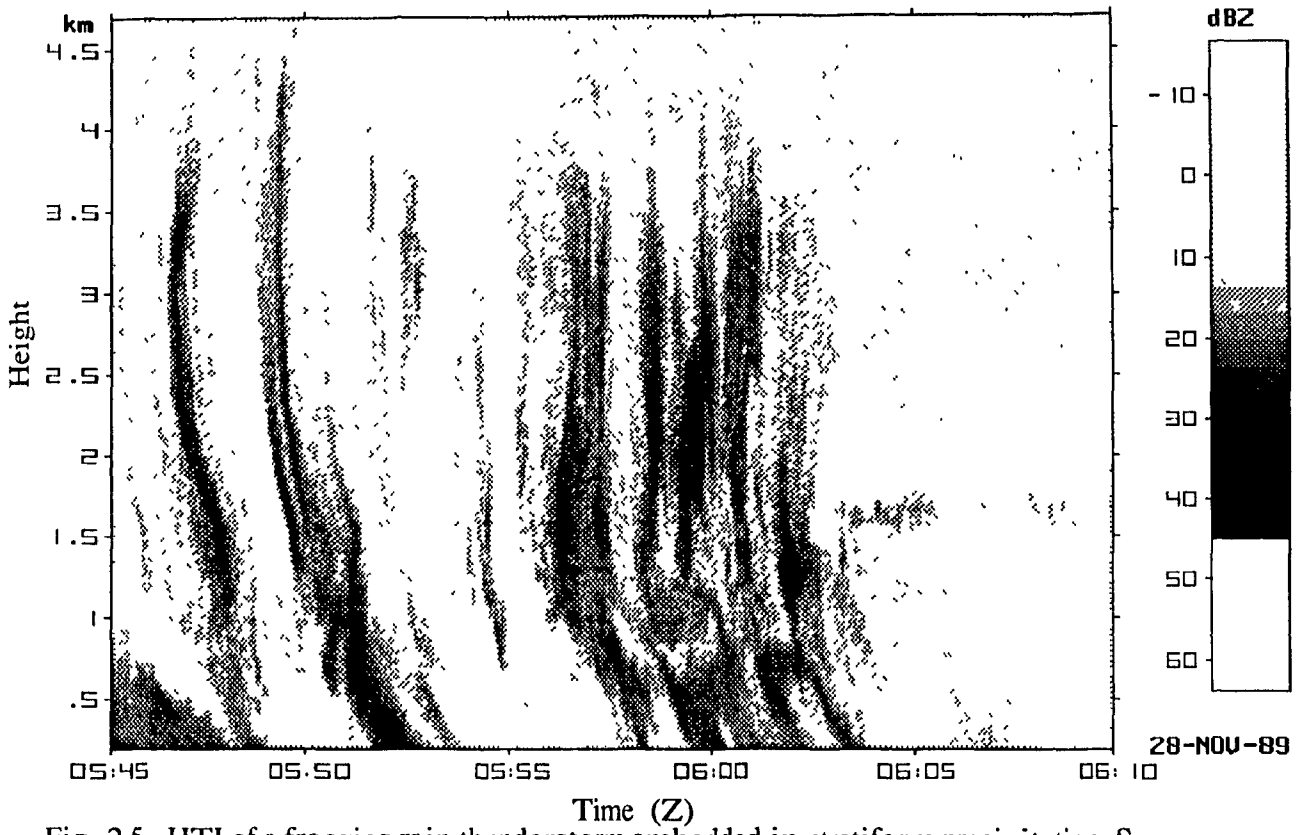

Fig. 2.5 - HTI of a freezing rain thunderstorm embedded in stratiform precipitation. Snow was reported before 5:45 and stratiform freezing rain started at 6:05. The surface temperature was -5°C.

of November 1989 and from the end of March until the end of April 1990. Due to the particularly rainy conditions especially in November, the relatively short collection period is rich in variety, including events from tornado generating convective rain to moderate snowfall and an unusual freezing rain thunderstorm (Fig. 2.5).

3 SIMULATION OF PRECIPITATION ESTIMATES BY RADAR

3.1 SIMULATION

The reflectivities measured by the zenith pointing radar were used as the initial field in a study of the effects of the sampling differences between radar and raingauges. A simulation was developed to estimate the ratio of the precipitation measured by a scanning radar and the surface precipitation as a function of range and of the beam height.

3.1.1 Input data

Most of the previous attempts to evaluate the discrepancies due to the sampling differences between precipitation estimates by radar and measurements by rain gauges were made using model rainfalls or focused primarily on convective precipitation events (Zawadzki, 1984; Chandrasekar and Bringi, 1987; Tees and Austin, 1989; Joss and Waldvogel, 1990). A similar attempt for stratiform precipitation is described in this chapter except that the high resolution reflectivity data obtained by the zenith pointing radar was used instead of a model or average rainfall or snowfall field.

To simulate what the scanning radar would have measured, it is assumed that the reflectivity sequence from the zenith pointing radar occurs over a point located at a distance r from the scanning radar. The four portions of events chosen from the data set collected, together with a description of the type of weather represented, are listed in Table 3.1.

Table 3.1 - Events dates and descriptions

	Date	Time	Shown in	Description
1.	November 9, 1989	9:05- 9:50	Figure 3.1	Low intensity stratiform rain
2.	November 9, 1989	16:50-18:25	Figure 3.3	Moderate stratiform rain
3.	November 16, 1989	16:50-17:25	Figure 3.5	Intense stratiform rain
4.	November 28, 1989	4:20- 5:45	Figure 3.7	Moderate snow

In all cases, the reflectivity of snow increased as it fell from its level of detection. For the first three events, the snow melted around 2 or 3 km giving rise to a region of enhanced radar reflectivity known as the bright band. Below the melting layer, the reflectivity was almost constant down to the ground except for the first event (Figure 3.1) where the reflectivity increased with decreasing height. It should be noted that for that particular event the rain rate enhancement was more significant when the precipitation was weak, suggesting that the observed stratus clouds under the melting layer may have caused raindrops growth by accretion (Austin, 1987).

An important problem is that reflectivity data in four dimensions is usually required for this kind of simulation to properly evaluate the effects of gradients or of attenuation. However, the initial field has only two dimensions, one in space and one in time. To compensate for one of the two missing dimensions, at least two scenarios can be proposed.

In the first scenario, the weather sequence moves towards the radar at a velocity v. Using Taylor's approximation, the time-height data can be converted into range-height data. Then, reflectivity information is present at all distances between the scanning radar

and the point over which rainfall is estimated. This scenario is appropriate for attenuation studies. But there is data only for one azimuth, which makes the estimation of the effects of reflectivity gradients with a widening beam almost impossible.

In the second scenario, the weather sequence moves tangentially to the radar and Taylor's approximation is again used to get data for the dimension perpendicular to the line between the radar and the point studied. This scenario is more suitable for gradient studies but the study of attenuation must then be ignored since there is no data along the radial.

The subject of attenuation has been much discused in the literature (Hitschfeld and Borden, 1954; Atlas, 1964; Medhurst, 1965; Battan, 1973). Furthermore, attenuation studies are not greatly improved by the availability of high resolution data needed for gradient studies. Therefore, the second scenario was chosen for the simulation. For each simulation, the time-height data was transformed into time-distance data using Taylor's approximation. The echo velocity v needed for the transformation was taken from the storm displacement as measured by the McGill operational radar tracking program SHARP (Bellon and Austin, 1978).

In addition, the initial reflectivity field was modified at low levels, typically less than 300 meters, because of the ground clutter contamination and of the inadequacy of the T.R. cell correction described in the previous chapter.

3.1.2 Scanning radar characteristics

The observation of the initial reflectivity field by an horizontally scanning radar is then simulated. The model antenna beam has a pencil beam radiation pattern and consists

of two gaussian lobes. The main lobe has a 1 degree beam and the sidelobe is 0.5 degree wide and located 2 degrees from the main beam with a peak in intensity 40 dB below that of the main lobe. The height of the radar horizon is taken with respect to a hypothetical curved earth of radius $4/3R_{earth}$ (Bean and Dutton, 1968) which accounts for the effects of the earth's curvature and normal refraction of a Standard Atmosphere. The contribution to the reflectivity of weather under the horizon is set to zero. The radar suffers no attenuation for the reasons explained above and has no minimum reflectivity threshold. It is assumed to be in a flat country where no obstacles can reduce its observation capabilities at far range. Time sampling effects (Wilson and Brandes, 1979) are not considered and the sampling interval of the radar is of the order of two seconds.

3.1.3 Radar accumulation computation

The radar accumulations are computed as a function of the range of the target and of the height at which the center of the beam is sampling. For each set of range and height, the weighting function of the model antenna beam is computed. Every time step, a reflectivity is measured by the scanning radar by weighting the height-distance reflectivity data with the antenna pattern function. For the rainfall cases, the reflectivity is converted into a rainfall rate whatever the height at which it has been measured. The rainfall rate at that instant is computed using the Z-R relationship derived from the drop-size distribution measured by Marshall and Palmer (1948)

$$Z = 200R^{1.6}$$

For the snowfall case, the snowfall rate is computed using the Z-R expression of Sekhon and Srivastava (1970):

$$Z = 1780R^{2.21}$$

An accumulation is finally computed by summing the contribution from each time step.

3.1.4 Gauge accumulation computation

Surface rainfall measurements cannot be used as ground truth for the evaluation of gauge-radar sampling differences because other sources of errors such as variations in the Z-R relationships or errors in measuring the initial radar reflectivity factor would influence the final result (Wilson and Brandes, 1979). The surface rainfall estimation must then come from the initial reflectivity field itself. To compute a simulated gauge accumulation, all the reflectivity measurements taken at 300 meters by the zenith pointing radar were converted into instantaneous rainfall or snowfall rates using the Z-R relationships described above. The rainfall rates were then integrated to obtain the surface accumulations.

3.2 RESULTS

The results of this simulation for each event are shown as contour plots in Figures 3.2, 3.4, 3.6 and 3.8. These figures show the ratio between the radar and gauge estimated accumulations (ER/EG).

3.2.1 Stratiform rainfall cases

The first three cases, which correspond to rainfall events, have at least three features in common. First, the bright band which is between 2 to 3 km for the 3 events significantly affects the estimation of rainfall. When only the bright band is sampled, the rainfall can be overestimated by a factor 4.5 at near range (Fig. 3.4, just above 2 km). Its

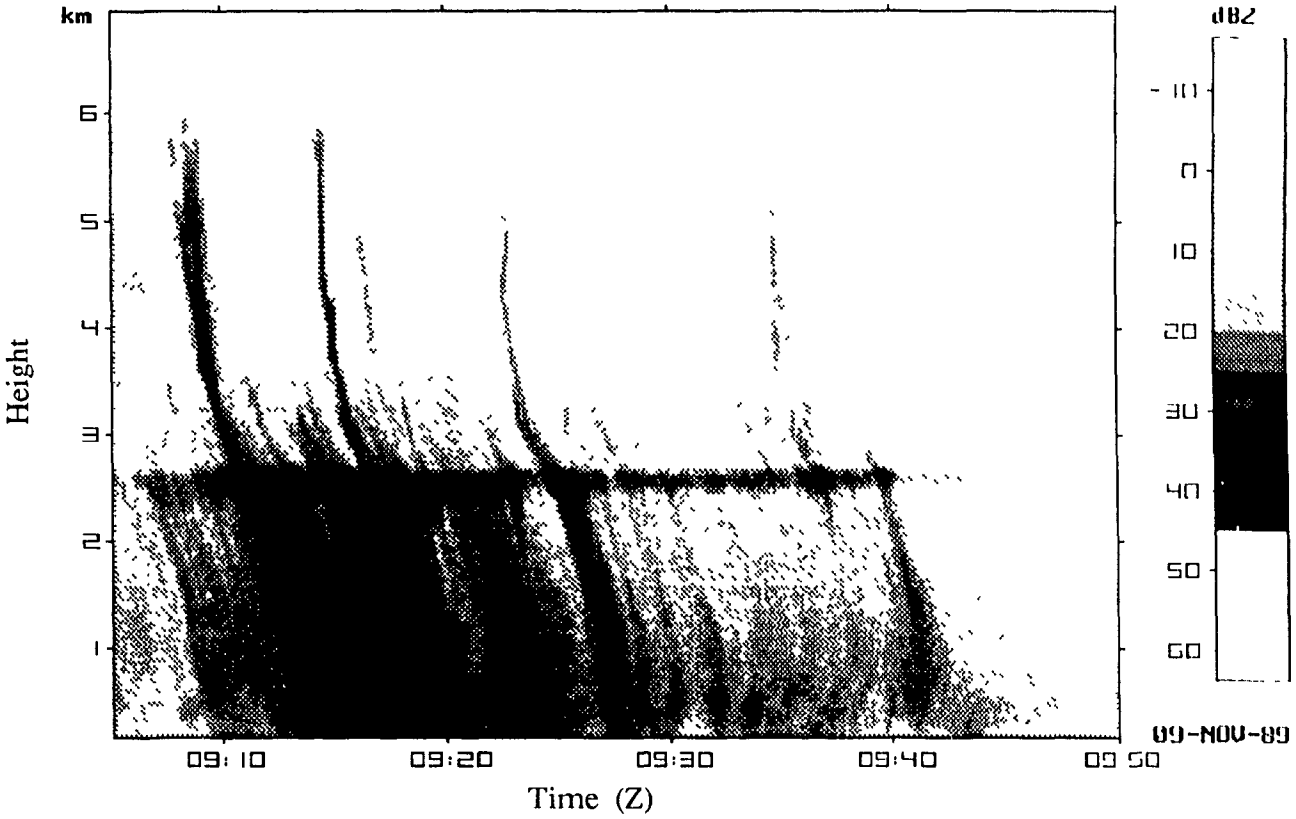

Fig. 3.1 - HTI of a light rainfall event.

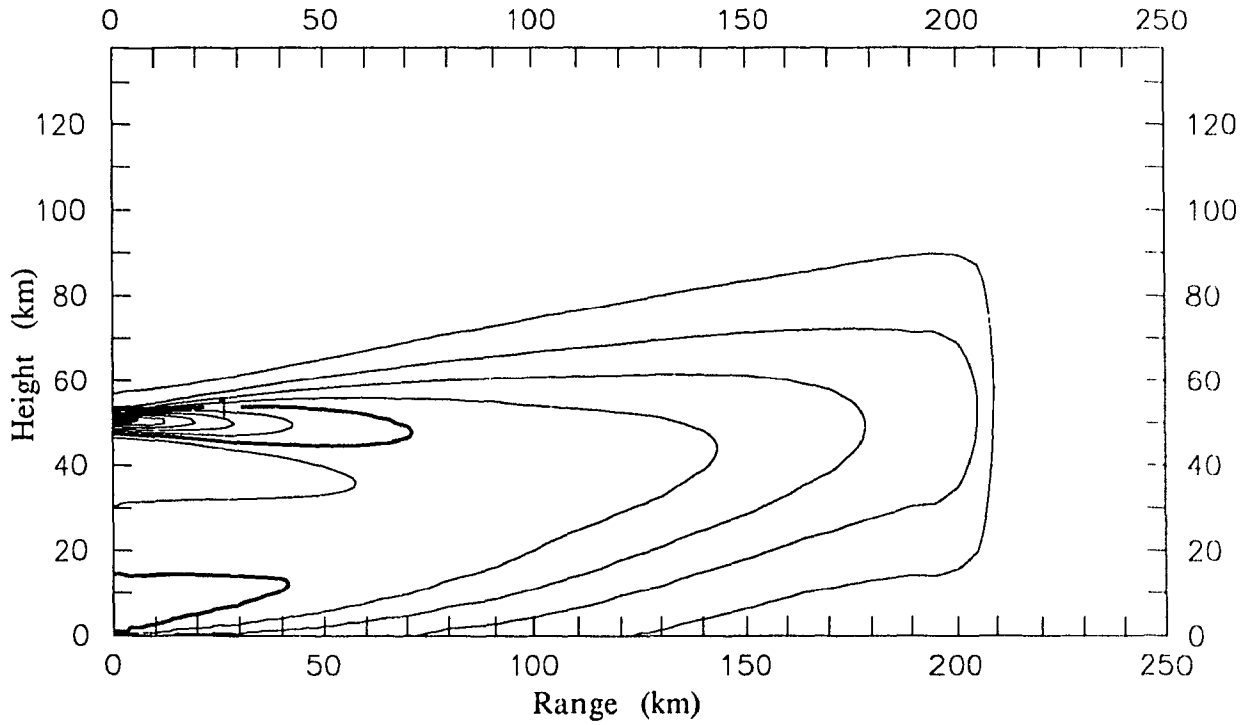

Fig. 3.2 - Contour plot of the ratio of the radar estimated rainfall and of the surface rainfall as a function of range and height pointed by the beam axis for the event shown above. The contour interval is 0.2. Dark contour interval is 1.

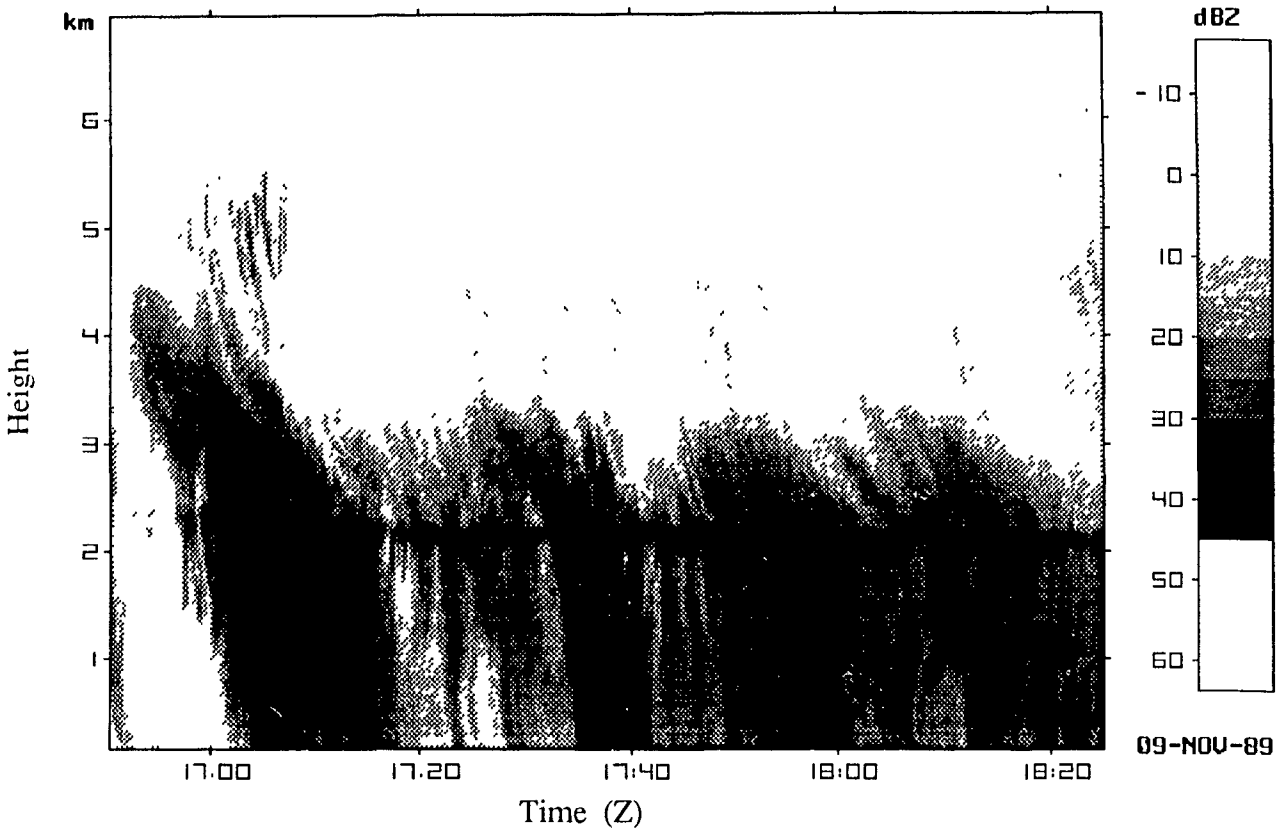

Fig. 3.3 - HTI of a moderate rainfall event.

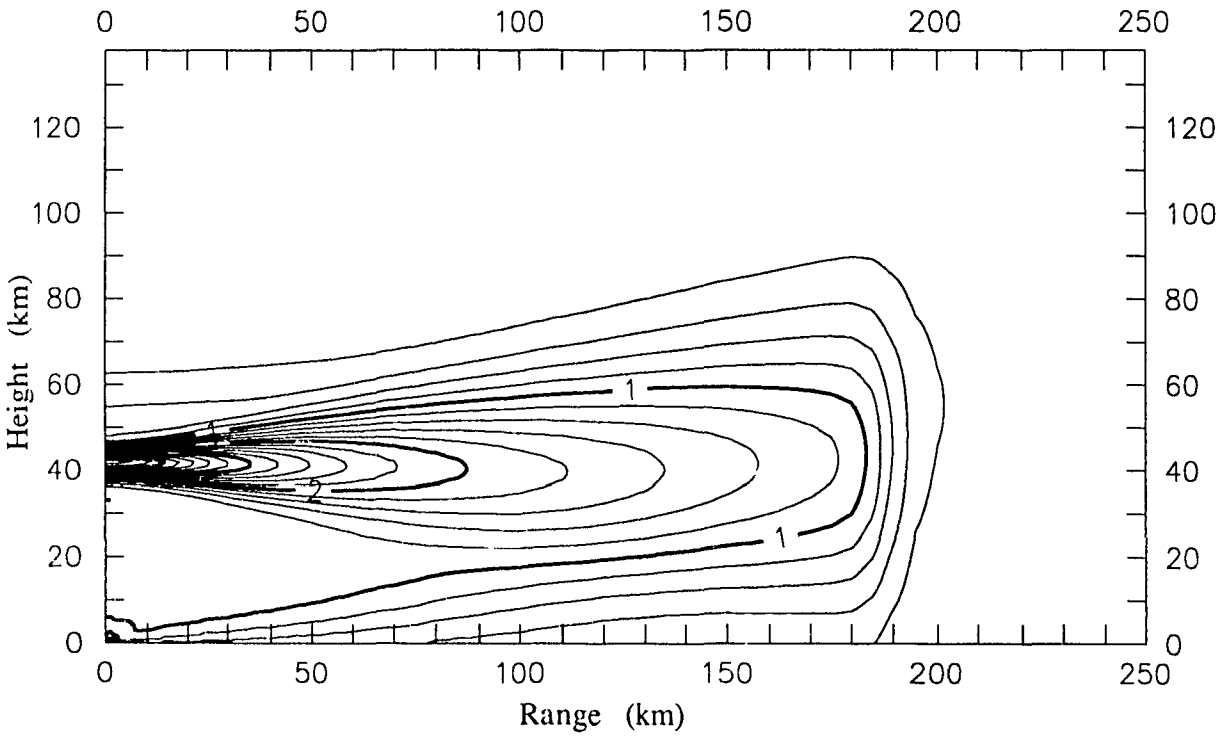

Fig. 3.4 - Same as Fig. 3.2 but for the event shown above.

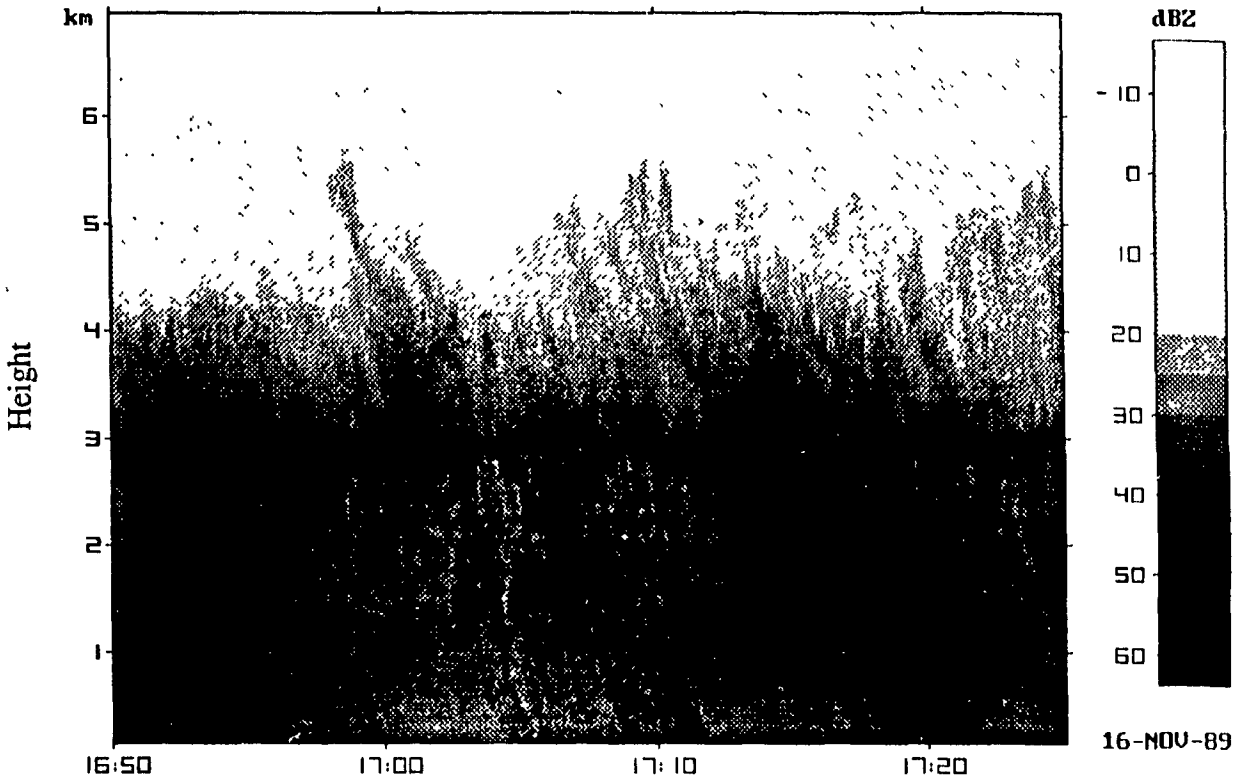

Fig. 3.5 - HTI of a strong rainfall event.

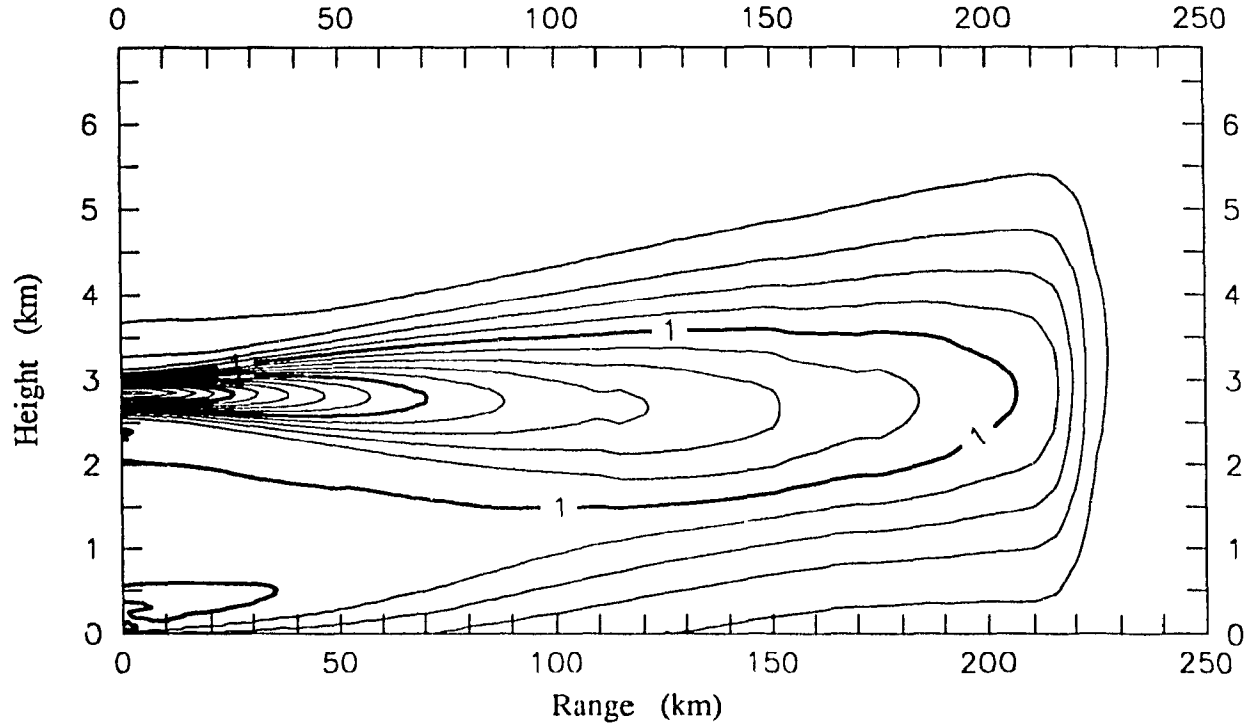

Fig. 3.6 - Same as Fig. 3.2 but for the event shown above.

influence weakens with range but spreads in heights as shown by the torch-like shape of the rainfall estimation contours around the height of the bright band. This feature is less obvious in the first case where precipitation increases significantly under the bright band and where the enhancing effect of the bright band is moderated by the relatively weak precipitation at that level.

The second common feature is the increase in height with range of the lowest contour. As shown by Donaldson (1964) for convective rainfall, this effect translates in the apparent increase of the echo tops as a function of range. This is due to the widening of the beam with range. As the beam widens, it will sample reflectivities from a broadening range of heights. Hence, even if the center of the beam is above the precipitation, the radar will still measure a reflectivity due to the precipitation located in the bottom part of the beam.

The third obvious feature is the very strong drop in the estimates at a range of about 200 km. This sharp decrease in rainfall estimation occurs when the radar horizon, or the height that the beam would reach if it was at an elevation angle of 0 degree, reaches a level close to the bright band height. Beyond this range, the beam can only sample snow with weak reflectivities since the strong rain and bright band are now under the horizon. Therefore, the range of the sudden drop tends to be greater when the bright band is higher, a feature clearly visible when comparing the second event (Figure 3.4, 2.2 km bright band, range of drop at 185 km) with the third (Figure 3.6, 2.9 km bright band, range of drop at 215 km). The range at which the height of the radar horizon corresponds to the height of the melting layer can be computed:

$$r = \sqrt{4/3 \times 2hR_{earth} + h^2}$$

where r is the range and h is the height of the melting layer. Beyond that range any attempt to obtain quantitative rainfall estimates is extremely difficult. Furthermore this range is an upper bound to the maximum useful range for all elevation angle combinations: whether PPIs, CAPPIs or others are used, the maximum useful range will always be less or equal to r.

Another important consideration in obtaining good rainfall estimates is the elevation angle combination which must carefully avoid the bright band as much as possible. That is, there must be an appreciable distance between the bright band and the height at which reflectivities are measured. Being just under the bright band is not good enough because the effect of the bright band broadens with increasing range. For example, in the second event, the bright band is around 2.2 km. Measuring reflectivities at 1.5 km, some distance away from the bright band, at 100 km range would have still led to a 60% overestimation of the rainfall accumulation (Figure 3.4). Measuring reflectivities at too low a level is not a solution either because ground echoes contaminate the rainfall measurement and screen the radar beam at further range. Estimating bright band height in real time becomes essential in order to assess the quality of the real time rainfall estimates However when the bright band is too low, good rainfall estimates are impossible without trying to correct for its effect, a difficult task achieved with some success by the British Meteorological Office (Smith, 1986).

It is interesting to compare the results of the first and second simulations which use data only 8 hours apart. The two portions of events are apparently similar, both being

stratiform and having their bright band between 2 and 2.5 km. However, the contours of ER/EG changes dramatically at all ranges. Some investigators proposed a range dependent Z-R relationship based on climatological rainfall statistics to correct the variations of reflectivity with range. If such correction would have worked for one event, it would have been inappropriate eight hours later. Things can get worse if the bright band changes height as it was the case an hour after the second event (Fig. 4.5). Hence range corrections based on climatological data like the range dependent Z-R relationships proposed by Calheiros and Zawadzki (1987) or Atlas et al. (1989) are likely to give spurious corrections. This is especially true for stratiform precipitation where the vertical reflectivity profile can change drastically from one event (Fig. 3.1 and 3.3) to another (Fig. 2.3) a few days apart and even within events. Therefore any range correction of radar data should be based on information about the storm itself rather than on statistical methods.

The bright band height and the elevation angle combination used are then two important parameters affecting the quality of stratiform rainfall estimation. The evaluation of the performance of some elevation angle programs for case study 3 and 4 will be presented in section 3.3.

3.2.2 Snowfall event case

The problems related to accurate snowfall estimation are different than those for rainfall primarily because of the absence of the bright band. Instead of reaching a strong maximum at some height, the snow reflectivity profile tends to decrease with height (Figure 3.7). Hence, measured snowfall amounts decrease as the height of the observation increases. There is no sudden drop at a certain range but a gradual decrease in the

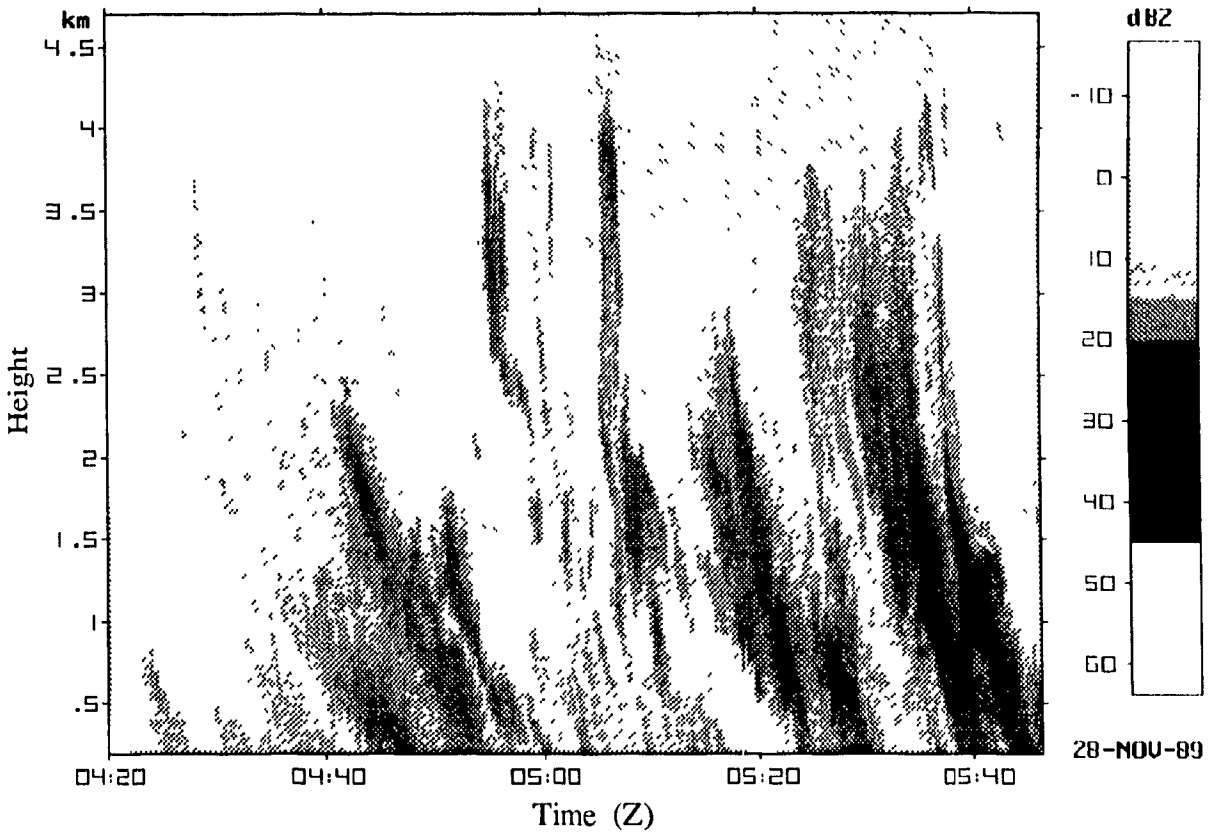

Fig. 3.7 - HTI of a moderate snowfall event.

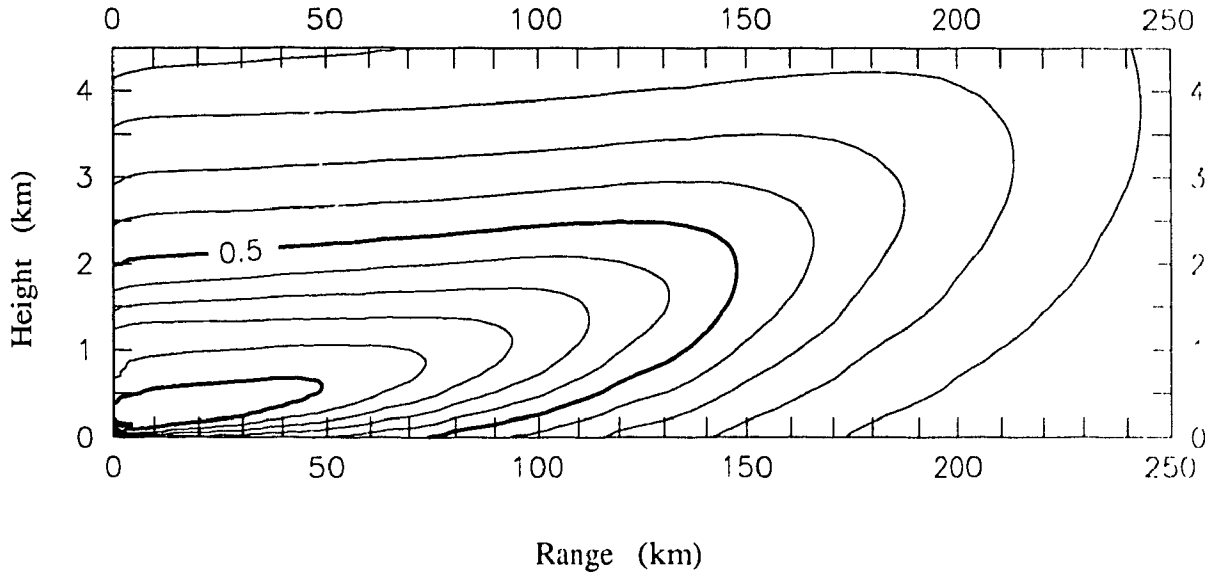

Fig. 3.8 - Contour plot of the ratio of the radar estimated snowfall and of the surface snowfall as a function of range and height pointed by the beam axis for the event shown above. The contour interval is 0.1. Dark contour interval is 0.5.

accuracy of the accumulation measurement (Figure 3.8). On the basis of this one case analyzed, the maximum range of accurate snowfall estimation is of the order of 70 km, which is much smaller than for the rainfall cases (200 km).

Since the reflectivity of snow decreases regularly with height, an horizontal stratification of the snowfall estimation contours can be observed: at close and medium range, ER/EG contours are roughly horizontal. However the range at which this stratification extends is a function of height: the higher the estimation is made, the further in range the bias of the estimation remains nearly constant. If an estimation of the snowfall accumulation is made at constant altitude between 1 and 3 km, it will be biased by the same amount for a range much longer than 70 km. Therefore, if the estimates are corrected by snow gauges measurements, the range of accurate snow accumulations could be extended by measuring the snowfall at a constant altitude above the surface. However, local low level orographic enhancement may render this task very difficult.

Snow echoes are weak. Therefore another problem not simulated might cause a problem for snowfall accumulation: the reflectivity might be under the detectability threshold. Since reflectivity decreases with height, it sets a constraint similar to that for the rainfall cases: in order to obtain good precipitation estimates, the radar must measure reflectivities at a low altitude, but still sufficiently high to avoid ground clutter problems. Here again the choice of a good elevation angle program for the scanning radar is critical.

3.3 PERFORMANCE OF DIFFERENT ELEVATION ANGLE PROGRAMS

The results of the simulations described in the previous paragraphs are difficult to use to estimate directly to what extent a radar using a given elevation angle combination

would have performed for any of these events. They are however very useful as a database on which several scenarios can be tried. This can be done by computing the height h at which the radar beam is pointing at range r. Then the ER/EG value at the (r,h) coordinate can be retrieved. This procedure was done for the third rainfall event and the snow event using three elevation angle combinations: a 0.5 degree PPI and two 1.5 km CAPPIs, one made with 4 elevation angles (0.5, 1.5, 2.5 and 4 degrees) and one with 24 (like the McGill radar, with angles listed in table 3.2 (Marshall and Ballantyne, 1975)).

Table 3.2 - Mc Gill radar elevation angles (deg)

#	Elevation	#	Elevation	#	Elevation	#	Elevation
1	0.3	2	0.5	3	0.7	4	0.9
5	1.1	6	1.4	7	1.8	8	2.2
9	2.7	10	3.4	11	4.1	12	4.9
13	5.9	14	7.1	15	8.6	16	10 3
17	12.3	18	14.6	19	17.2	20	20.3
21	23.8	22	27.7	23	32.1	24	34.4

The results for the rainfall event are shown in Figure 3.9 to 3.14. Figure 3.9, 3.11 and 3.13 show the result of the rainfall estimate simulation as in Figure 3.6 over which are plotted the 3 elevation angle combinations. Figure 3.10, 3.12 and 3.14 show the ratio of the measured over the real rainfall accumulation as a function of range. All three

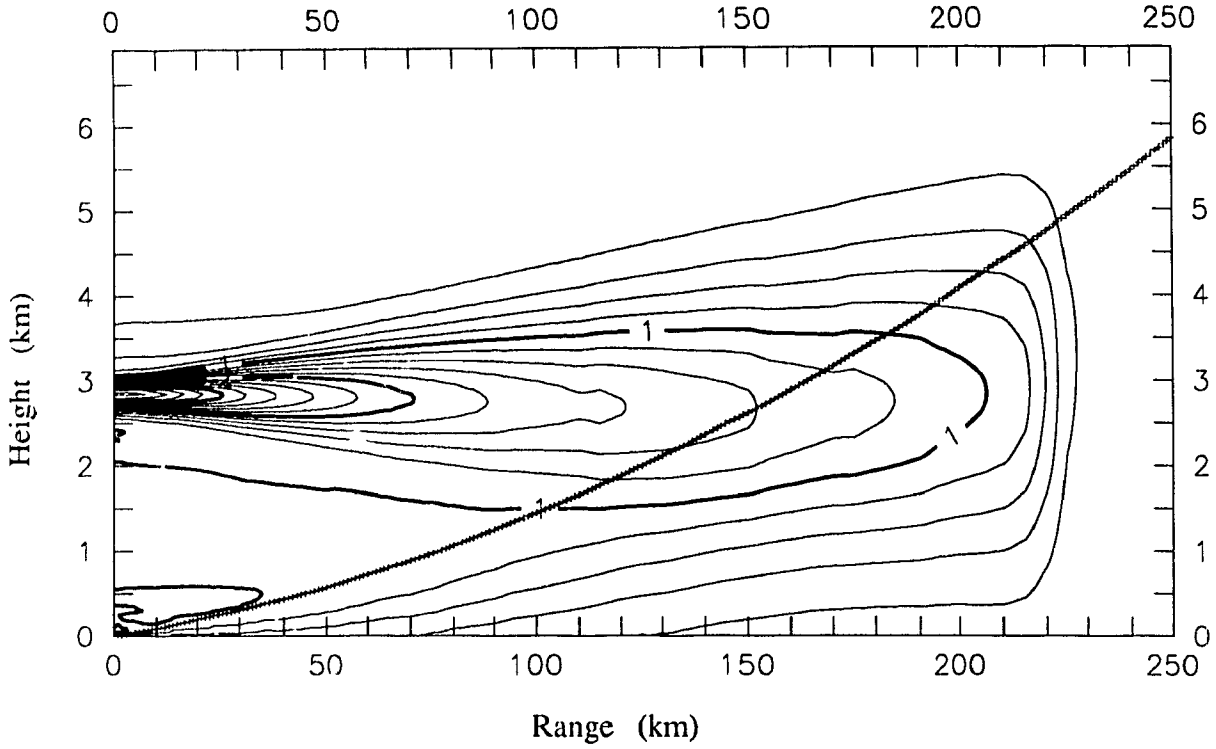

Fig. 3.9 - Results of the strong stratiform rainfall simulation over which is overlaid the height of a 0.5° PPI as a function of range.

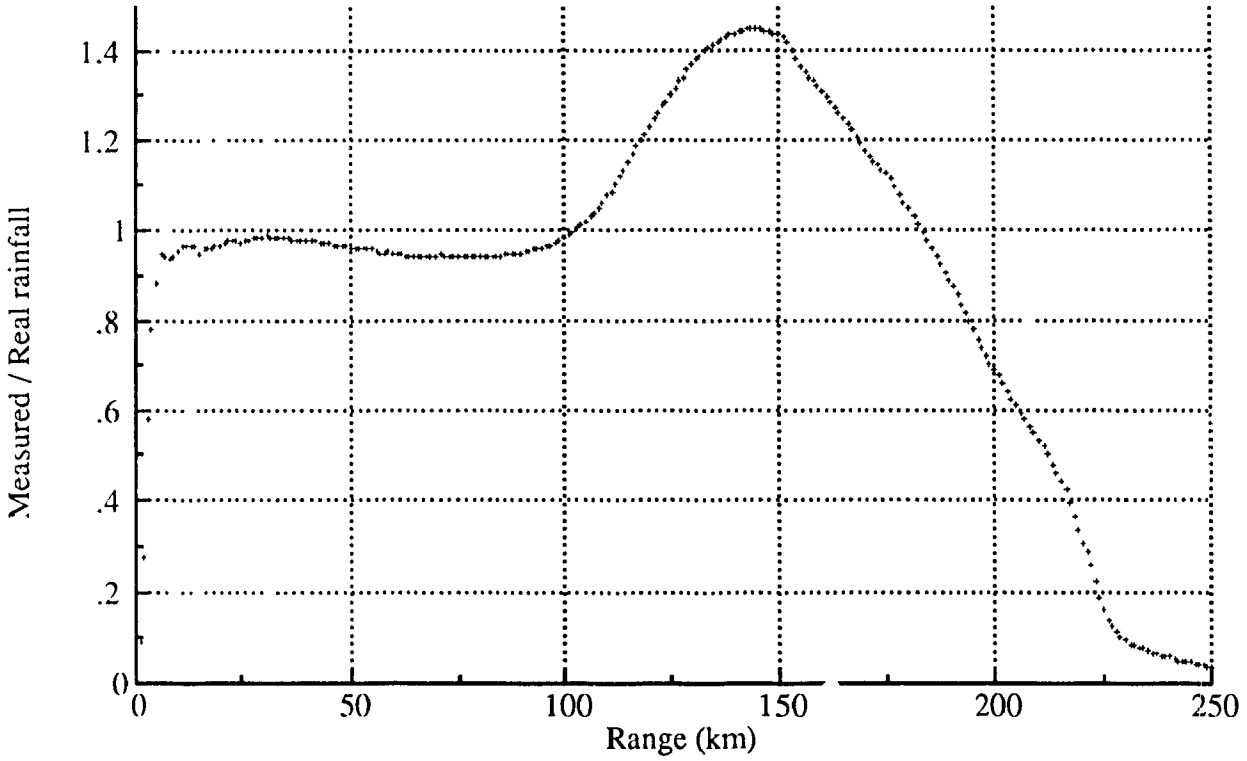

Fig. 3.10 - Ratio of the radar estimated rainfall and of the surface rainfall for the strong stratiform event if a 0.5° PPI is used.

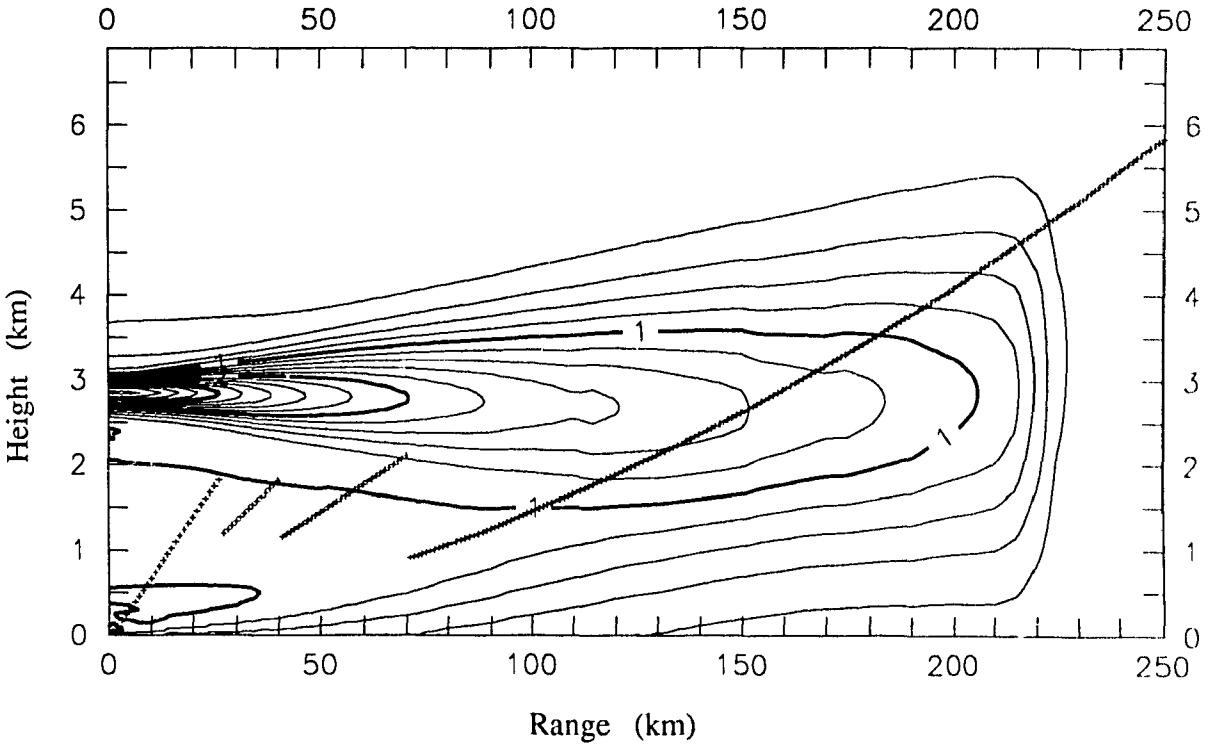

Fig. 3.11 - Results of the strong stratiform rainfall simulation over which is overlaid the height used by the 4 elevation angle 1.5 km CAPPI.

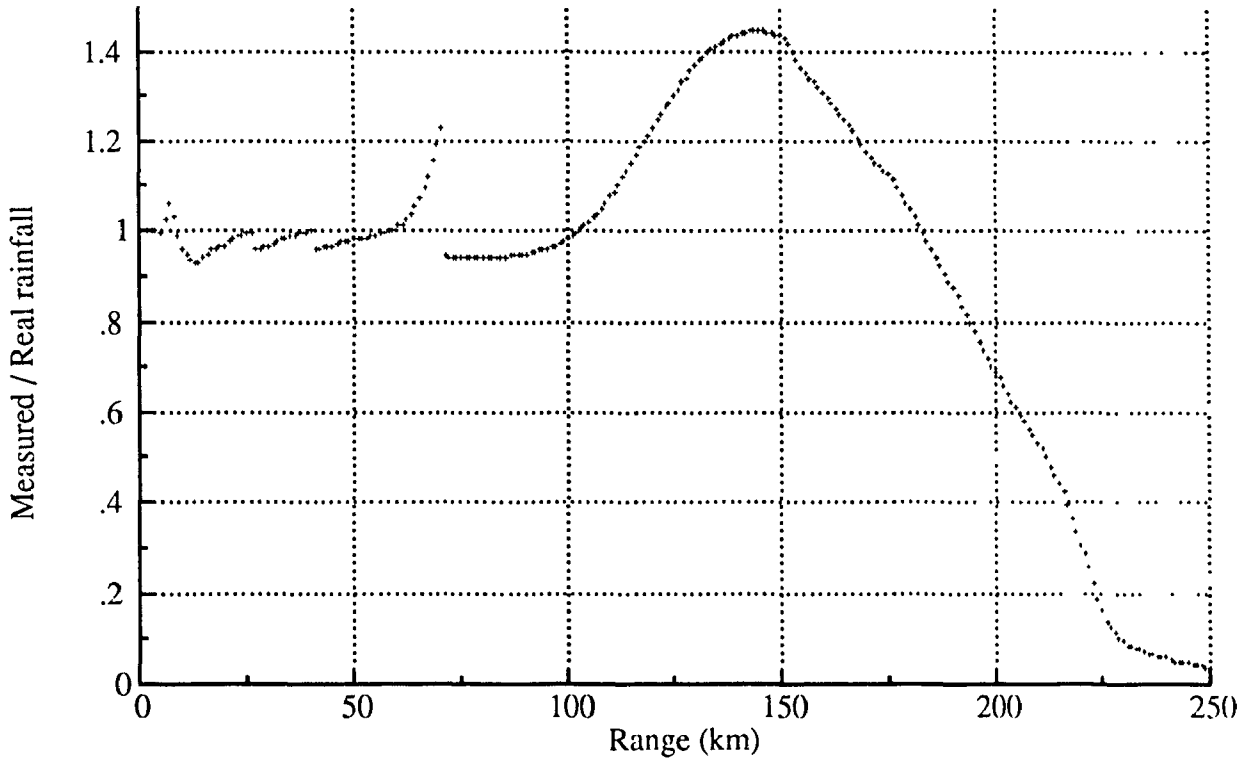

Fig. 3.12 - Ratio of the radar estimated rainfall and of the surface rainfall for the strong stratiform event if the 4 elevation angle CAPPI is used.

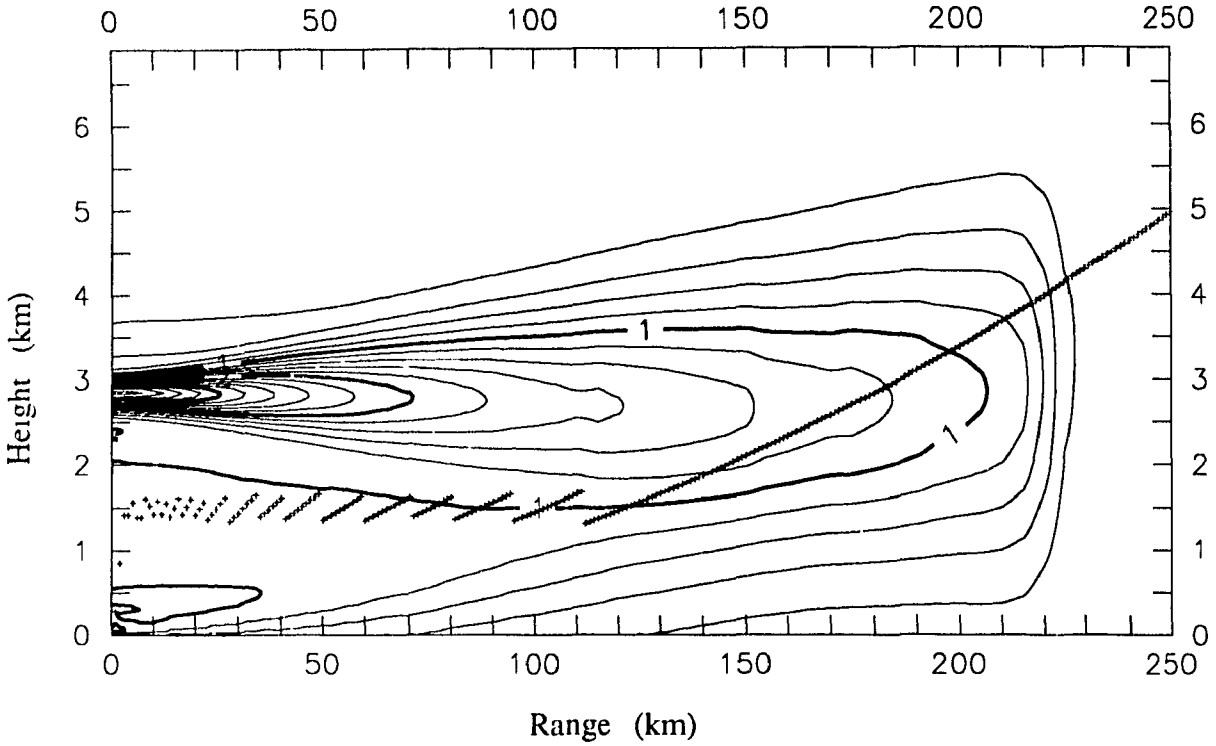

Fig. 3.13 - Results of the strong stratiform rainfall simulation over which is overlaid the height used by the 24 elevation angle 1.5 km CAPPI.

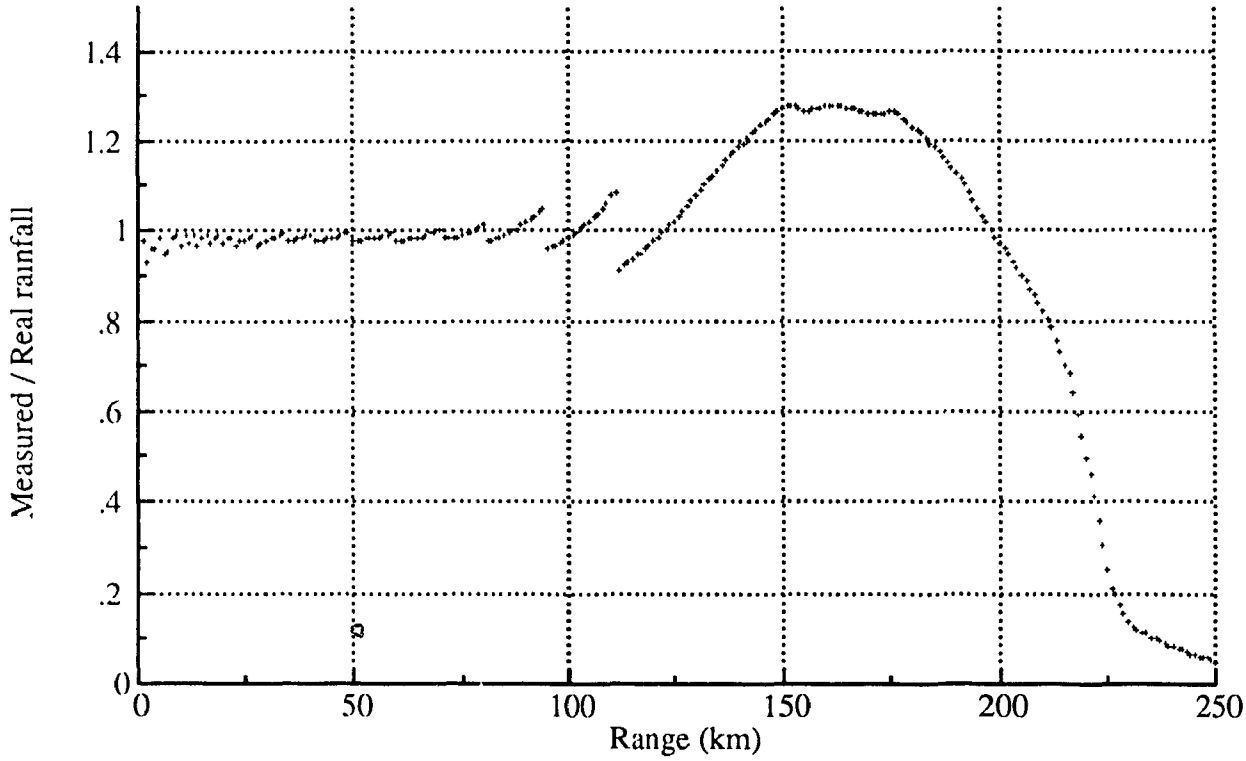

Fig. 3.14 - Ratio of the radar estimated rainfall and of the surface rainfall for the strong stratiform event if the 24 elevation angle CAPPI is used.

elevation angle combinations perform relatively well at short range. As the range is increased, the radar first overestimate the precipitation as the height of the observation traverses the bright band. Then the rainfall is underestimated as more and more snow fill the beam. Around 220 km, ER/EG quickly decrease as the range of sudden drop is reached. The first two elevation angle combinations are comparable in quality. At short range, the 4 elevation CAPPI is worse than the PPI mainly because the second angle penetrates too far into the zone of influence of the bright band. Both are equally accurate up to 110 km where the bright band begins to affect the rainfall estimates. Beyond 145 km where both elevation angle combinations overestimate the rainfall by more than 40%, the estimates decrease steadily up to 225 km. Even if the simulation shows similar performance, it should be noted that the estimations from the PPI are more likely to be contaminated by ground echoes than the CAPPIs. The 24 elevation angle CAPPI performs better by getting accurate rainfall estimates up to 130 km, and the overestimation due to the bright band is always less than 30%. The estimates are generally better up to 220 km where they quickly drop because from there on the beam only samples low reflectivity snow.

The results of the elevation programs test for the snowfall event are shown in Figures 3.15 to 3.20. Since snow decreases with height and the height of the PPI increases continuously with range, the snowfall estimates show a decrease with range. These are accurate up to 60 km from where they decrease steadily (Figure 3.16). This behavior is consistent with the measurements made by Jatila (1973; see also Wilson, 1976). The snowfall estimations from the four elevation based CAPPI are not accurate at any range and make several jumps each time a change in elevation is made (Figure 3.18). The 24 elevation CAPPI shows more interesting results. There is a systematic

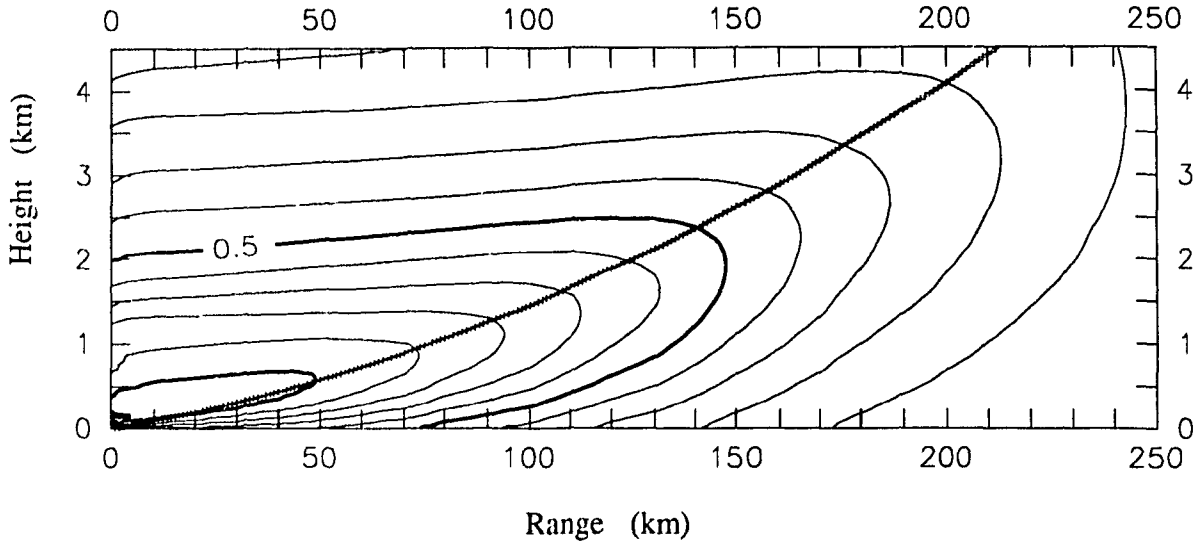

Fig. 3.15 - Results of the moderate snowfall simulation over which is overlaid the height of a 0.5° PPI as a function of range.

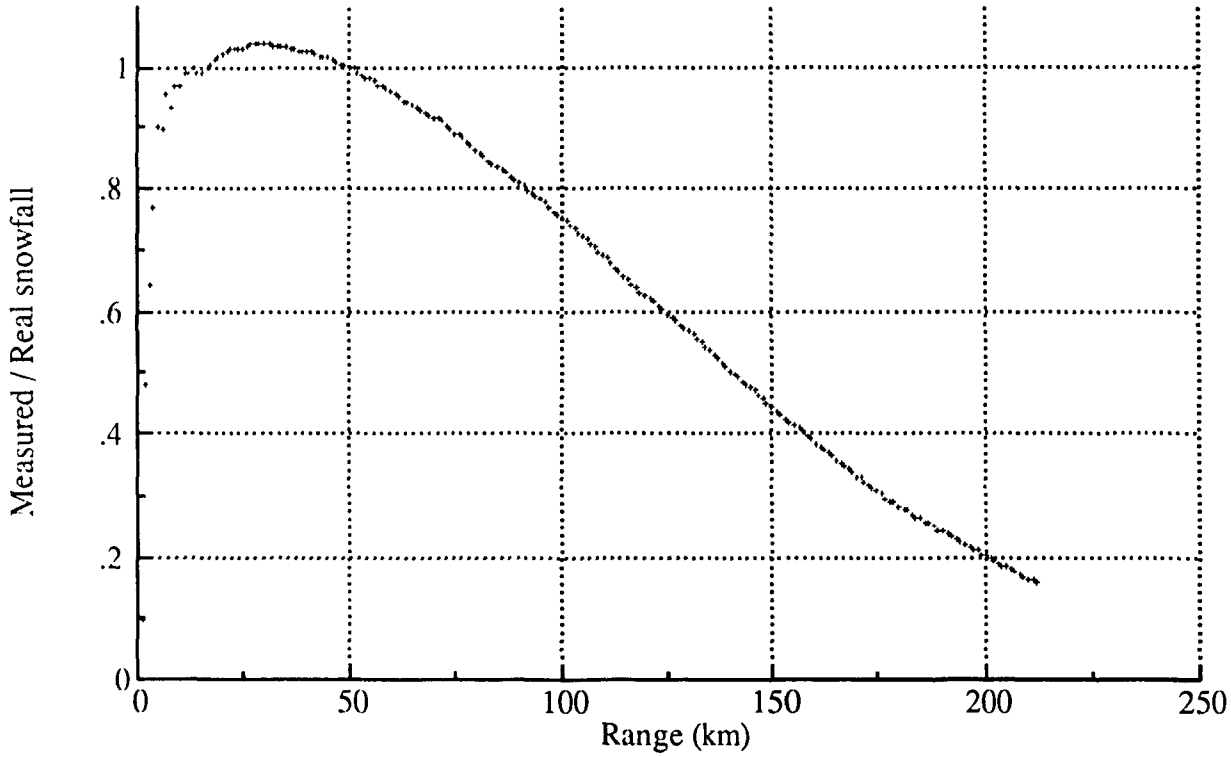

Fig. 3.16 - Ratio of the radar estimated snowfall and of the surface snowfall for the moderate snowfall event if a 0.5° PPI is used.

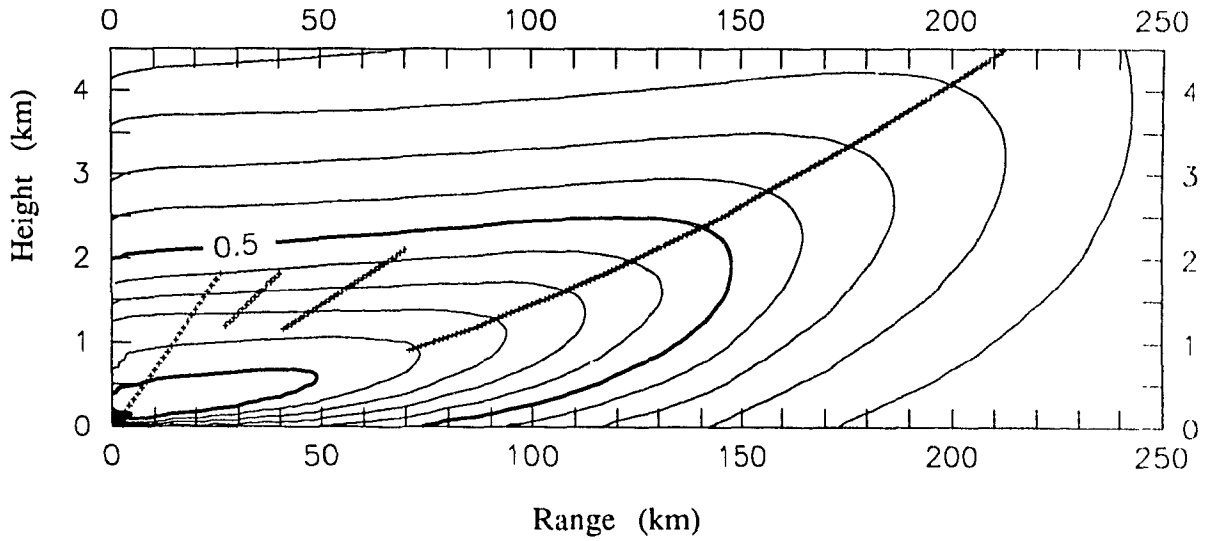

Fig. 3.17 - Results of the moderate snowfall simulation over which is overlaid the height used by the 4 elevation angle 1.5 km CAPPI.

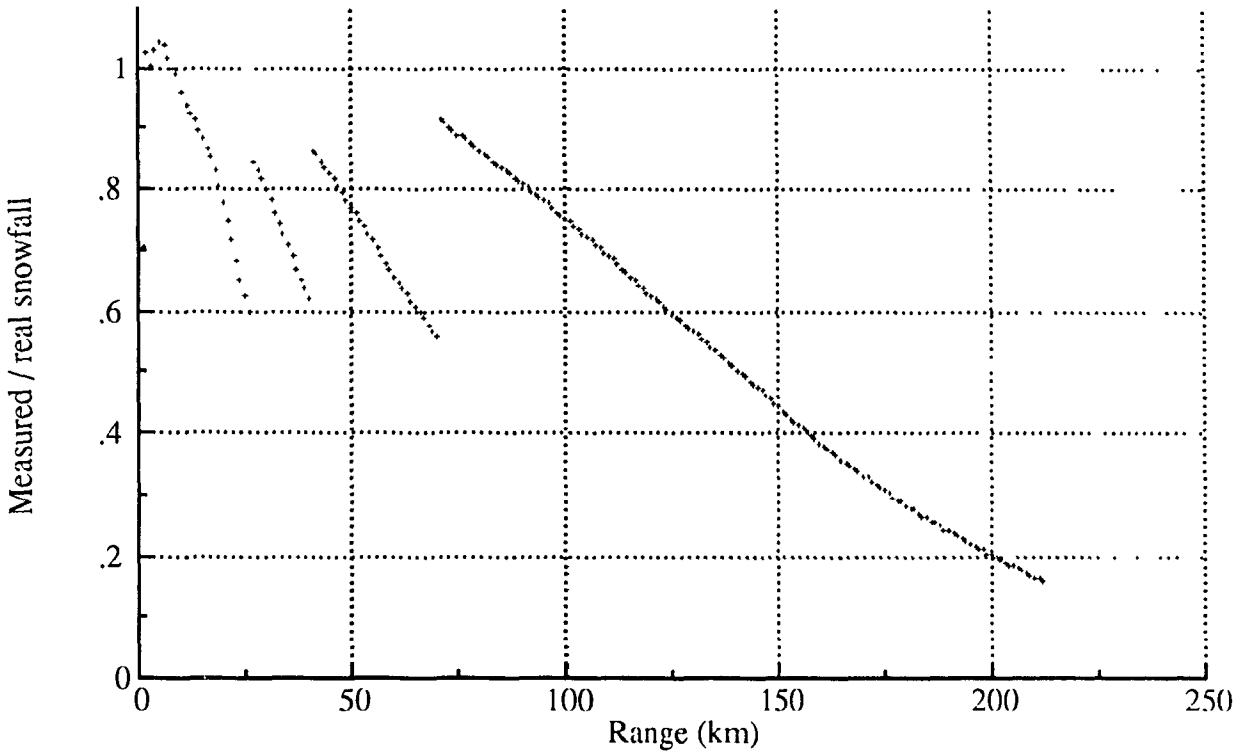

Fig. 3.18 - Ratio of the radar estimated snowfall and of the surface snowfall for the moderate snowfall event if the 4 elevation angle CAPPI is used.

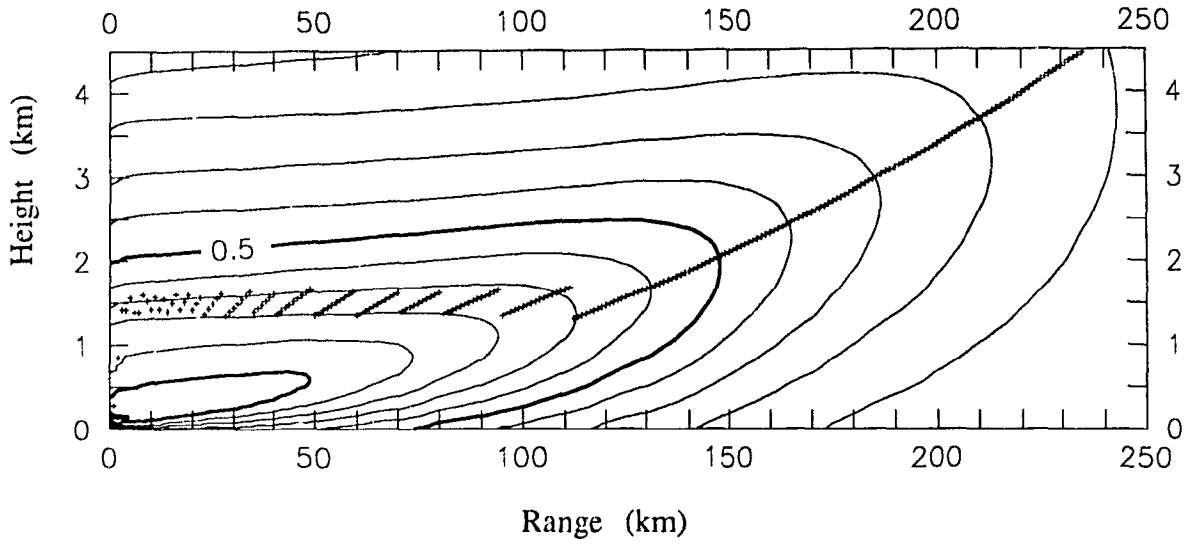

Fig. 3.19 - Results of the moderate snowfall simulation over which is overlaid the height used by the 24 elevation angle 1.5 km CAPPI.

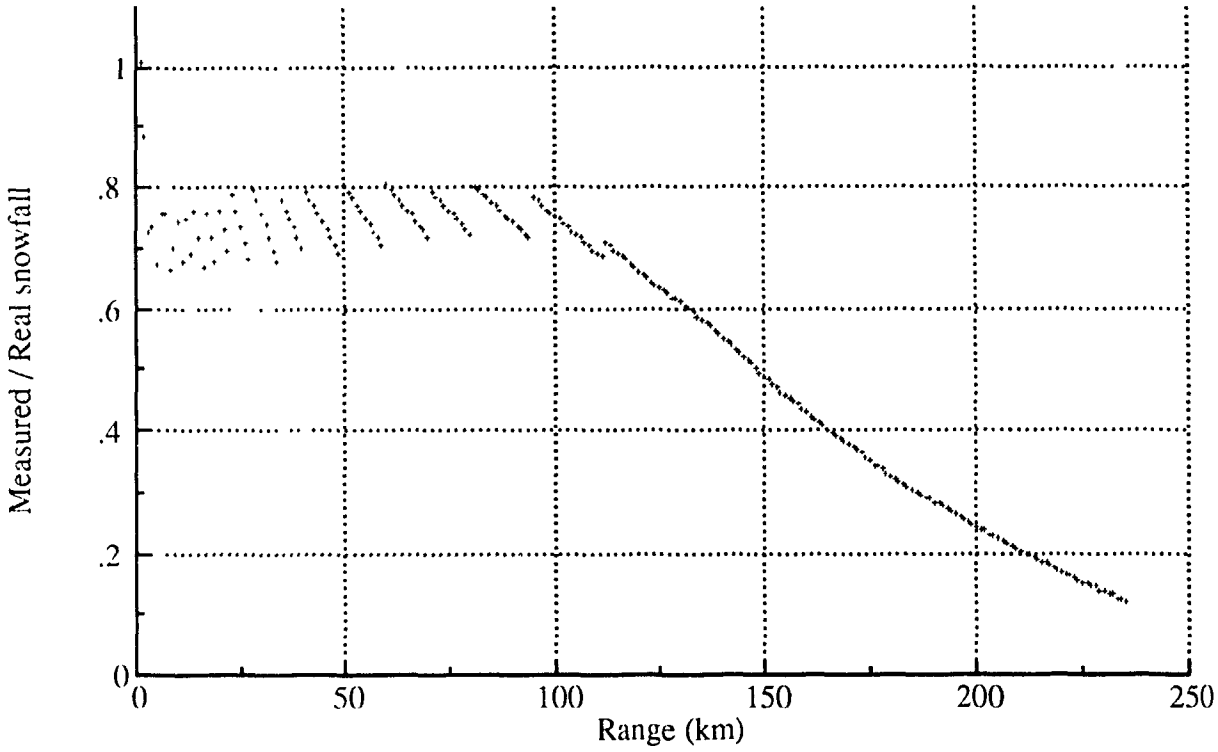

Fig. 3.20 - Ratio of the radar estimated snowfall and of the surface snowfall for the moderate snowfall event if the 24 elevation angle CAPPI is used.

underestimation by 25% up to 110 km. Beyond this range, the magnitude of the measurements decrease steadily (Figure 3.20). Since the underestimation within 110 km is constant, the radar can be calibrated with snowgauges and accurate snowfall estimates could be obtained up to range nearly two times greater than for the PPI (Carlson and Marshall, 1972).

The main advantage of using a CAPPI is to avoid the presence of ground echoes at close range. Furthermore, it leads to superior precipitation estimates with extended range if the number of elevation angles is sufficient. If the number of angles is too small, the quality of the precipitation estimates will suffer.

4 EFFECTS OF NON UNIFORM REFLECTIVITY IN THE BEAM ON ESTIMATES OF STRATIFORM PRECIPITATION

Non uniform reflectivity in the radar beam is one of the causes of disagreement between radar derived and rain gauge accumulations. In stratiform precipitation, the three main causes of these non uniformities are the bright band for rain, the incompletely filled beam for snow and the horizontal and vertical reflectivity gradients for both. Each of these causes and their effects on radar derived precipitation estimates are studied more closely in this chapter.

4.1 BRIGHT BAND IN RAIN EVENTS

The simulations in the previous chapter have shown that the bright band is the main cause of bias in rainfall estimations at short and medium range. The reflectivity enhancement corresponds to the region just under the 0°C isotherm where snowflakes melt into raindrops. The peak in reflectivity separates a region of weak reflectivities above corresponding to solid precipitation from a region of stronger reflectivity below corresponding to rain (Austin and Bémis, 1950; Battan, 1973; Sauvageot, 1982). A typical vertical reflectivity profile using data from the zenith pointing radar is shown in Figure 4.1. However, the bright band shape, strength and thickness vary considerably from storm to storm and even within storms (Waldvogel and Steiner, 1986; Figure 4.2 and 4.5).

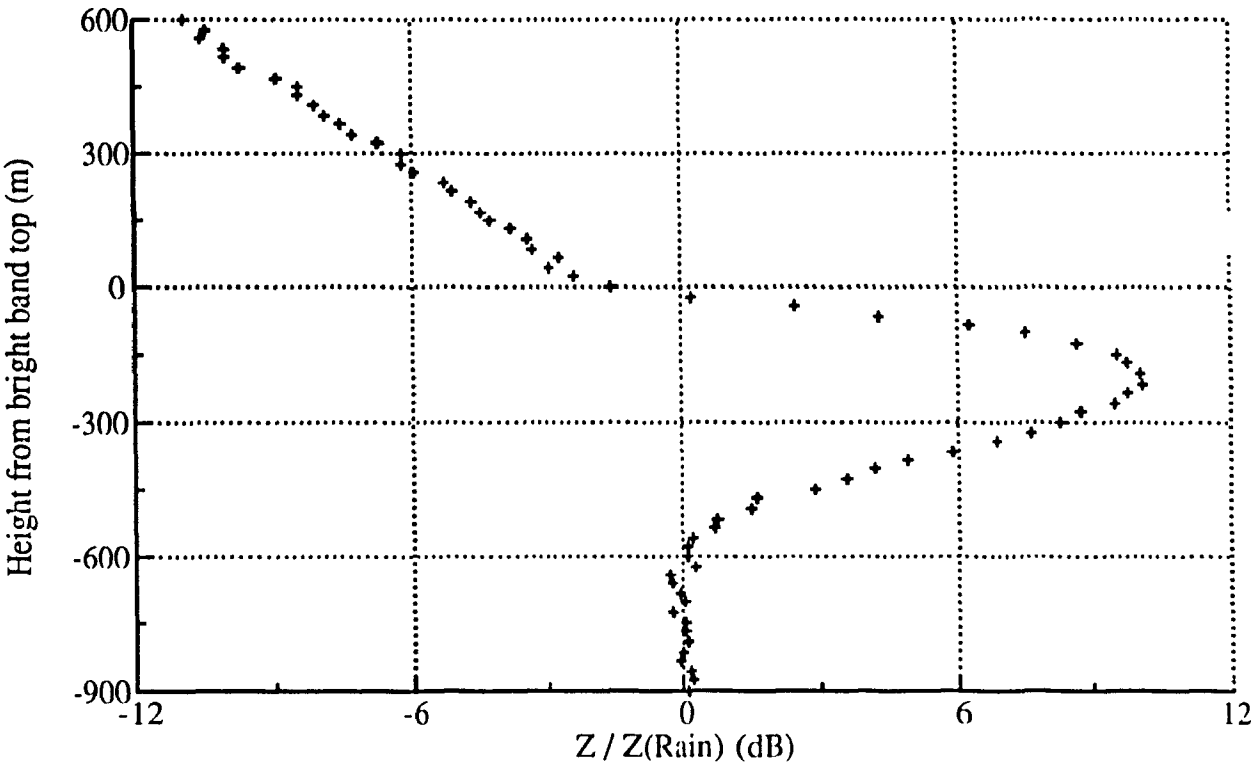

Fig. 4.1 - Typical bright band profile based on 10 minute averaged data.

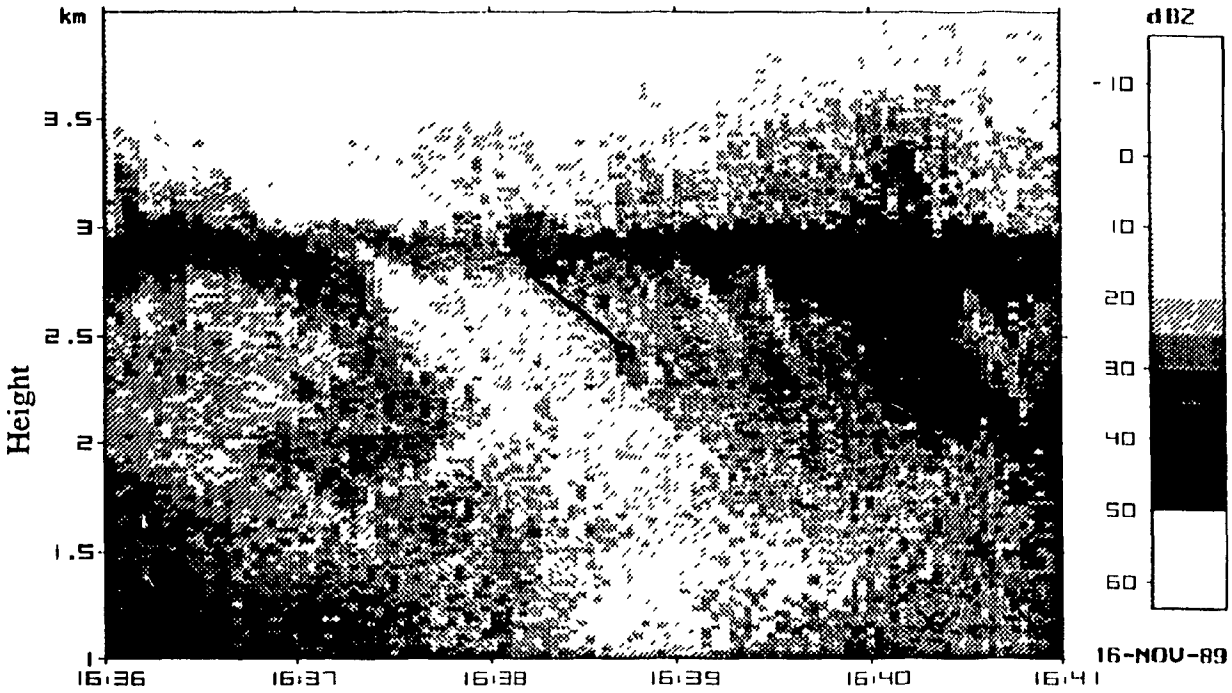

Fig. 4.2 - The bright band thickness measurement program evaluates the instantaneous bright band thickness and correlates it with the rainfall rate at some distance below the bright band accounting for the drifting of precipitation trail echoes.

4.1.1 Bright band thickness measurement technique

Before attempting any corrections for the bright band, the thickness and the intensity of the reflectivity enhancement must be known. The zenith pointing radar data collected in fall 1989 and spring 1990 is used to determine bright band characteristics. This calculation was performed for each series of measurements. To determine the instantaneous bright band thickness, the maximum vertical gradient in reflectivity on each side of the bright band $\left(\frac{dZ}{dh}\right)_{max}$ is found. The bright band limits are then defined as the first points beyond the maximums where the vertical gradient in reflectivity is half of the maximum found on each slope (when $\frac{dZ}{dh} \leq \frac{1}{2}\left(\frac{dZ}{dh}\right)_{max}$). Even if this definition is unorthodox, it gives good results: using this definition, the bright band on Figure 4.1 would be about 520 meters thick which closely corresponds to a subjective estimate. The rainfall reflectivity associated with the bright band thickness is also measured (Figure 4.2) taking into account the drift of the rainfall trail due to wind shear (Marshall, 1953; Sauvageot, 1982).

4.1.2 Results of thickness measurements

Figure 4.3 shows the results of the frequency of occurrence of bright band thickness for all the data where the reflectivity was above or equal to 6 dBZ (or rainfall above or equal to 0.1 mm/hr) just below the bright band. This graph is similar to the one made by Steiner and Waldvogel (1989) except that it is a composite of three months of rainfall data. A mean thickness of 346 meters is found but there is a wide scatter as 95% of the measurements are from 160 meters to 560 meters. The mean thickness of the bright band and its standard deviation for each 5 dBZ interval of rain reflectivity is shown in Figure 4.4. On the bottom part of the graph, the frequency distribution of rainfall reflectivity is shown to give additional information about the distribution of rain rates in the data set.

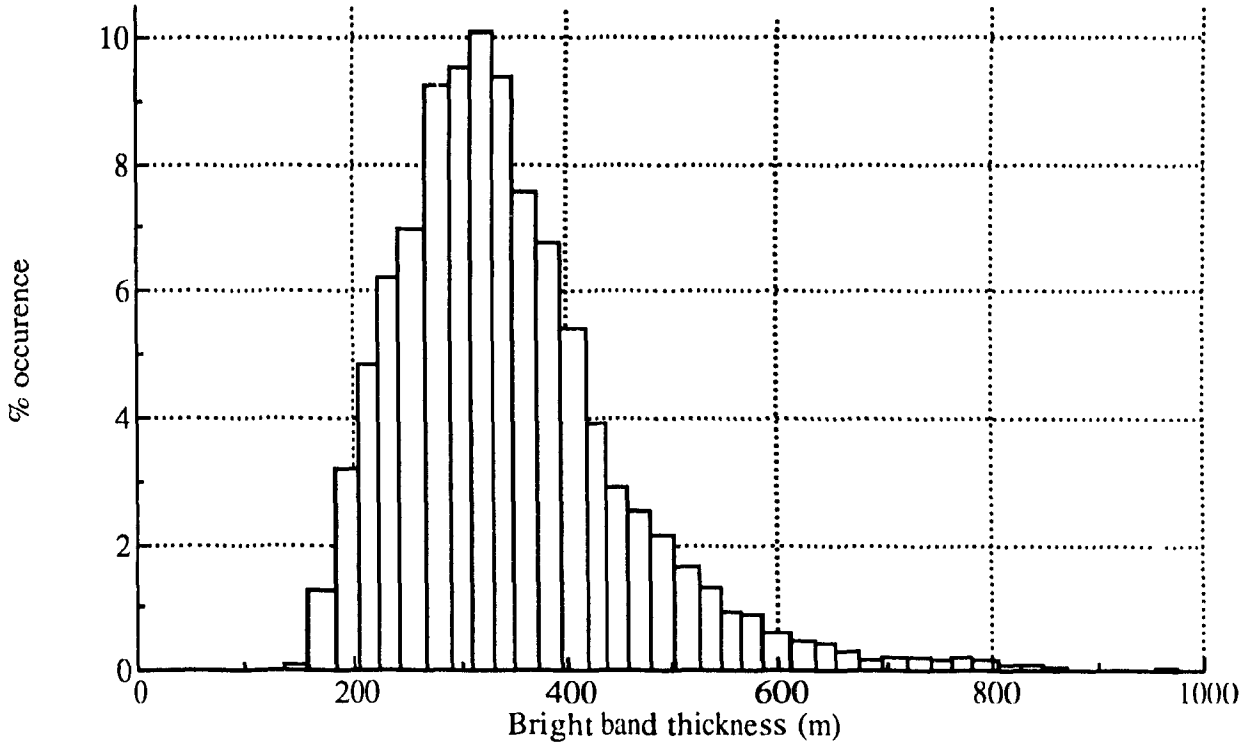

Fig. 4.3 - Frequency of occurence of bright band thickness for all the rainfall collected in the fall of 1989 and the spring of 1990 when the rate was greater than 0.1 mm/hr.

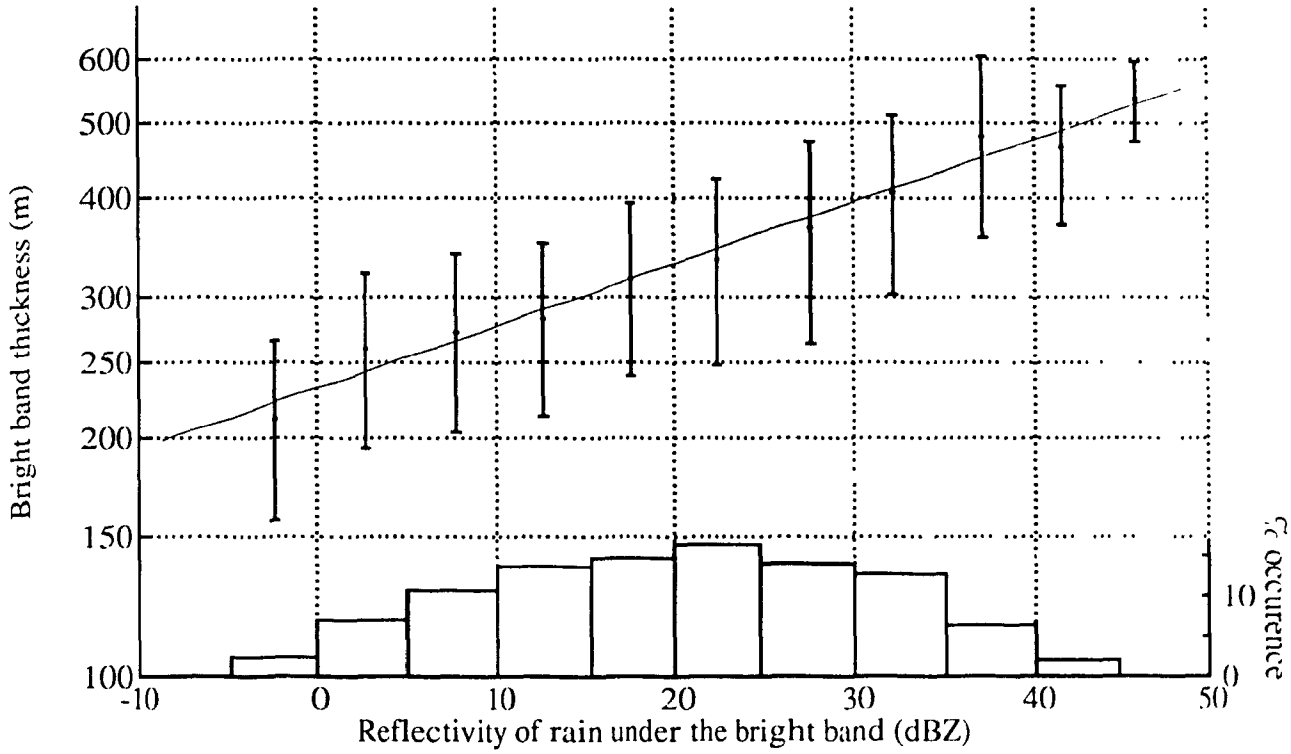

Fig. 4.4 - Mean bright band thickness with the standard error of measurement as a function of the reflectivity of the rain. The bar chart shows the frequency of occurence of each rain reflectivity interval for the entire data set.

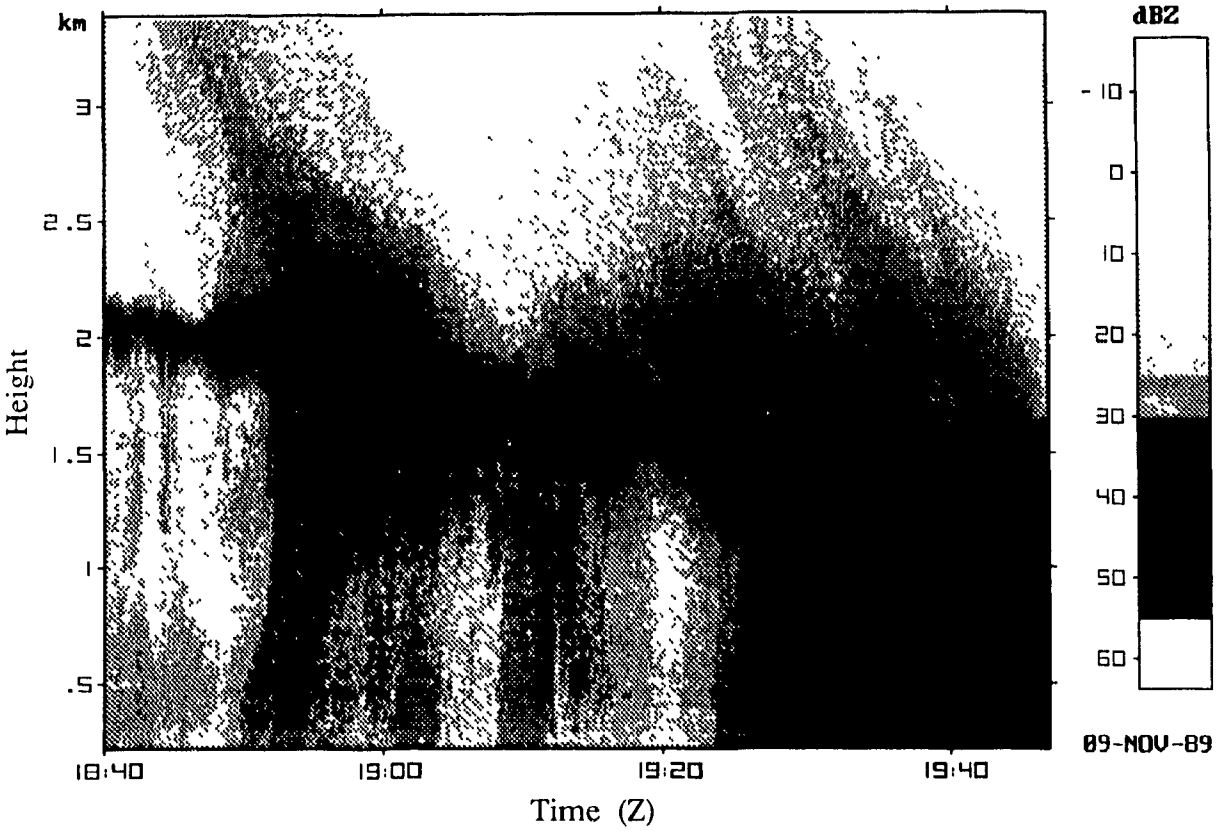

Fig. 4.5 - HTI of a portion of the November 9th rainfall showing important changes in bright band thickness.

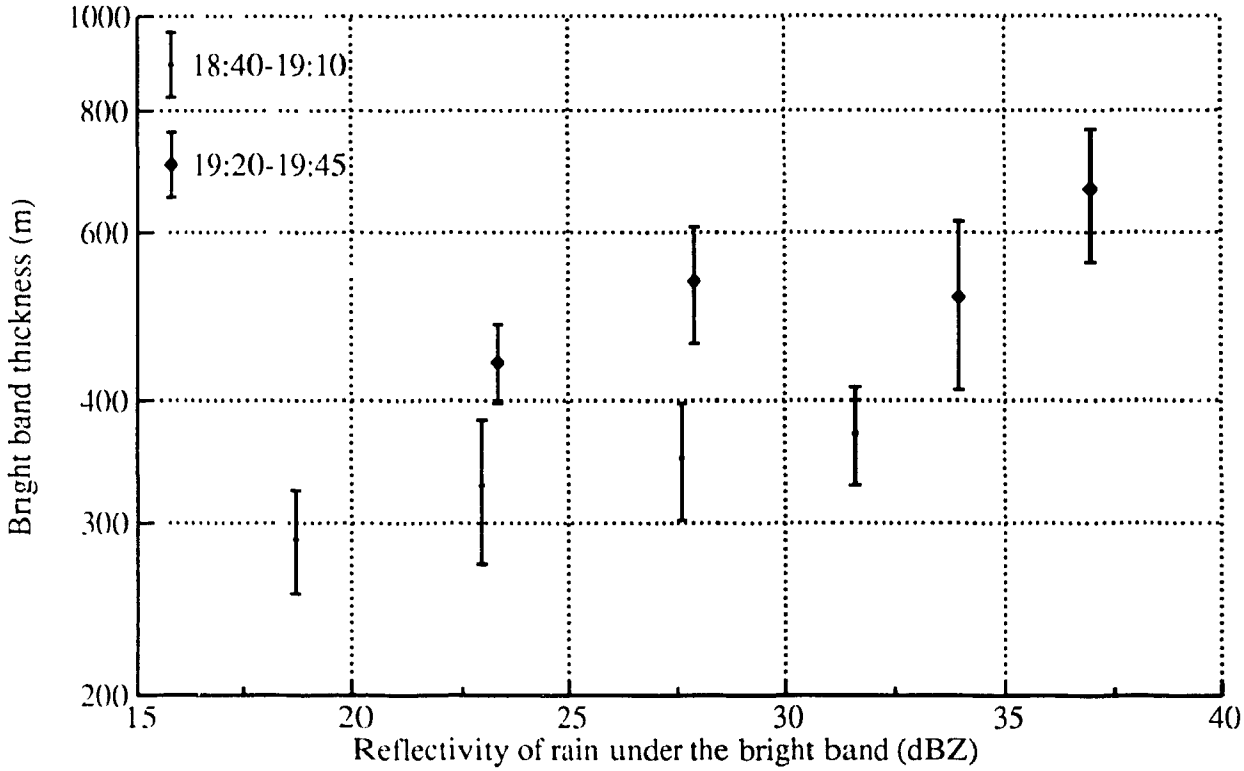

Fig. 4.6 - Bright band thickness vs rain reflectivity for two time periods of the event shown above.

The dependence of the bright band thickness on rain reflectivity for the entire data set is comparable to what Klaassen (1988) obtained using 49 1-minute averaged thickness measurements.

The distribution of rain reflectivity looks normal on the dBZ scale (Figure 4.4). Hence, the distribution of rainfall rates is log-normal, which is generally the case for sufficiently long periods of time. The mean bright band thickness increases exponentially with the logarithm of the rainfall reflectivity. This is due to the fact that the larger snowflakes associated with higher rainfalls takes more time to melt and travel a longer distance before they melt since they fall faster ($v = 160D^{0.3}$; Langleben, 1954). Since the distribution of rain reflectivity is normal on the dBZ scale and since the bright band thickness increases exponentially on the same scale, the bright band thickness should follow a log-normal distribution when the contribution from all rainfall rates are combined. Although the distribution in Figure 4.3 does not include data for rainfall rates under 0.1 mm/hr, it appears to be log-normal.

Even for rainfalls having similar rates, there is still wide scatter in the bright band thickness measurements. The standard deviation of each measurement is relatively large as can be seen by the size of the error bars in Figure 4.4. This reflects the fact that the bright band shows large variations between different events as well as within a distinct event. A good example can be seen in Figure 4.5. The bright band of a normal depth became quickly wider after 19:20. This sudden change is also illustrated in Figure 4.6 which shows that the change in thickness is not simply associated with a variation in rainfall intensity but also to a variation in conditions.

The scatter in the measurement can have several origins:

a) *changes in the temperature profile or the lapse rate* around 0°C affecting the melting duration;

b) the presence of an *updraft or downdraft* which can shorten (updraft) or lengthen (downdraft) the size of the melting layer;

c) *changes in fall speed related with the height of the bright band* because the higher the bright band, the faster the hydrometeors. The friction due to air is reduced at high altitudes where the air pressure is reduced and the velocity is proportional to $P^{-0.5}$;

d) *changes in the snowflake size distribution* where the presence of a few exceptionally large snowflakes (or their absence) will affect the size of the bright band;

e) *the width of each interval* (5 dBZ) for which all the thickness measurements are combined;

f) *algorithm induced scatter* such as errors in the thickness measurements due to the noisy data or in the rainfall measurement. The matching of a rainfall rate with the associated thickness can be difficult because of changes in the slope of trails (Figure 4.2, left versus right) or in the intensity of precipitation between the bright band and the level at which the rainfall is measured.

4.1.3 Discussion on bright band correction techniques

Obtaining the best information about the vertical profile of the precipitation is essential before attempting any bright band corrections. One way to retrieve it with a scanning radar is to use the data from several elevation angles. For example, Collier et al. (1980) used the ratio between the reflectivity obtained with two CAPPIs to determine

whether the echo received was from stratiform, convective or ground echoes. Knowing that information, it is then possible to eliminate the ground echoes and correct the reflectivity of the stratiform and convective precipitation to obtain the best rainfall rate map.

Corrections for the enhancement of the bright band have been attempted by a few investigators. Harrold and Kitchingman (1975) first proposed a scheme which used the ratio of reflectivity measurements taken at two different elevation angles to correct for any vertical variations in the reflectivity. However, the algorithm was however numerically unstable and minor improvement in the overall accuracy was observed. The current method used operationally by the British Meteorological Office is described in Smith (1986). The technique builds on the one proposed by Harrold and Kitchingman but only attempts to correct for low level bright bands. It obtains reasonable success in real-time with limited computing power using a conservative approach.

The aforementioned techniques assume that the bright band stays at the same height everywhere or that the vertical structure is horizontally uniform. This condition is necessary otherwise regions of strong precipitation might be confused with reflectivity enhancement due to the bright band and corrections would be incorrectly applied. However, a bright band can rise or sink (Figure 2.3 and 4.5), appear or disappear (Figure 2.5 and 4.7), become discontinuous (Harrold et al., 1968) and even split in two parts (Plank et al., 1955; Figure 4.8) over distances smaller than the radar range. Therefore the restriction of a constant bright band height is a serious limitation. One way to reduce the problem is to correct the radar reflectivity using raingauges (Collier, 1986). But this attacks the symptoms rather than the problem and errors in precipitation estimates in

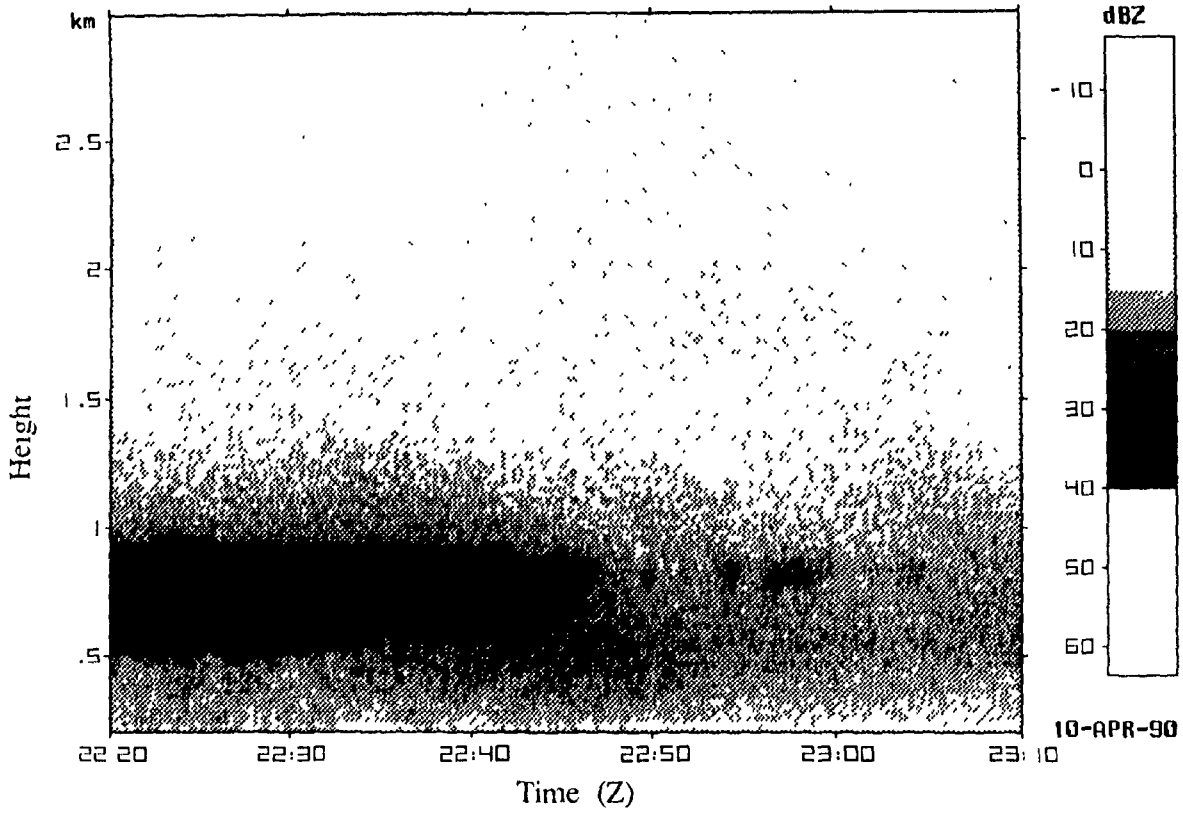

Fig. 4.7 - Decaying bright band with the passage of a cold front. The freezing rain mixed with snow changed to snow as the bright band vanished.

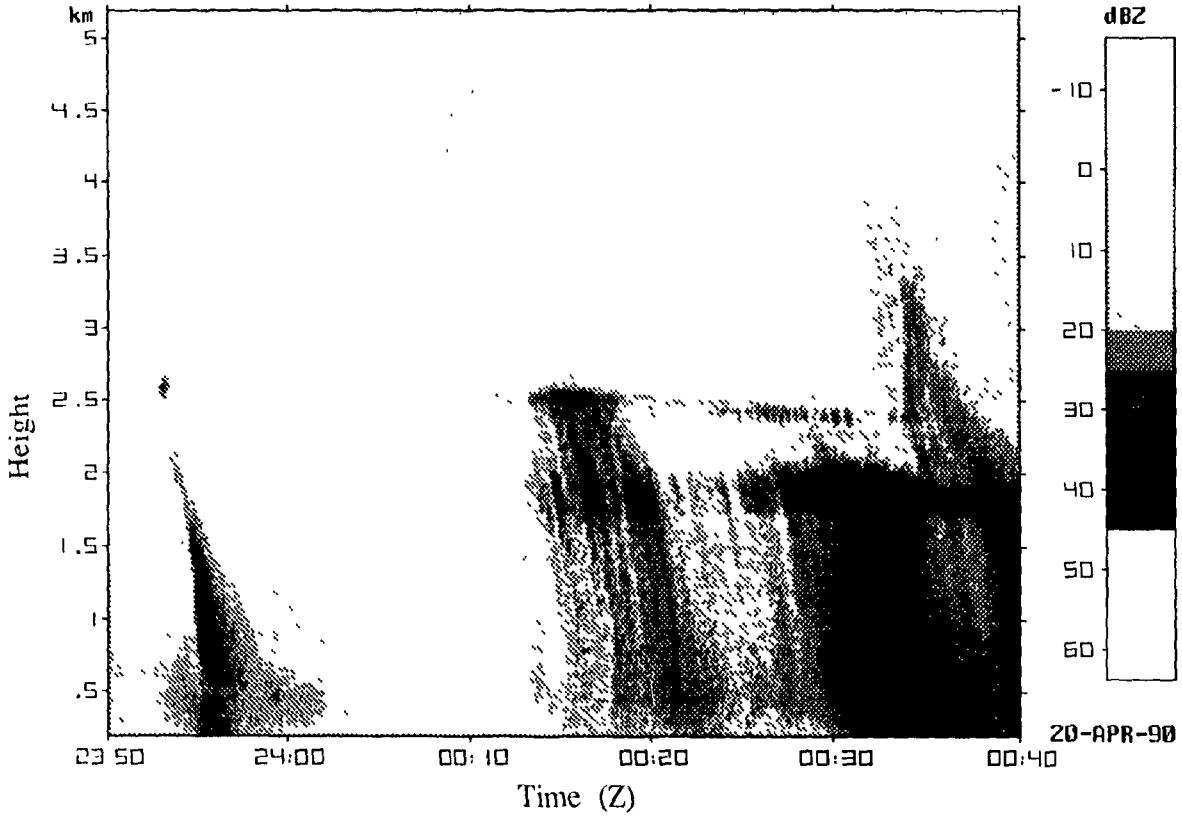

Fig. 4.8 - Splitting bright band with the passage of a cold front. The bright band originally at 2.6 km (23:55) split in two parts because of the temperature inversion. The top bright band vanished and the bottom bright band around 1.8 km persisted after 0:35.

bright band cases are still on the average several times larger than in no bright band cases (Browning and Collier, 1989). Since bright band height or thickness variations occur on scales much smaller than the radar range, any correction of rainfall estimation over a small region must be carried out using local information. For example, a zenith pointing radar installed in or close to a city could correct scanning radar data for any variations of reflectivity with height much more accurately for the urban area than a scanning radar using several elevation angles. The accuracy would be improved mostly because the vertical resolution of such radar could easily be 20 meters or less compared with the scanning radar whose beamwidth is 1 km or more at ranges in excess of 50 km. This kind of correction could readily be done in real time. Furthermore, the zenith pointing radar could give information about the bright band thickness and intensity to the scanning radar. If the bright band height remains constant over the scanning radar range (i.e. if the time-history of the bright band on the zenith pointing radar shows constant height and if the bright band height measurements from the two radars match), the bright band characteristics measured precisely by the zenith pointing radar could be used for the correction for the whole radar scan. This could be done for all bright band heights, even over 1000 meters where the scanning radar starts to have problems evaluating bright band characteristics (Smith, 1986). If the bright band height changes in time or space, the information provided by the zenith pointing radar could be used for local correction only In this case, the time-history of bright band heights could also be used with synoptic maps to help to determine a bright band height map, assuming that these features are only advected with the mean flow as measured using radar echo tracking. This map could be used for the bright band correction yielding to more accurate corrections than available before. Hence, a zenith pointing radar or a small network of them, could be used not only

for research on microphysical processes but also to help to correct operational radars for vertical variations in reflectivity. Clearly this is practical only if the cost of a zenith pointing radar can be made much smaller than appropriate scanning radars. Cost studies not included as part of this thesis suggest that non-Doppler high resolution zenith pointing radars may be deployed for as little as 17,000 US$ and a plan to deploy such a system in northern England where stratiform rain predominates is under way.

4.2 INCOMPLETE BEAM FILLING IN SNOW EVENTS

When measuring a low altitude phenomenon like snowfall, it is likely that beyond a certain range, the radar beam will be high and large enough to be not completely filled with precipitation. In order to evaluate the magnitude of this effect, a new simulation was done for the snowfall event.

The simulation for the snowfall case (Figure 4.9) was done for two beam widths in order to study the advantage of using a shorter wavelength other radar parameters being equal. It was thought that a narrower beam being completely filled with precipitation would lead to better estimates of snowfall than a wider beam which would be partially filled after a certain range (Giguère and Austin, 1989). Figure 4.10a shows the results for the 1 degree beam and Figure 4.10b those for the 0.3 degree beamwidth corresponding roughly to the beam widths of the McGill radar in its summer (S-band) and winter (X-band) mode respectively. A comparison of the two simulations shows a close similarity between the ER/EG contours. Some small differences can be noticed. First, at short range and at some distance from the ground, the returns from the S-band radar are very similar in magnitude to those from the X-band radar. The S-band radar beam may

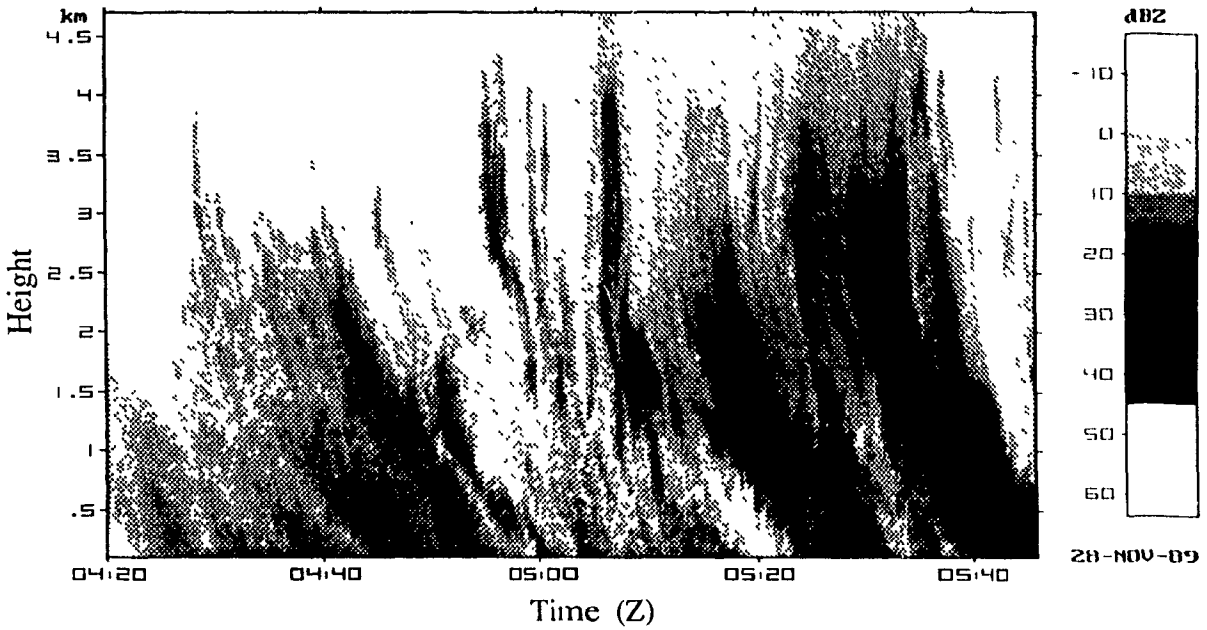

Fig. 4.9 - HTI of a moderate snowfall event.

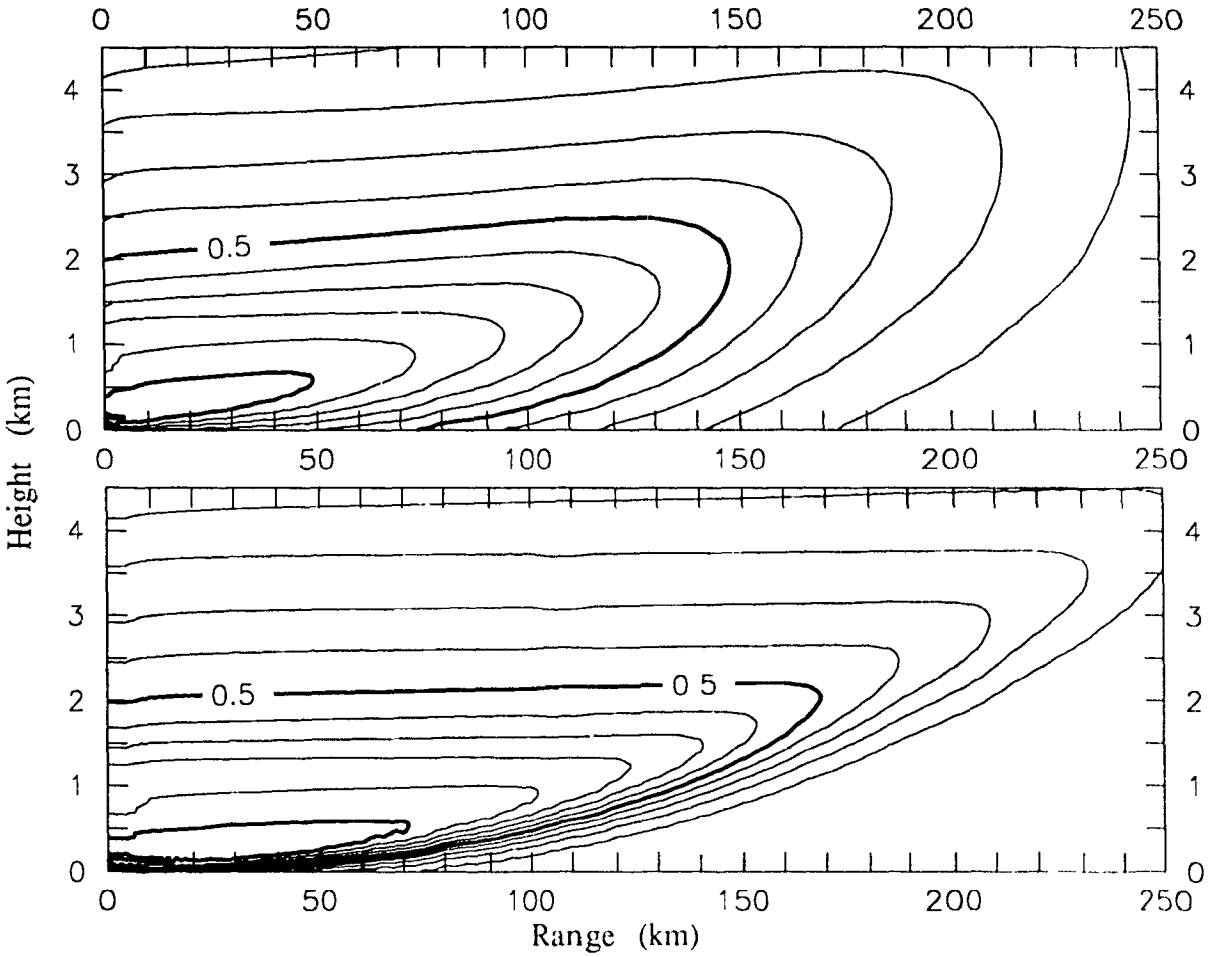

Fig. 4.10 - Contour plot of the ratio of the radar estimated snowfall and the surface snowfall as a function of range and height pointed by the beam axis for the event shown above. Top: using a radar with a 1° beam. Bottom: using a radar with a 0.3° beam.

miss some snow in the top part of its beam because of partial beam filling, but this is compensated for by the stronger snow echo it gets in the bottom part. The beam filling argument then appears to be wrong. However at long range (150 km) and for low elevations (corresponding to angles between 0 and 0.3 degree), the X-band radar is slightly superior to the S-band. In this case, a significant part of the wide S-band beam is below the horizon while the narrow X-band beam does not suffer from this problem. Furthermore, ground echo problems are more likely and stronger when using a wide beam and a long wavelength than with a narrow beam at a short wavelength (Ulaby et al., 1981). To extend the useful range when measuring snowfall, a beam at low elevation is essential. Since a narrow beam radar can be pointed at a lower elevation angle than a wider beam, it is therefore slightly superior for snowfall accumulation estimates. As can be seen when comparing the two figures, the difference between the performance of the two radars is notable if the sampling is done at very low levels (like in a PPI) but relatively modest if made at constant height (like in a CAPPI). Hence, most of the improvement in quantitative estimation of snowfall of the McGill X-band radar over the S-band radar described in Giguère and Austin (1989) probably comes from the 4.6 dB improvement in sensitivity in favor of the X-band radar, rather than from beam filling effects.

4.3 GRADIENTS IN RAIN AND SNOW

There are two ways gradients in the reflectivity field can affect the reflectivity measurement or the rainfall rate estimation at a point. First, if strong gradients are present in the volume sampled instantaneously by a beam, the rainfall rate for the whole region will be underestimated even if the reflectivity measurement is correct. For example if a 1

mm/hr rain (23 dBZ reflectivity using the Marshall and Palmer relationship) is present over half of the region and the other half is precipitation free, the radar will measure the rainfall to be 0.65 mm/hr (20 dBZ) for the whole region. However, if radar measurements are interpreted as the rainfall rate at the center of the beam, the rainfall rate might be either underevaluated or overevaluated depending on the shape of the reflectivity function in the beam (Zawadzki, 1982). Secondly, reflectivity measurements can be made incorrect at the post-detection integration step in the presence of gradients. Depending on the way reflectivity data is averaged, logarithmically versus linearly for example, additional errors can be produced in the presence of strong gradients or if the area over which reflectivities are averaged is large (Rogers, 1971; Zawadzki, 1982).

The magnitude of gradients in stratiform rain varies significantly from storm to storm depending primarily on whether the precipitation is generated from isolated snow trails (Figure 3.1 or 4.11), shower-type cells (Figure 3.3) or roughly uniformly (Figure 3.5). The snow trail generated events tended to have the stronger gradients. In order to appreciate their strength, the reflectivity function along a line at 1.5 km (Figure 4.11) is shown in Figure 4.12. To generate that function, the reflectivities from each measurement of the two bins closest to 1.5 km were averaged and then plotted on the reflectivity-time graph. The field is relatively noisy (1 dBZ root mean square) because only 40 pulses are averaged to reduce the statistical fluctuations. Most of the large scale reflectivity variations seem to follow an exponential power law (Shaffner et al., 1981). The most severe variations are close to step functions in appearance. Changes in reflectivity of more than 15 dB are observed on periods smaller than 30 seconds. More intense gradients

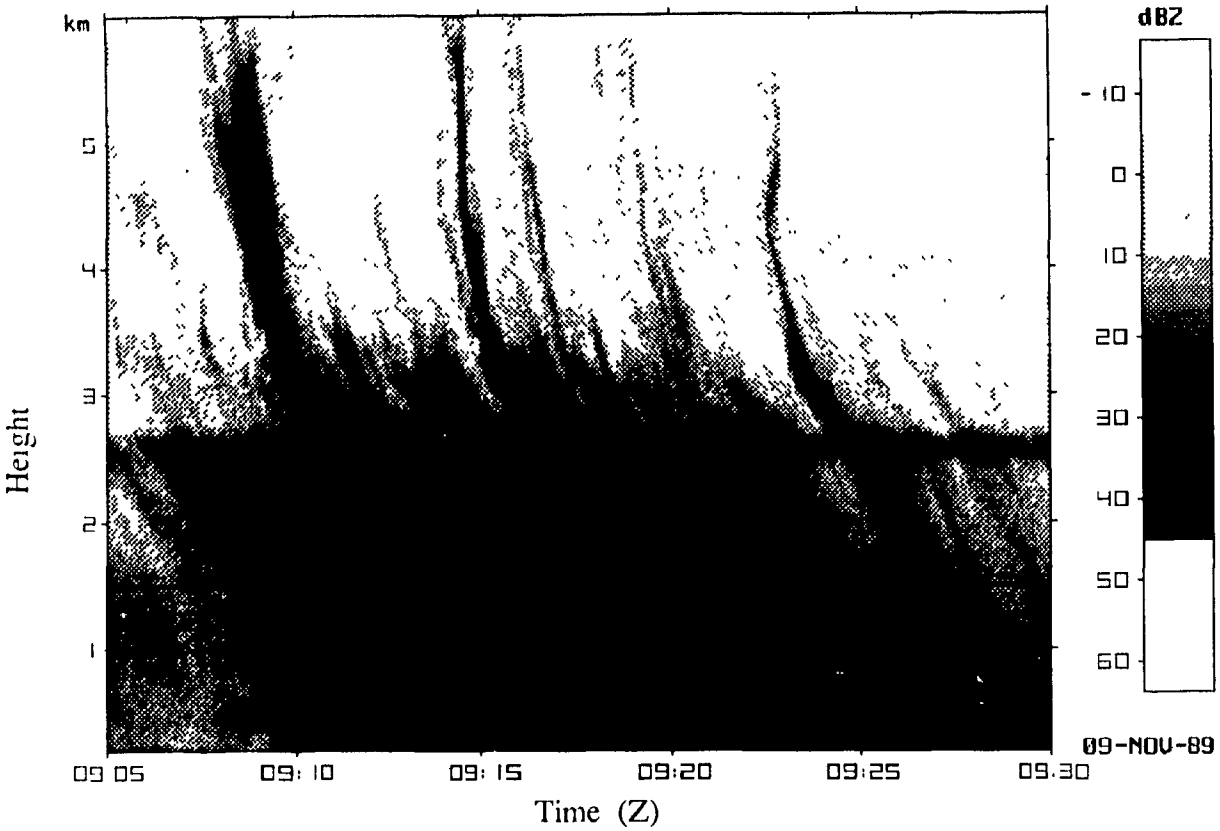

Fig 4.11 - HTI of a portion of the event #1. The line at 1.5 km shows the path along which the data for the graph shown below is collected.

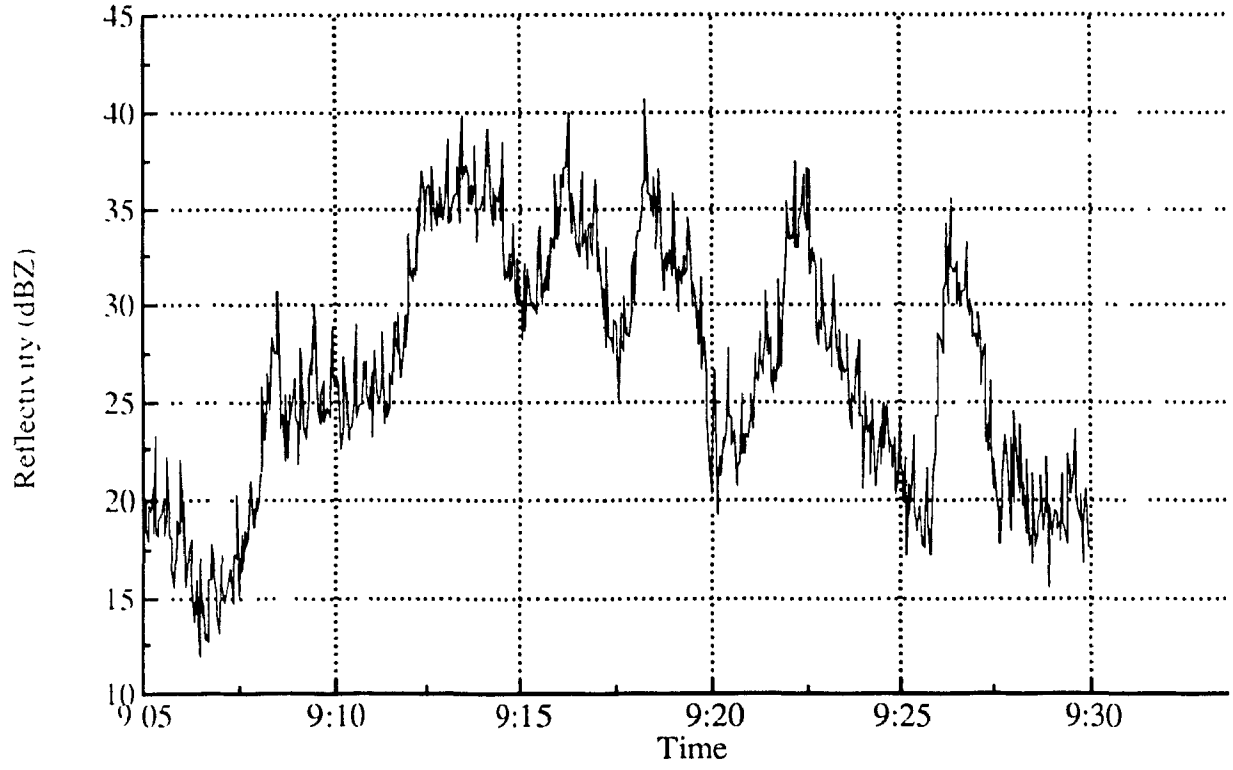

Fig 4.12 - Reflectivity at 1.5 km for the portion of event shown above as a function of time. Some of the "noise" is due to the fact that each reflectivity measurement has a root mean square error of 1 dBZ.

tend to be observed at higher altitudes in the snow from where the often narrow trails originate. Variations of 30 dBZ over 100 meters (vertical) or 10 seconds (horizontally) were observed for several events.

The next question is to what extent these important and numerous changes in the reflectivity field on some stratiform events bias the rainfall estimation. Since there are several ways for gradients to bias the rainfall measurements depending on the way reflectivities are derived and on whether point, surface or volume rainfall is considered as the ground truth, the focus will be on how gradients bias the rainfall estimation for the volume illuminated by the beam at an instant. The effect of post-detection integration will not be investigated here. To answer this question, we must compare the actual rainfall estimation with what the radar would have observed if no reflectivity gradients were present.

The four precipitation events studied earlier were reexamined to study the effects of reflectivity gradients on stratiform precipitation estimation. The first step consists of computing the mean vertical reflectivity profile of each event. These average profiles were then used as in Joss and Waldvogel (1990) to determine what a scanning radar would have seen as a function of range and height assuming the event was horizontally stratified. The result is a simulation similar to the one shown in chapter 3 (Fig. 3.2, 3.4, 3.6 and 3.8) except using data having a constant vertical reflectivity profile. The ratio of the results simulation with the original data and the results from the simulation with a constant vertical reflectivity profile will then give a measure of the effects of gradients on the precipitation estimations.

The data used for the simulation fluctuates somewhat because of the modest number of samples averaged. To some extent, this might introduce artificial reflectivity fluctuations and hence nullify the study. However, Figure 4.12 suggests that this effect is going to be small compared with the one due to real fluctuations. To further support this assumption, an additional test was made. Averaging 20 pulses gives reflectivity measurements accurate to less than 1.5 dBZ. If the radar reflectivity in the beam is constant at 23 dBZ, a rainfall rate of 1 mm/hr is measured. If the reflectivity in the beam is inhomogeneous, with half at 24.5 dBZ and half at 21.5 dBZ, a rainfall of 1.022 mm/hr is measured. Since the probability distribution of $Z_{measured} / Z_{real}$ is not gaussian (Marshall and Hitschfeld, 1953) and low values are slightly more probable than high values when averaging 20 pulses, the bias caused by the fluctuation of the input data then becomes negligible.

The results of the study of the effects of gradients are shown in Figures 4.13 to 4.16 corresponding to the events shown in Figures 3.1, 3.3, 3.5 and 3.7 respectively. The contour lines used are the same for all the four graphs. The bias contour plots are noisier than those of the rainfall estimates because the contour intervals are much smaller.

First, the bias due to reflectivity variations becomes more important with height as the field becomes less and less homogeneous. There is a strong correlation between the regions in the graph where enhancement is weak and where the contribution to the rainfall estimation came primarily from rain and bright band echoes. There is a sudden increase around the echo top height and contours above that height are artificially high and mostly due to the few peaks of radar noise that went high enough to register as reflectivity measurements. These were then interpreted by the simulation as localized

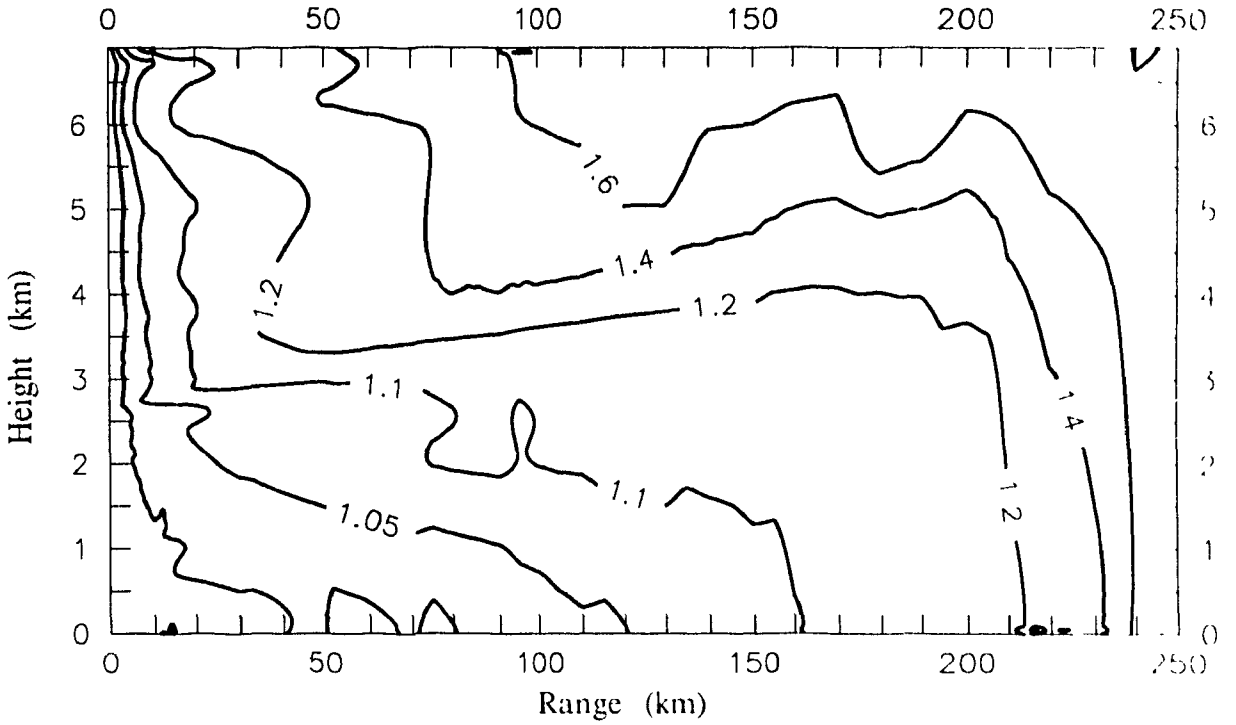

Fig. 4.13 - Contour plot of the overevaluation due to gradients for the light rainfall event as a function of range and height. The graph shows the ratio of what the radar estimated with what it would have estimated if the reflectivity field was horizontally stratified. Contour lines are 1.02, 1.05, 1.1, 1.2, 1.4 and 1.6.

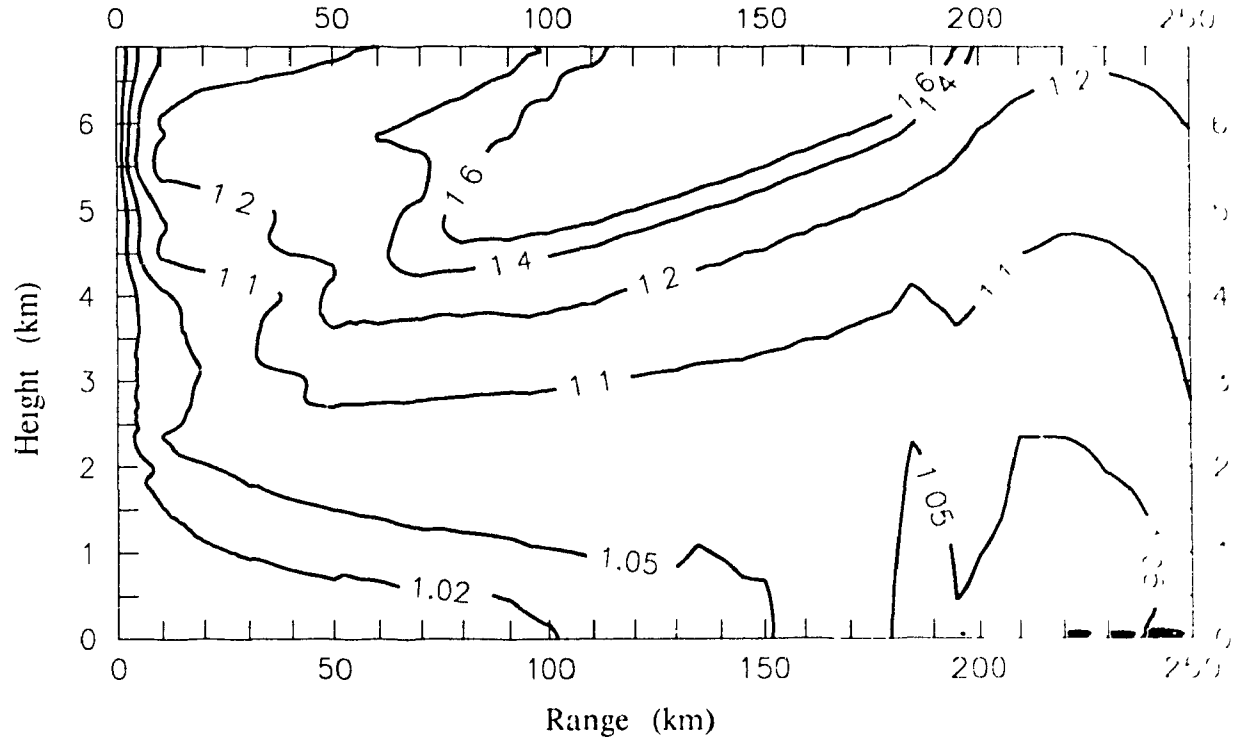

Fig. 4.14 - Same as Fig. 4.13 but for the moderate rainfall event

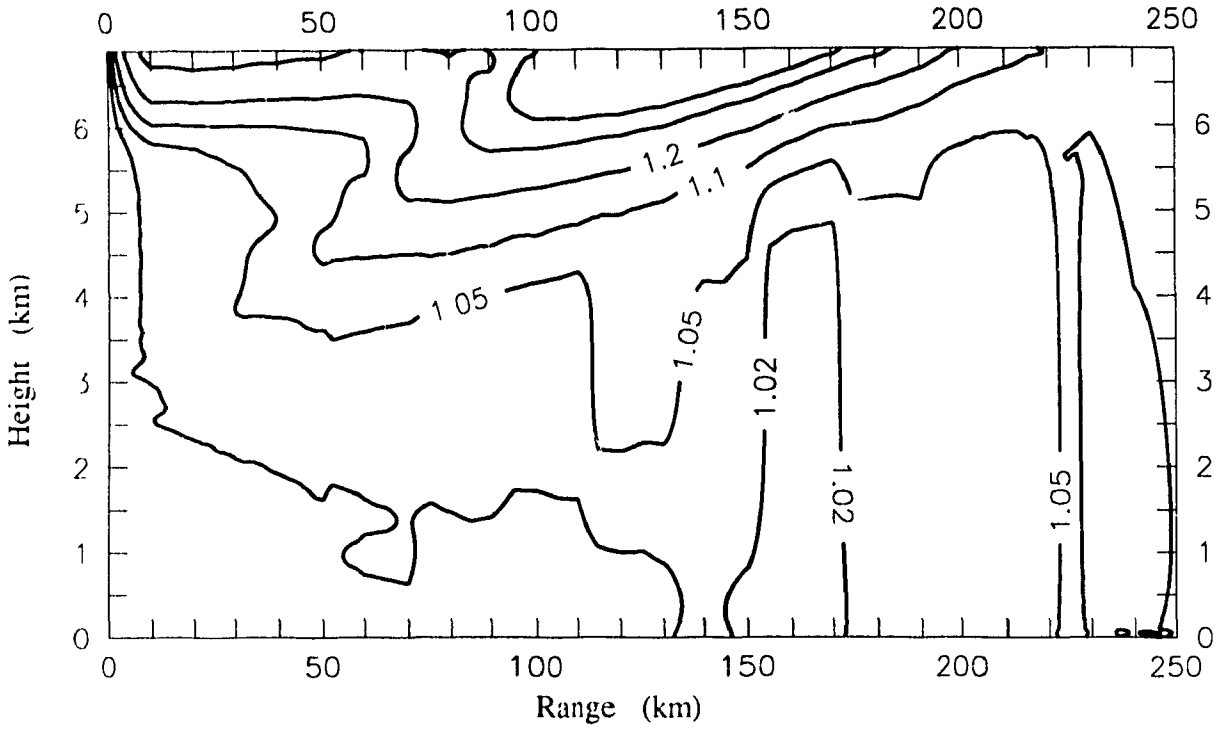

Fig. 4.15 - Same as Fig. 4.13 but for the strong rainfall event.

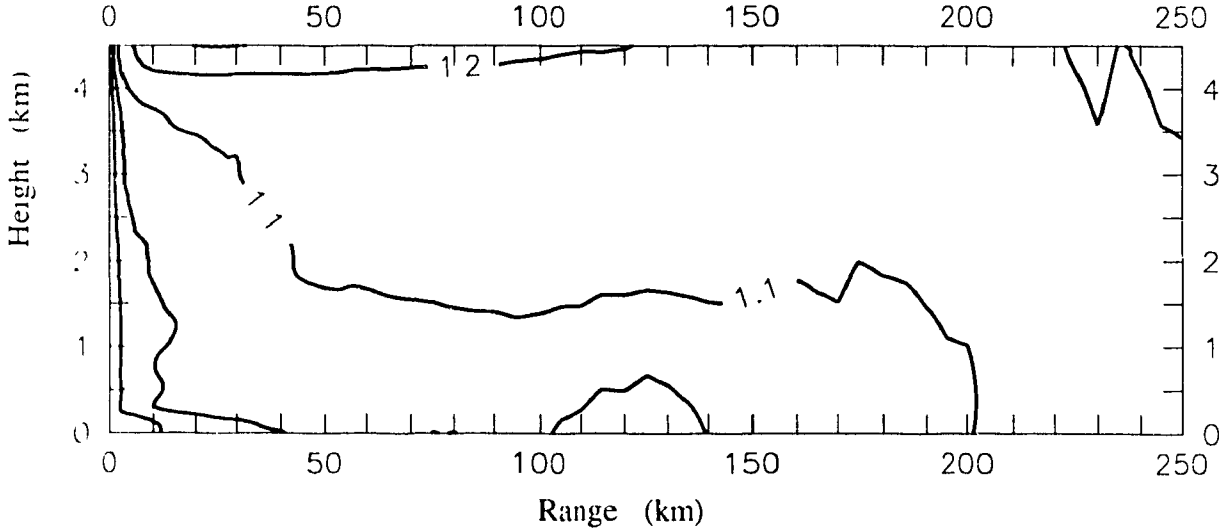

Fig. 4.16 - Same as Fig. 4.13 but for the moderate snowfall event.

precipitation echoes in the middle of an echo free region.

All four events show little enhancement due to gradients at very low levels. For the first rainfall event, it is partly due to the fact that precipitation increased as it approached the ground due to raindrop accretion in a low level stratus. The weaker rain increased significantly while the moderate rain did not increase as much, which caused a weakening of the gradients. But the main cause for the too weak enhancement at low levels for the first and the other events is artificial: at low levels where the reflectivity data was inaccurate, the reflectivity values were set to the value around 300 meters (Section 3.1.1), wiping out all vertical reflectivity gradients. Hence only the horizontal only gradients contribute to the enhancement at low levels.

The first rainfall event which had the greatest variations in reflectivity shows the greatest precipitation estimation enhancement. In the portion under 2.5 km corresponding to rain, the enhancement increases with range as more and stronger gradients fit in the widening beam. For ranges smaller than 150 km, beyond which rainfall estimations are inaccurate for that event, the bias is just above 10%. The same is true for the snowfall event for ranges under which accurate estimations are possible. For the second event, the bias is even smaller and almost negligible for the strong stratiform event. Since beyond these ranges the rainfall estimations drop while the effect of gradients tends to increase ER/EG, it can be concluded that in stratiform cases, variations in reflectivity do not play an important role in biasing rainfall estimation by radar.

The results of the reflectivity gradient simulation were made using a 2-D reflectivity field. The effect of the 3rd dimension varies with scenarios. If we consider a standard radar beam, the length of the radar pulse which is along this third dimension is 150

meters for a typical 1 microsecond pulse. This is a short distance compared to the diameter of the beam which is of the order of a few kilometers. Therefore it is unlikely that the results of the 2-D simulation are going to be modified significantly by the addition of the third dimension. This might not be true if what happens at the post-detection integration level is included in the analysis. If the averaging method is logarithmic or the surface over which reflectivities are averages is large, significant bias could be induced.

5 CONCLUSION

5.1 CONCLUSION

Reflectivity data of fall and spring Montreal weather was collected by a high resolution X-band zenith pointing radar. The data was used to try to evaluate the effects of the sampling differences between a scanning radar and gauges, and how their magnitude varies with range.

Accurate stratiform precipitation estimates are challenging to obtain even when only the effects of radar gauge sampling differences are studied. For rainfall, the bright band must be avoided by measuring reflectivities well below the bright band If this condition is met, the different simulated elevation angle combinations performed reasonably well A CAPPI with several elevation angles was found to be superior to a PPI or a pseudo CAPPI using a few elevations angles as it is less sensitive to vertical changes in reflectivity and also avoids much of the ground clutter. After a certain range which increases as a function of the height of the bright band, rainfall estimates are severely underestimated and are probably uncorrectable since most of the reflectivities could be under the minimum detectable threshold of the radar. For snowfall where reflectivity decreases with height, only the simulated CAPPI with several elevation angles obtains reasonable results up to a range which is about half the one for the rainfall events

Non uniform reflectivity in the radar beam is one of the causes of disagreement between radar derived and rain gauge accumulations. The problems associated with partial beam filling, gradients and the bright band were investigated separately The beam

filling problem related to snow detection was found to be inexistant at short range and modest at medium and far range. The advantage of using a radar with a smaller beam was hence found to be modest unless a gain in sensitivity is obtained. Even if variations in the reflectivity field can be sudden, their overall effect on the estimation of rainfall was minor at the ranges and heights where accurate precipitation estimation was possible. Of the three main causes of non uniformities in stratiform rain investigated, the most important one is the bright band. Bright band thickness increases exponentially as a function of the logarithm of radar reflectivity or rain rate. However, even for similar rainfall rates, there can be large scatter of thickness from storm to storm and even within storms, as well as large changes in bright band height. This is the reason why current bright band corrections using data from one scanning radar together with other climatological data are not likely to be successful. It is believed that these techniques could be significantly improved by using zenith pointing radars to detect bright band heights and thickness changes.

In fact all the information necessary for a range correction of the reflectivity measurement could be provided by a zenith pointing radar except for the effects related to attenuation and beam blockage. A technique using zenith pointing radars to provide reflectivity corrections could be implemented in real-time using the data from the actual event. Therefore, such a technique would be more precise than the statistical range correction procedures advocated by Calheiros and Zawadzki (1987) or Atlas et al. (1989).

5.2 FUTURE WORK

The results here suggest some additional work which could be undertaken. First, simulations similar to the one done in chapter 3 could be used to study other events. For example, the accuracy and scatter of instantaneous rainfall estimations by radar as a function of range could be investigated and compared with the results obtained for accumulations estimations. Simultaneously, the accuracy of real-time raingauge calibration could be investigated by comparing the reflectivity aloft and at the surface for short periods The accuracy of radar accumulation and instantaneous estimations in convective storms as a function of range and height could also be tested. Secondly, the convective storm estimations might be more easily biased by gradients in the reflectivity field then the ones for stratiform precipitation. A study of the effect of gradients in convective storms could hence yield to interesting results. Finally, the feasibility and the accuracy of zenith pointing made bright band or vertical reflectivity variation corrections could be tested in field experiments and in real time. High resolution vertical data close to the ground could also be useful to study orographic enhancement of precipitation such as the one due to seeder-feeder mechanism.

6 BIBLIOGRAPHY

ATLAS, D., 1964: Advances in radar meteorology. In *Advances in Geophysics*, Academic Press, New York, **10**, 318-478.

ATLAS, D., D. ROSENFELD and D. A. SHORT: The estimation of convective rainfall by area integrals 1: the theoretical and empirical basis. *Journal of Geophysical Research*, **95 D3**, 2153-2160.

AUSTIN, P.M., 1987: Relation between measured radar reflectivity and surface rainfall. *Monthly Weather Review*, **115**, 1053-1070.

AUSTIN, P.M. and A.C. BEMIS, 1950: A quantitative study of the «bright band» in radar precipitation echoes. *Journal of Meteorology*, **7**, 145-151.

BATTAN, L.J., 1973: *Radar observation of the atmosphere*. University of Chicago Press, Chicago, 324 pp.

BEAN, B.R. and E.J. DUTTON, 1968: *Radio Meteorology*, Dover Books, New York.

BELLON, A. and G.L. AUSTIN, 1978: The evaluation of two years of real-time operation of a short-term precipitation forecasting procedure (SHARP). *Journal of Applied Meteorology*, **17**, 1778-1787

BOUCHER, R.J., 1957: Synoptic-dynamic implications of 1.25 cm vertical beam radar echoes. *Preprints, 6th conference on Radar Meteorology*, American Meteorological Society, 179-188.

BROWNING, K A. and C.G. COLLIER, 1989: Nowcasting of precipitation systems. *Reviews of Geophysics*, **27**, 345-370.

CALHEIROS, R V. and I. ZAWADZKI, 1987: Reflectivity-Rain rate relationships for radar hydrology in Brazil. *Journal of Climate and Applied Meteorology*, **26**, 118-132.

CARLSON, P.E and J.S. MARSHALL, 1972: Measurement of snowfall by radar. *Journal of Applied Meteorology*, **11**, 494-500.

CHANDRASEKAR, V. and V.N. BRINGI, 1987: Simulation of radar reflectivity and surface measurements of rainfall. *Journal of Atmospheric and Oceanic Technology*, **4**, 464-478.

COLLIER, C.G., 1986: Accuracy of rainfall estimates by radar, Part I: Calibration by telemetering raingauges. *Journal of Hydrology*, **83**, 207-223.

COLLIER, C.G., S. LOVEJOY and G.L. AUSTIN, 1980: Analysis of bright bands from 3-D radar data. *Preprints, 19th conference on Radar Meteorology*, American Meteorological Society, 44-47.

DONALDSON, R.J., 1964: A demonstration of antenna beam errors in radar reflectivity patterns. *Journal of Applied Meteorology*, **3**, 611-623.

DOUGLAS, R.H., K.L.S. GUNN and J.S. MARSHALL, 1957: Pattern in the vertical of snow generation. *Journal of Meteorology*, **14**, 95-114.

DOVIAK, R.J., 1983: A survey of radar rain measurement techniques. *Journal of Climate and Applied Meteorology*, **22**, 832-849.

GIGUERE, A. and G.L. AUSTIN, 1989: On the significance of radar wavelength in the estimation of snowfall. *Proceedings of the International Symposium on Hydrologic Applications of Weather Radar*, Salford.

GOSSARD, E.E and R.G. STRAUCH, 1983: *Radar observations of clear air and clouds* Elsevier, Amsterdam, 280 pp.

GUNN, K L.S., M.P. LANGLEBEN, A.S. DENIS and B.A. POWER, 1954. Radar evidence of a generating level for snow. *Journal of Meteorology*, **11**, 20-26.

HARROLD, T.W. and P.G. KITCHINGMAN, 1975: Measurement of surface rainfall using radar when the beam intersects the melting layer. *Preprints, 16th conference on Radar Meteorology*, American Meteorological Society, 473-478.

HARROLD, T.W., K.A. BROWNING and J M. NICHOLLS, 1968: Rapid changes in the height of the melting layer. *Meteorological Magazine*, **97**, 327-332

HITSCHFELD, W. and J. BORDAN, 1954. Errors inherent in the radar measurement of rainfall at attenuating wavelengths. *Journal of Meteorology*, **11**, 58-67.

JATILA, E. (1973): Experimental study of the measurement of snowfall by radar. *Geophysica*, **12**, No.2, 1-10.

JOSS, J. and A. WALDVOGEL, 1989: Precipitation estimates and vertical reflectivity profile corrections. *Preprints, 24rd conference on Radar Meteorology*, American Meteorological Society, 682-688.

JOSS, J. and A. WALDVOGEL, 1990: Precipitation measurement and hydrology: A review. In *Radar in Meteorology*, American Meteorological Society.

KLAASSEN, W., 1988: Radar observations and simulation of the melting layer of precipitation. *Journal of the Atmospheric Sciences*, **45**, 3741-3753.

KOISTINEN, J., 1986: The effect of some measurement errors on radar-derived Z-R relationships. *Preprints, 23rd conference on Radar Meteorology*, American Meteorological Society, JP50-JP53.

LANGLEBEN, M.P., 1954: The terminal velocity of snow flakes. *Quarterly Journal of the Royal Meteorological Society*, **80**, 174-181.

LHERMITTE, R.M. and D. ATLAS, 1963: Doppler fall speed and particle growth in stratiform precipitation. *Preprints, 12th conference on Radar Meteorology*, American Meteorological Society, 297-302.

MARSHALL, J.S., 1953: Precipitation trajectories and patterns. *Journal of Meteorology*, **10**, 25-29.

MARSHALL, J.S., 1957: The constant-altitude presentation of radar weather patterns. *Preprints, 6th conference on Radar Meteorology*, American Meteorological Society, 321-324.

MARSHALL, J.S. and E.H. BALLANTYNE, 1975: Weather surveillance radar. *Journal of Applied Meteorology*, **14**, 1317-1338.

MARSHALL, J.S. and W.M.K. PALMER, 1948: The distribution of raindrops with size. *Journal of Meteorology*, **5**, 165-166.

MARSHALL, J.S. and W. HITSCHFELD, 1953: Interpretation of the fluctuating echo from randomly distributed scatterers -- Part I. *Canadian Journal of Physics*, **31**, 962-993.

MEDHURST, R.G., 1965: Rainfall attenuation of centimeter waves - Comparison of theory and measurement. *IEEE Transactions on Antennas and Propagation*, **AP-13**, 550-564.

PLANK, V.G., D. ATLAS and W.H. PAULSEN, 1955: The nature and detectability of clouds and precipitation as determined by 1.25 centimeter radar. *Journal of Meteorology*, **12**, 358-370.

RICHTER, S.H., 1969: High resolution tropospheric radar sounding. *Radio Science*, **4**, 1261-1268.

ROGERS, R.R., 1971: The effect of variable target reflectivity on weather radar measurements. *Quartely Journal of the Royal Meteorological Society*, **97**, 154-167.

SAUVAGEOT, H., 1976: Observation directe d'une cellule génératrice de traînée de précipitations soumise à un cisaillement de vent (In French). *Journal de Recherches Atmosphériques*, **10**, 119-122.

SAUVAGEOT, H., 1982: *Radarmétéorologie* (in French). Editions Eyrolles et CNET-ENST, Paris, 296 pp.

SEED, A. and G.L AUSTIN, 1989: Variability of summer Florida rainfall and its significance for the estimation of rainfall by gages, radar, and satellite. *Journal of Geophysical Research*, **95 D3**, 2207-2215.

SELIGA, T.A. and V.N. BRINGI, 1976: Potential use of radar differential reflectivity measurements at orthogonal polarizations for measuring precipitation. *Journal of Applied Meteorology*, **15**, 69-76.

SEKHON, R.S. and R.C. SRIVASTAVA, 1970: Snow size spectra and radar reflectivity. *Journal of the Atmospheric Sciences*, **27**, 299-307.

SHAFFNER, M., R. CARBONE and E. GORGUCCI, 1981: Information from bias measurements. *Preprints, 20th conference on Radar Meteorology*, American Meteorological Society, 523-528.

SIRMANS, D. and R.J. DOVIAK, 1973: Meteorological radar signal intensity estimation. *NOAA Technical Memorandum ERL/NSSL 64*, 80 pp.

SMITH, C.J., 1986: The reduction of errors caused by bright bands in quantitative rainfall measurements made using radar. *Journal of Atmospheric and Oceanic Technology*, **3**, 129-141.

SMITH, P.L., 1964: Interpretation of the fluctuating echo from randomly distributed scatterers -- Part III. *Stormy Weather Group report MW-39.*

STEINER, M. and A. WALDVOGEL, 1989: The bright band and its influence on microphysics. *Preprints, 24th conference on Radar Meteorology*, American Meteorological Society, 5-8.

TEES D. and G.L. AUSTIN, 1989: The effect of range on the radar measurement of rainfall. *Proceedings of the International Symposium on Hydrologic Applications of Weather Radar*, Salford.

ULABY, F.T., R.K. MOORE and A.K. FUNG, 1981: *Microwave remote sensing.* Addison-Wesley, 2162 pp.

ULBRICH, C.W. and D. ATLAS, 1975: The use of radar reflectivity and microwave attenuation to obtain improved measurements of precipitation parameters. *Preprints, 16th conference on Radar Meteorology*, American Meteorological Society, 496-503

WALDVOGEL, A. and M. STEINER, 1986: Small scale structures in the bright band. *Preprints, 23rd conference on Radar Meteorology*, American Meteorological Society, JP276-279.

WALLACE, P.R., 1953: Interpretation of the fluctuating echo from randomly distributed scatterers -- Part II. *Canadian Journal of Physics*, **31**, 995-1009.

WILSON, J.W., 1976: Radar-rain gage precipitation measurements: a summary. *Preprints Conference on Hydrometeorology*, American Meteorological Society, 72-75.

WILSON, J.W. and E.A. BRANDES, 1979: Radar measurement of rainfall - A summary. *Bulletin of the American Meteorological Society*, **60**, 1048-1058.

ZAWADZKI, I., 1982: The quantitative interpretation of weather radar measurements. *Atmosphere-Ocean*, **20**, 158-180.

ZAWADZKI, I., 1984: Factors affecting the precision of radar measurements of rain. *Preprints, 22nd conference on Radar Meteorology*, American Meteorological Society, 251-256.

Appendix A: Algorithm for the averaging of the returned power

A-1 THE OBSERVER'S PROBLEM

Marshall and Hitschfeld (1953) showed that the intensity of individual echoes from a random array of scatterers fluctuates randomly with an exponential distribution. Hence, in order to obtain a good estimate of the reflectivity value, several measurements must be averaged. Calculations and simulations of different averaging techniques have been done by several authors (Marshall and Hitschfeld, 1953; Smith, 1964; Sirmans and Doviak, 1973; Seed and Austin, 1989). All these studies point out that the techniques that are computationally easy to obtain such as logarithmic averaging or exponential smoothing perform much worse than averaging reflectivities which requires handling numbers spanning on several orders of magnitude. This becomes even worse when reflectivity variations are present when averaging pulses downrange (Rogers, 1971; Zawadzki, 1982).

A-2 Z AVERAGING TECHNIQUE

It was felt that to obtain precise measurements from the zenith pointing radar, the reflectivity measurements should be averaged linearly. However, the radar receiver has a logarithmic amplifier. Furthermore, exponentiating a measurement in real time required computing power far above the capabilities of the Micro-PDP 11/73 logging the data. Logging all measurements for subsequent averaging would have required too much disk space. In order to obtain fast linear averaging, a technique was developed and

implemented with success.

The digitizer outputs a value proportional to the logarithm of the power received:

$$k \ln(P_{n+1})$$

Suppose that the sum of n measurements is already stored as an integer in memory in the form

$$k \ln(\Sigma P_i)$$

If c is define as the difference between the two

$$c = k \ln(P_{n+1}) - k \ln(\Sigma P_i)$$

then

$$\ln\left(\frac{P_{n+1}}{\Sigma P_i}\right) = \frac{c}{k} \quad \Rightarrow \quad P_{n+1} = (\Sigma P_i) \exp\left(\frac{c}{k}\right)$$

The new received power measurement is now added to the previous ones:

$$(\Sigma P_i) + P_{n+1} = (\Sigma P_i)\left(1 + \exp\left(\frac{c}{k}\right)\right)$$

$$\therefore \quad k \ln(P_{n+1} + \Sigma P_i) = k \ln(\Sigma P_i) + k \ln\left(1 + \exp\left(\frac{c}{k}\right)\right)$$

The equation has two terms: the first one is the previous sum stored in the same form as previously and the second term is a function of c only. Since the new value comes from a

digitizer and the sum is in integer form, c can only take a discrete number of values. Since the number of values of c is limited, a table of values of the second term can be stored in the computer and accessed using c as an index.

The first measurement coming from the digitizer is transferred directly to the sum since it already has the correct format. For the next measurements, the summing algorithm is relatively simple: first the sum is subtracted from the new measurement. The value obtained is then used as an index to get a number from the table of pre-calculated second term values. This number is then added to the sum. When all the measurements are integrated, the sum of received powers can be easily converted to numbers proportional to the logarithm of reflectivities by making a correction for range and for the number of measurements that entered in the computation of the sum. Since the averaging technique is simple and does not require floating point or large integer calculations, it can be done easily in real-time by the microcomputer as the measurements are taken. The processing time for 250 bins is more or less equal to the time it takes to wait to get a reflectivity measurement independent to the previous one (of the order of 5 ms; Sauvageot, 1982)

Appendix B: Sample HTIs

The following nine pages show some of the HTIs collected for the thesis. Two HTIs are displayed on each page and they are related to the same event. The top image shows the complete event while the bottom image zooms on a particular or strange feature of the event.

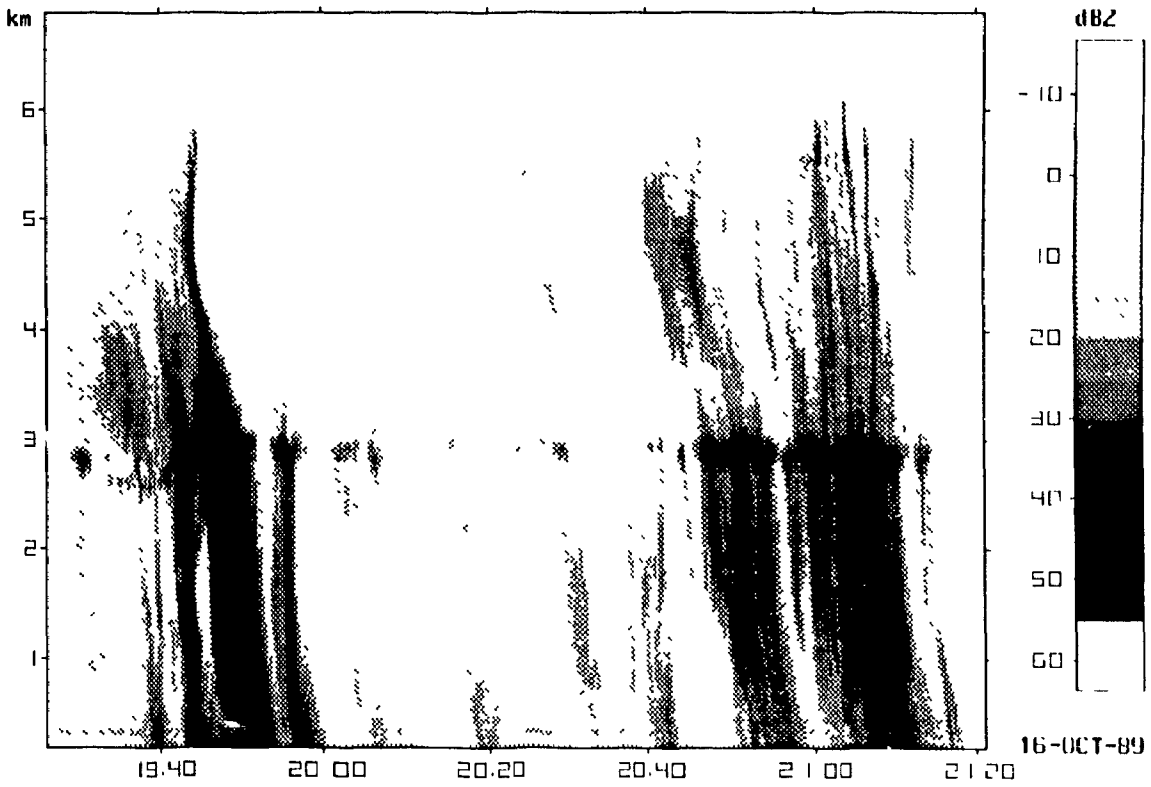
km
6
5
4
3
2
1
dBZ
- 10
0
10
20
30
40
50
60
19.40
20 00
20.20
20.40
21 00
21 20
16-OCT-89

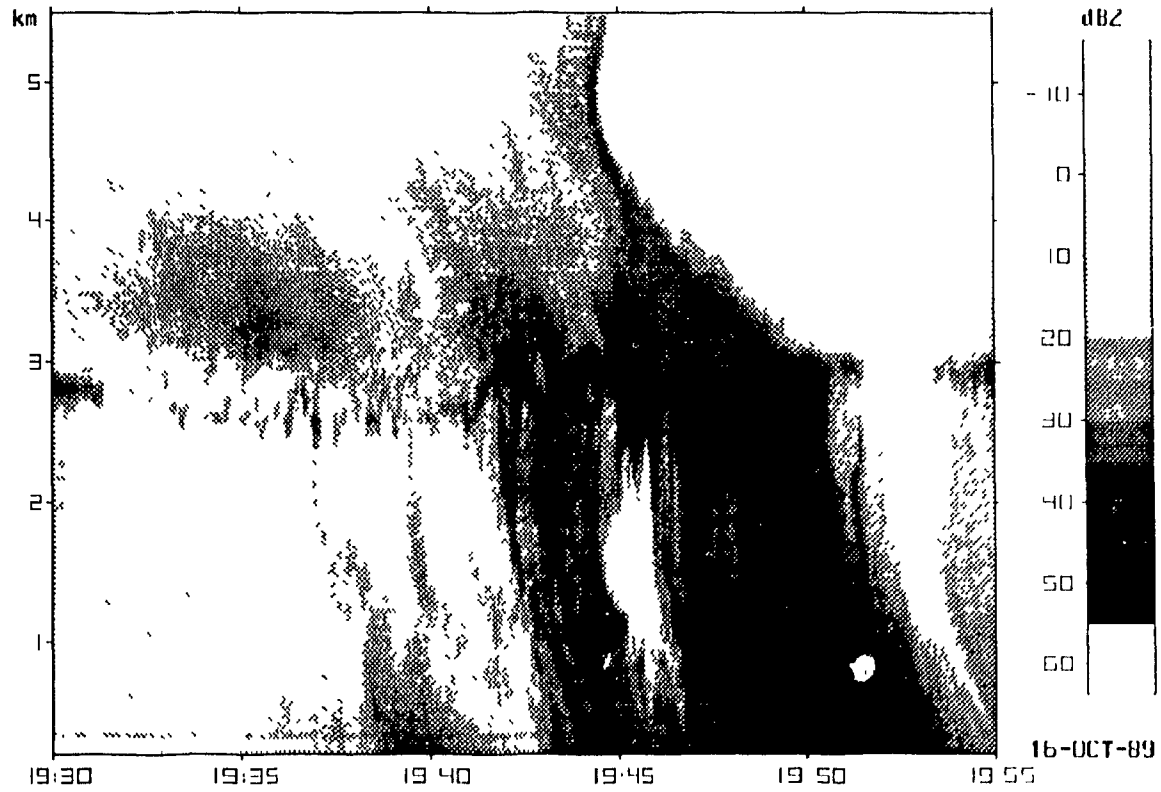
km
5
4
3
2
1
dBZ
- 10
0
10
20
30
40
50
60
19:30
19:35
19 40
19:45
19 50
19 55
16-OCT-89

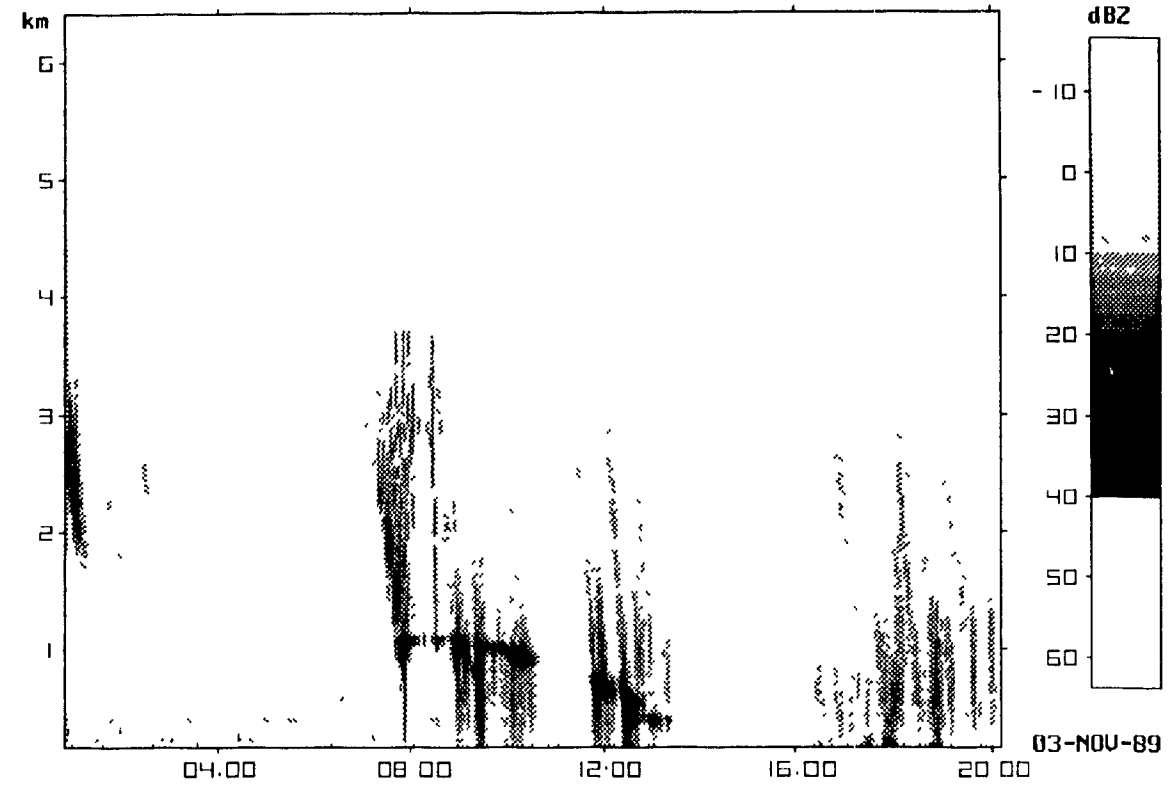
km
6
5
4
3
2
1
04.00
08 00
12:00
16.00
20 00
dBZ
- 10
0
10
20
30
40
50
60
03-NOV-89

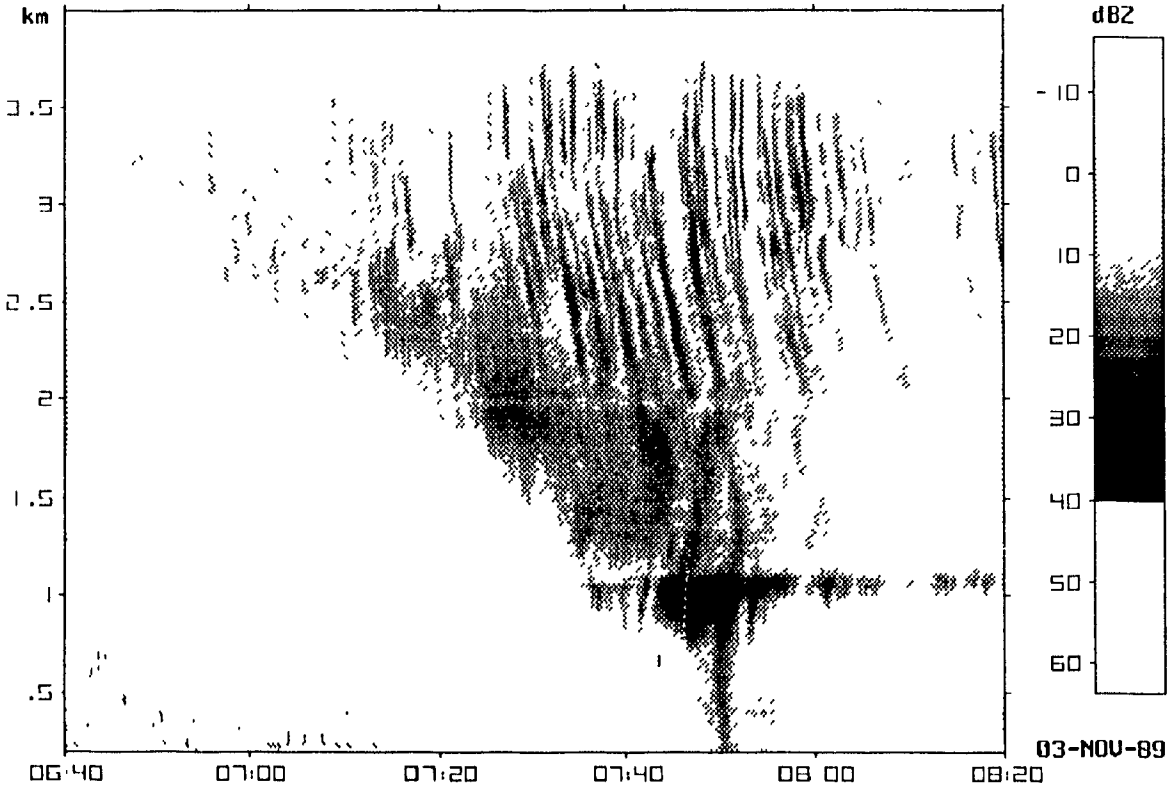
km
3.5
3
2.5
2
1.5
1
.5
06:40
07:00
07:20
07:40
08 00
08:20
dBZ
- 10
0
10
20
30
40
50
60
03-NOV-89

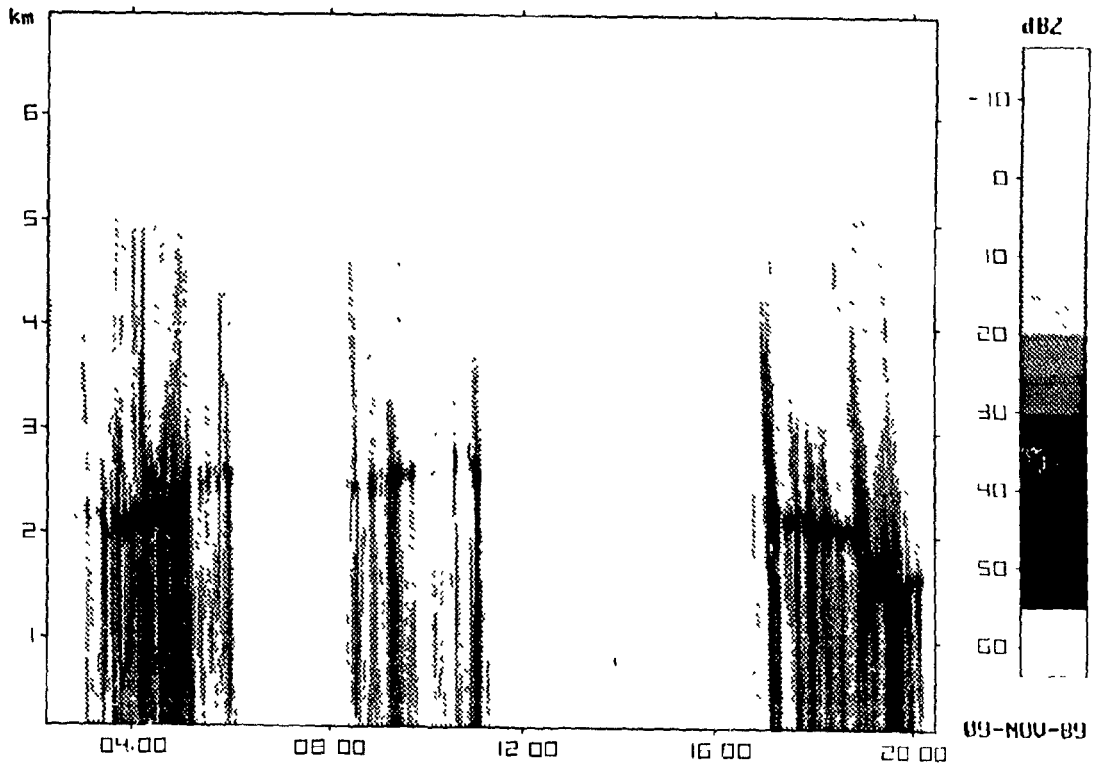
km
6
5
4
3
2
1
04.00
08 00
12 00
16 00
20 00
dBZ
- 10
0
10
20
30
40
50
60
09-NOV-89

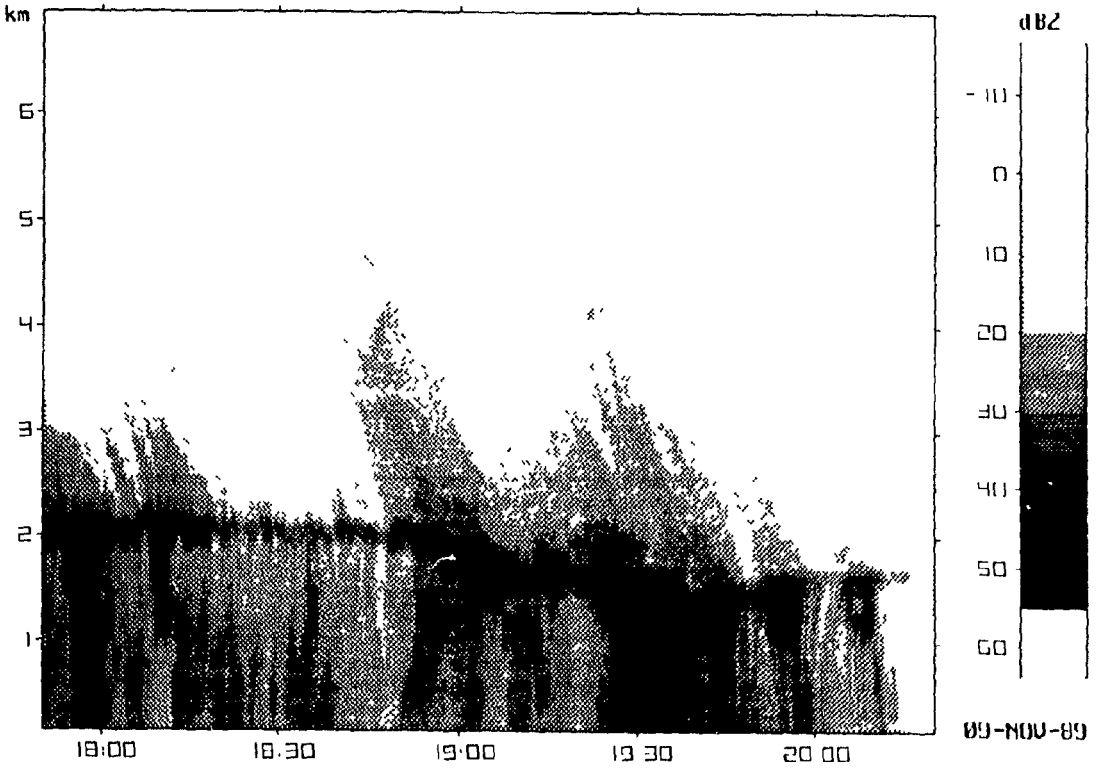
km
6
5
4
3
2
1
18:00
18:30
19:00
19 30
20 00
dBZ
- 10
0
10
20
30
40
50
60
09-NOV-89

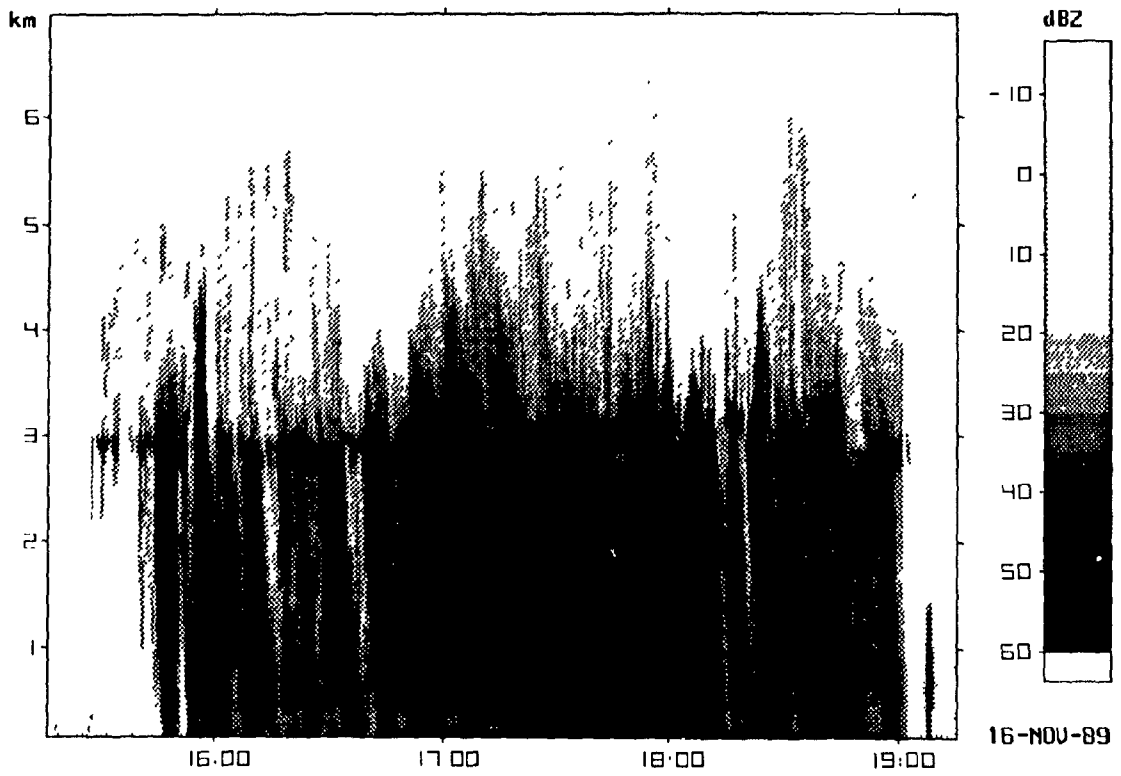
km
6
5
4
3
2
1
16:00
17:00
18:00
19:00
dBZ
-10
0
10
20
30
40
50
60
16-NOV-89

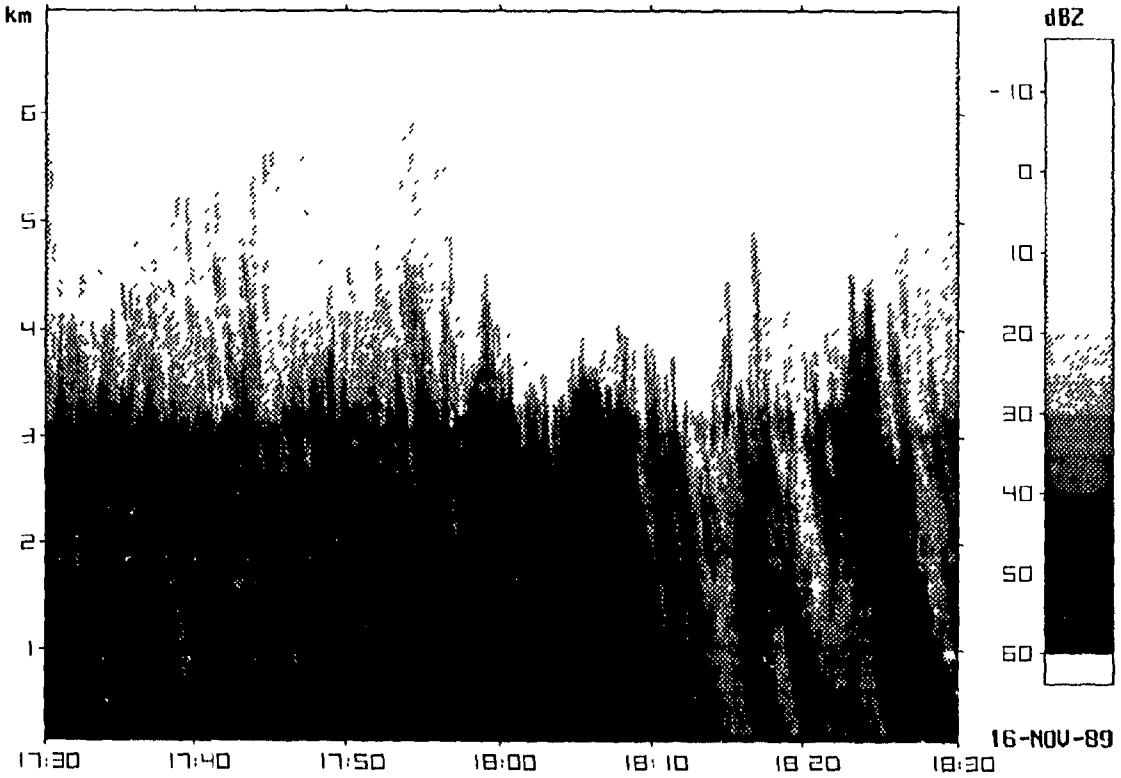
km
6
5
4
3
2
1
17:30
17:40
17:50
18:00
18:10
18:20
18:30
dBZ
-10
0
10
20
30
40
50
60
16-NOV-89

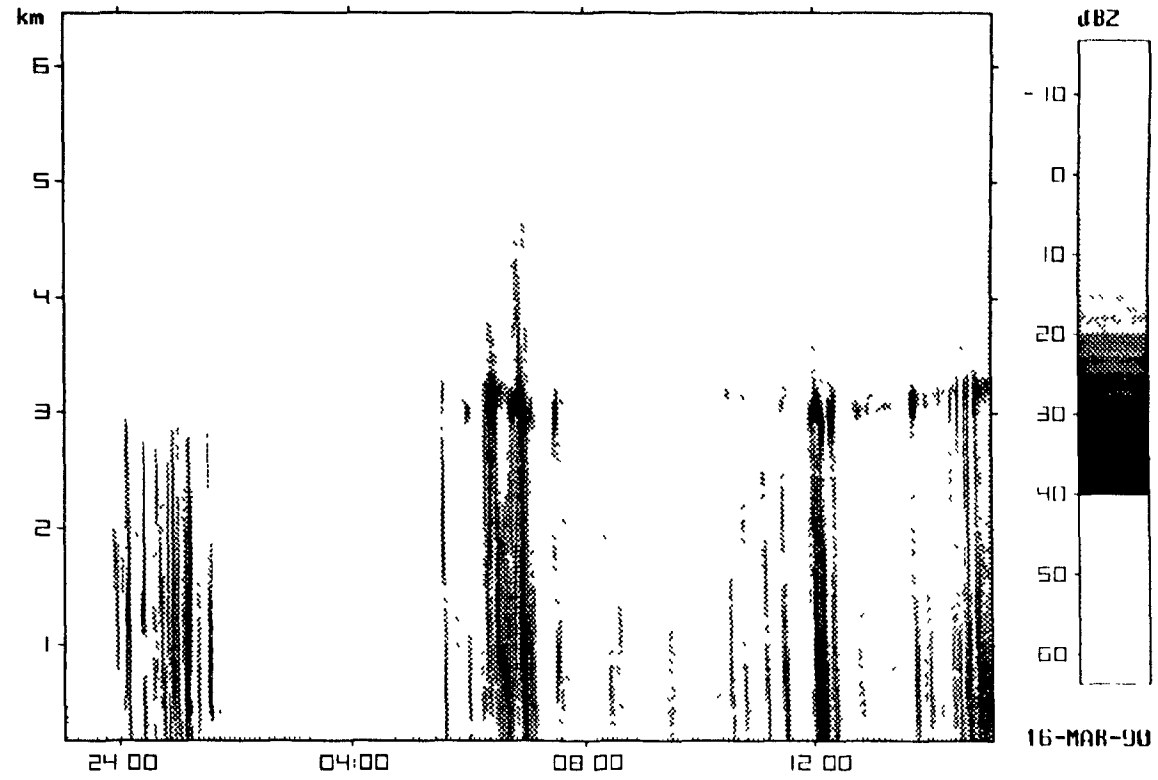
km
6
5
4
3
2
1
24 00
04:00
08 00
12 00
dBZ
- 10
0
10
20
30
40
50
60
16-MAR-90

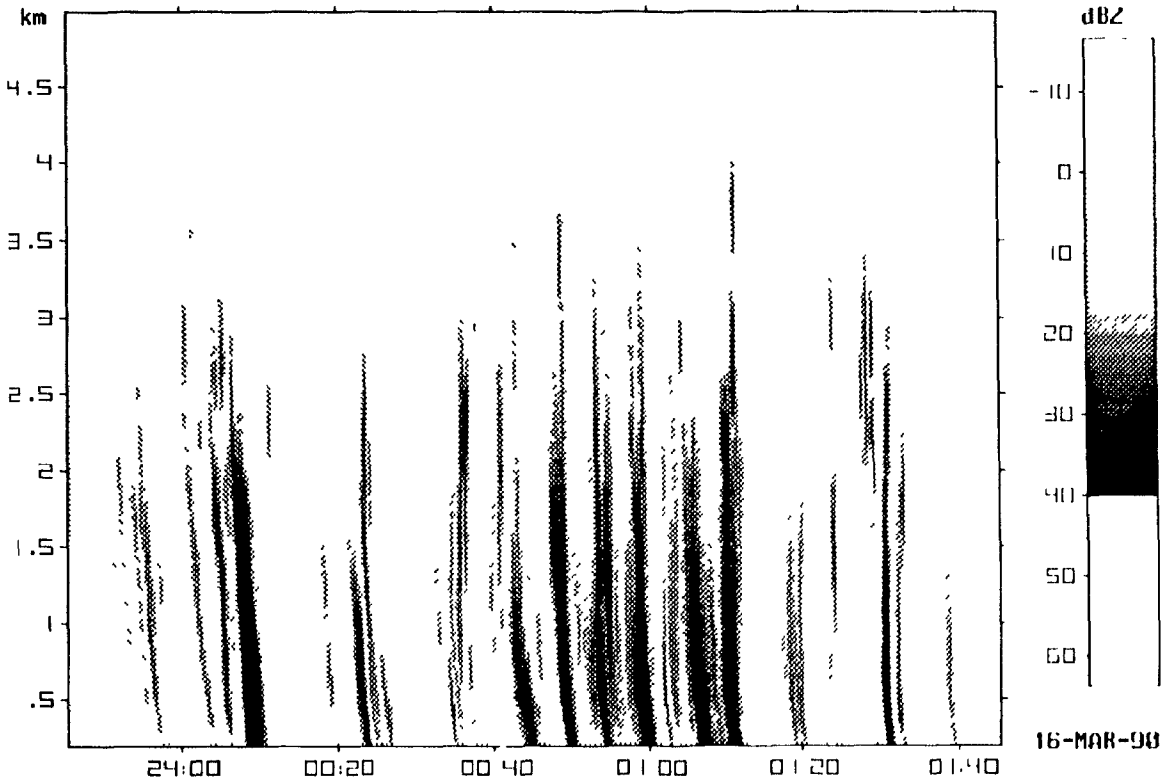
km
4.5
4
3.5
3
2.5
2
1.5
1
.5
24:00
00:20
00 40
01 00
01 20
01:40
dBZ
- 10
0
10
20
30
40
50
60
16-MAR-90

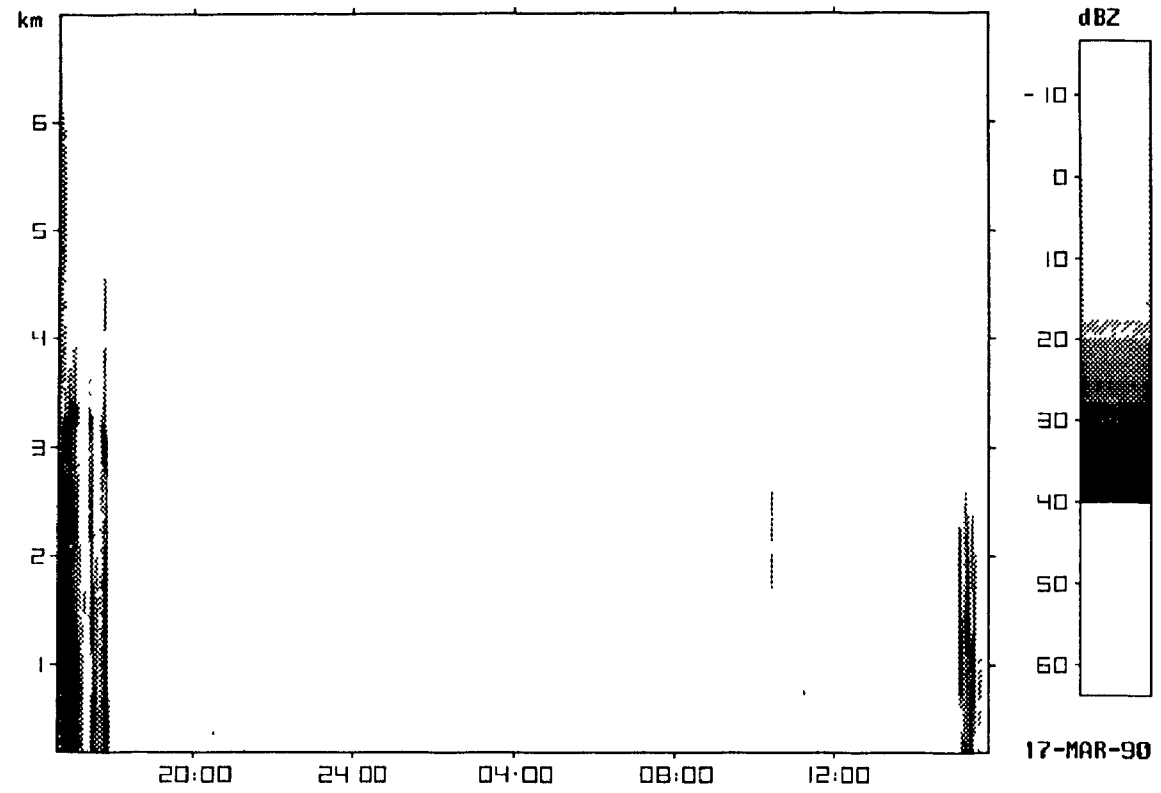
km
6
5
4
3
2
1
20:00
24 00
04:00
08:00
12:00
dBZ
- 10
0
10
20
30
40
50
60
17-MAR-90

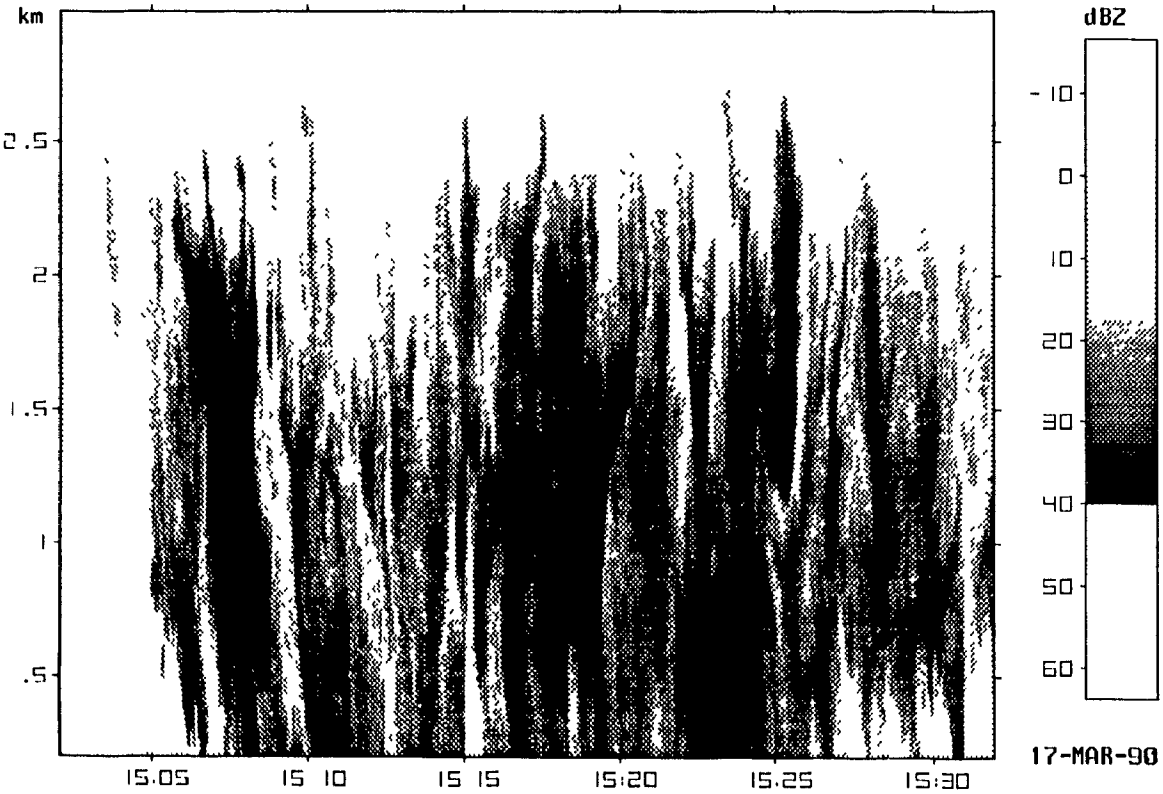
km
2.5
2
1.5
1
.5
15:05
15 10
15 15
15:20
15:25
15:30
dBZ
- 10
0
10
20
30
40
50
60
17-MAR-90

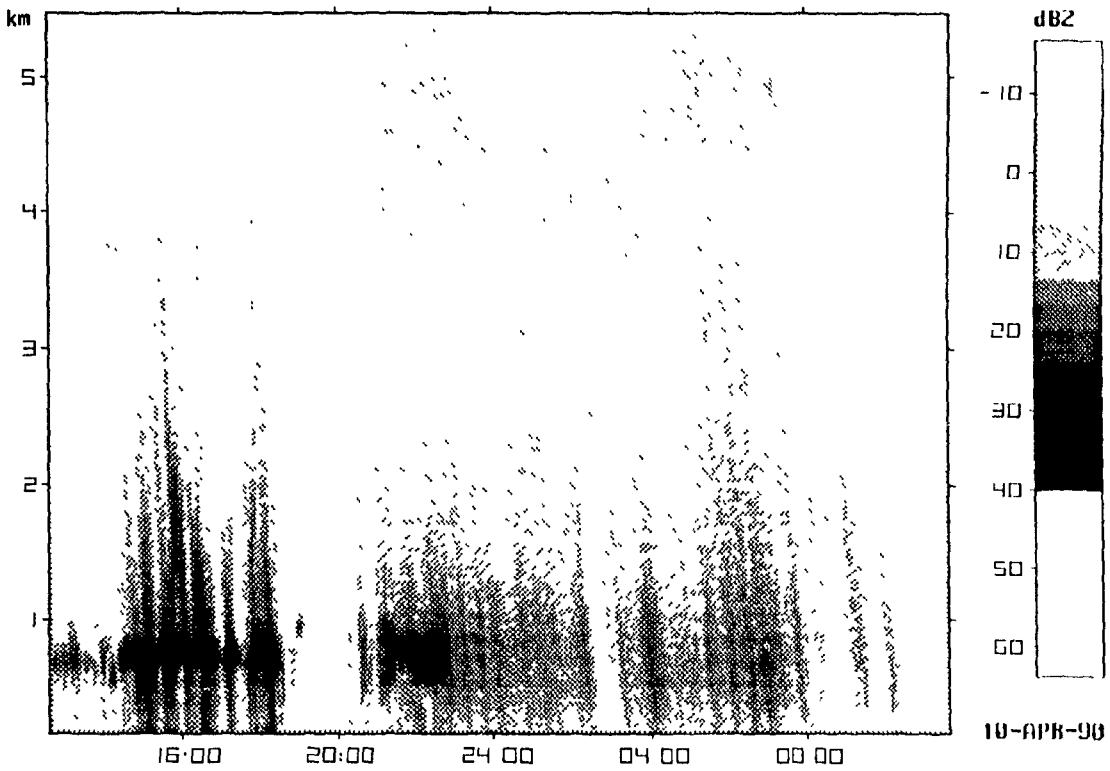
km
5
4
3
2
1
16:00
20:00
24 00
04 00
00 00
dBZ
- 10
0
10
20
30
40
50
60
10-APR-90

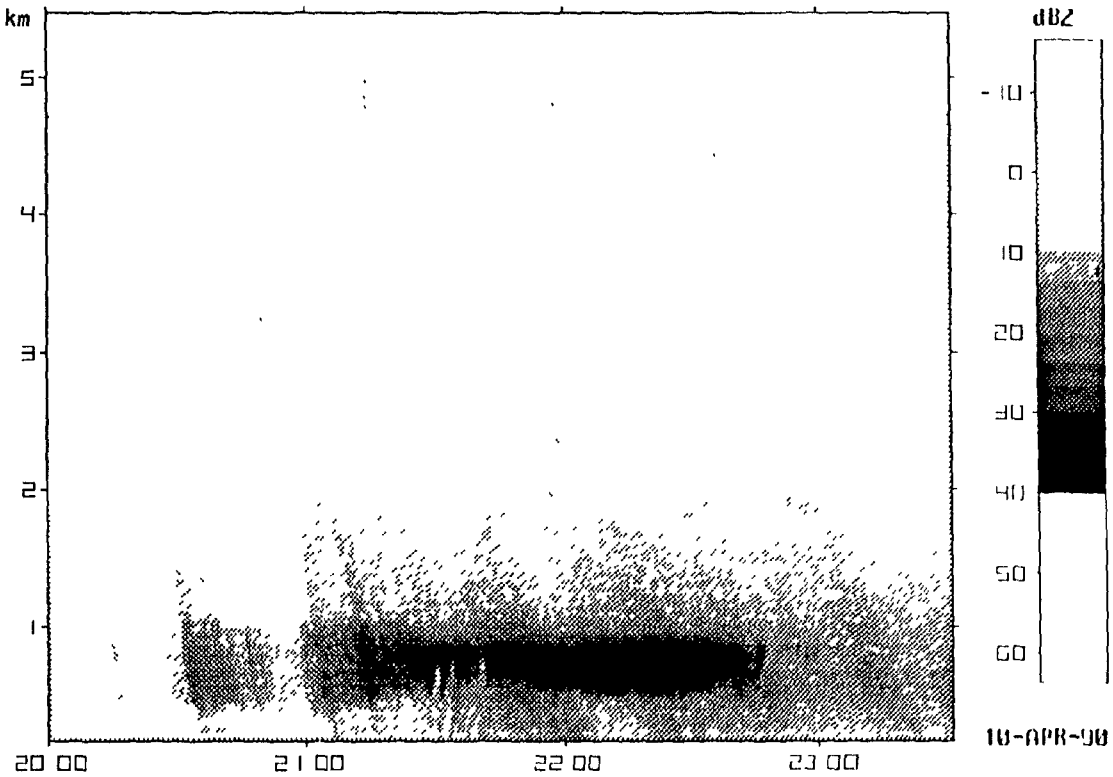
km
5
4
3
2
1
20 00
21 00
22 00
23 00
dBZ
- 10
0
10
20
30
40
50
60
10-APR-90

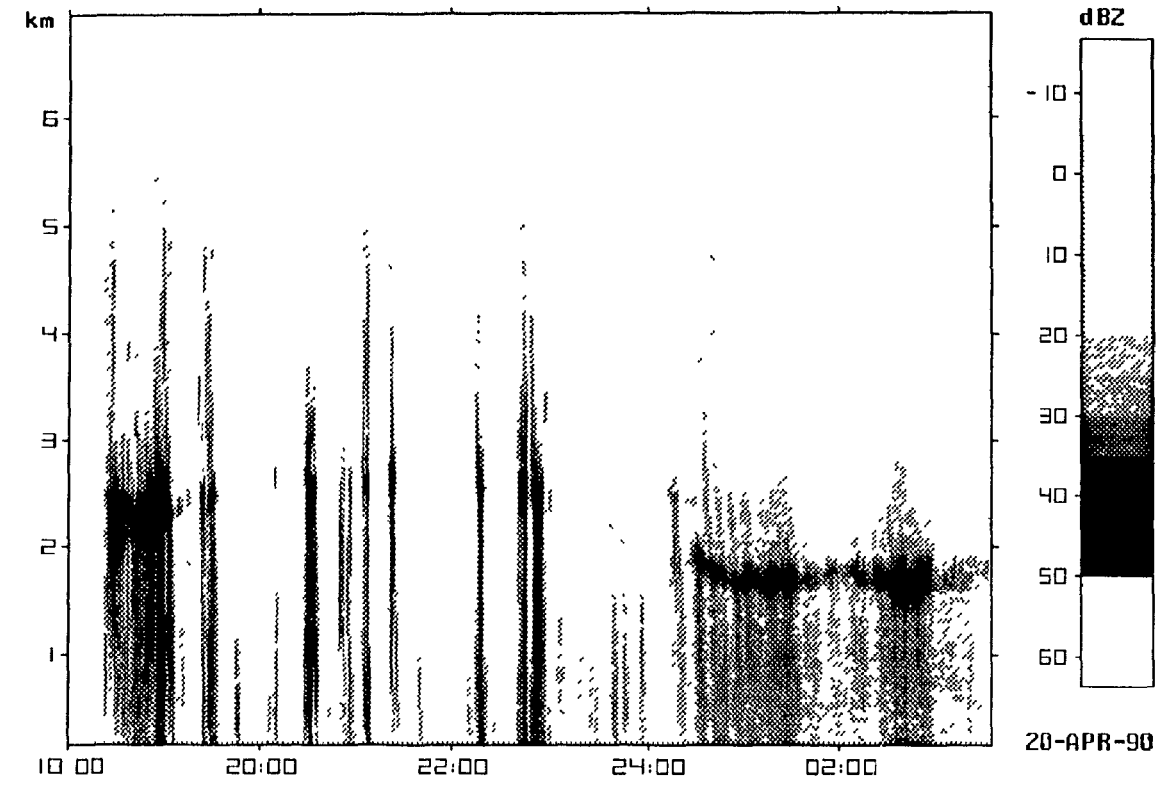
km
6
5
4
3
2
1
10 00
20:00
22:00
24:00
02:00
dBZ
-10
0
10
20
30
40
50
60
20-APR-90

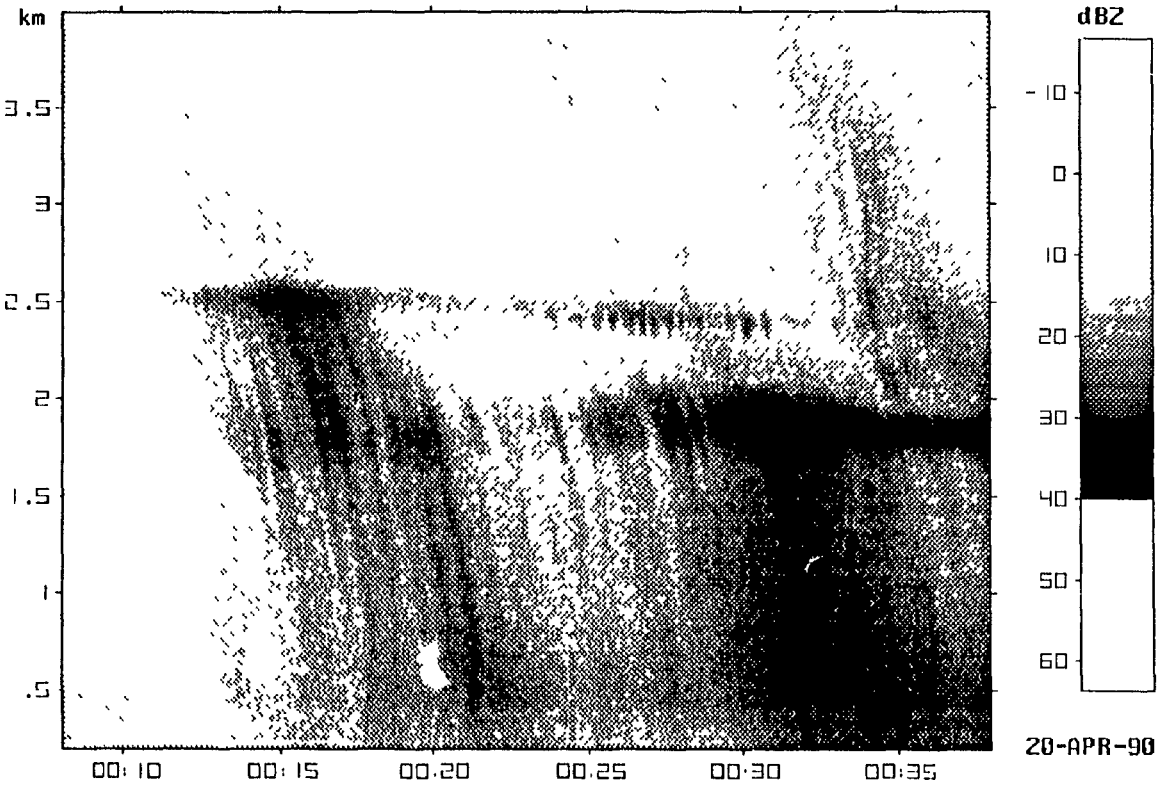
km
3.5
3
2.5
2
1.5
1
.5
00:10
00:15
00:20
00:25
00:30
00:35
dBZ
-10
0
10
20
30
40
50
60
20-APR-90

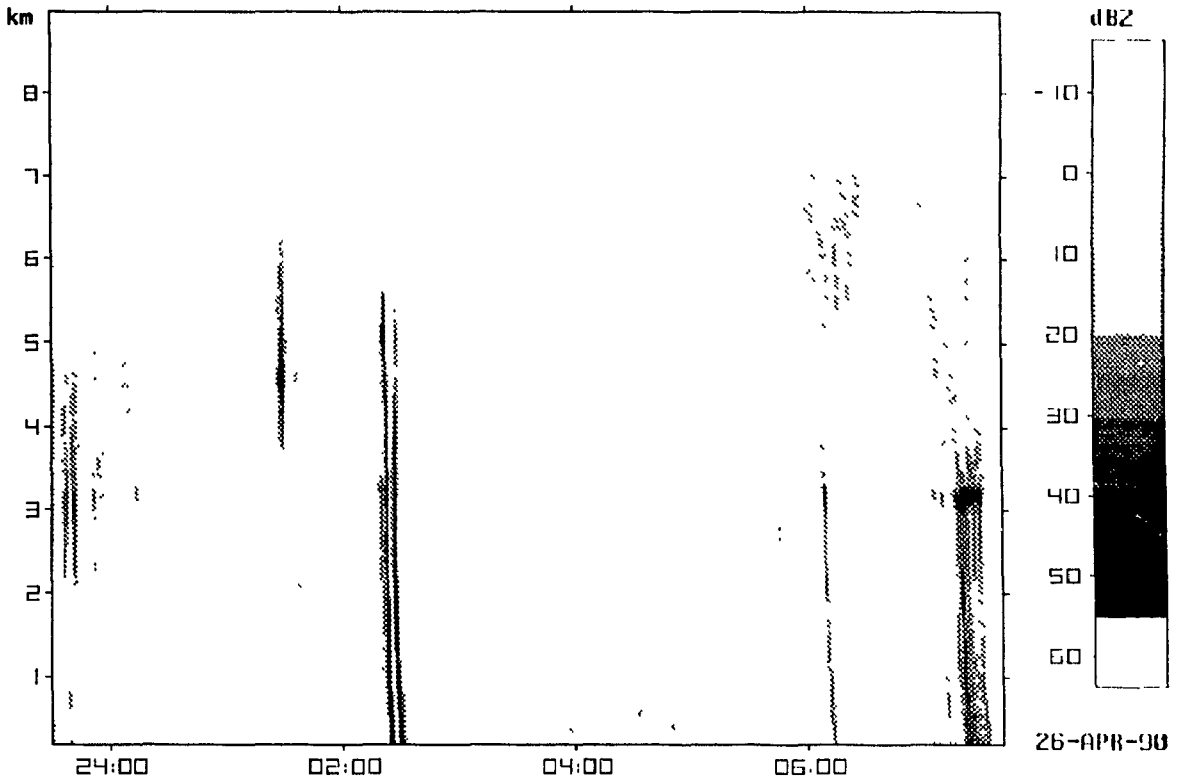
km
8
7
6
5
4
3
2
1
24:00
02:00
04:00
06:00
dBZ
-10
0
10
20
30
40
50
60
26-APR-90

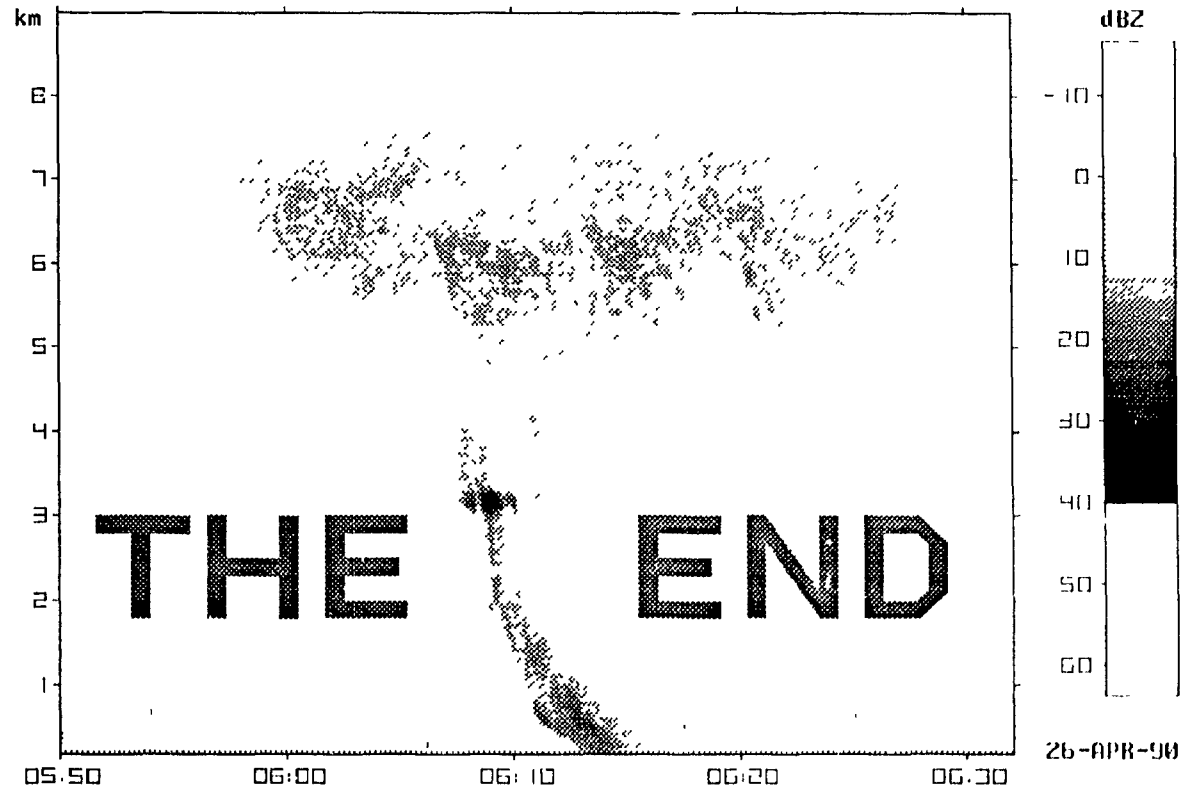
km
8
7
6
5
4
3
2
1
THE END
05:50
06:00
06:10
06:20
06:30
dBZ
-10
0
10
20
30
40
50
60
26-APR-90